Characterizing the Structural Neuroplasticity of Focal Epilepsies with Magnetic Resonance Imaging

By
Daniel Yuchen Chu

A dissertation submitted in partial fulfillment of
the requirements for the degree of

Doctor of Philosophy
(Neuroscience)

at the
UNIVERSITY OF WISCONSIN-MADISON
2023

Date of final oral examination: 11/06/2023

The dissertation is approved by the following members of the Final Oral Committee:
Vivek Prabhakaran, Professor, Radiology, Neurology, and Psychiatry
M. Elizabeth Meyerand, Professor, Biomedical Engineering and Medical Physics
John Paul Yu, Assistant Professor, Radiology
Elizabeth Felton, Assistant Professor, Neurology
Aaron Struck, Assistant Professor, Neurology
Nagesh Adluru, Associate Scientist, Waisman Center

Acknowledgements

It has been a tremendous honor and privilege to study and work alongside some of the most inspiring mentors, colleagues, physicians, and surgeons in my MD-PhD training odyssey to becoming a physician scientist. My gratefulness for them is immeasurable, and no words can fully express the magnitude of my appreciation for all of their support in these past several years.

To **Dr. Irene Chen**, my undergraduate advisor at the University of California, Santa Barbara. You were the first professor to truly believe in me. You gave me my very first basic science research experience. You were instrumental in helping me become fiercely independent and unapologetically curious of the biomedical sciences and gave me the unique opportunity of leading my own pilot project in the microbial metagenome of wound environments. Thank you for all those times you opened your office doors to me for my never-ending questions, my ideas, and even discussions about life in general. To this day, I still think about how lucky I was to have had such a caring and inspiring mentor like you, and it is one of my continuous motivations to become the best physician-scientist I can possibly be.

To **Dr. Jeffrey Cohen**, my IRTA fellowship advisor at the National Institute of Health. You are one of the most dedicated physician-scientists I have ever had the pleasure of working with. You are still one of best physicians I have ever witnessed in action. Your bedside manner continues to inspire me. It was absolutely magical. Shadowing you has allowed me to understand and appreciate the importance of the art of medicine.

To **Dr. Tho Pham**, my advisor at the Stanford School of Medicine. Thank you for being one of my greatest advocates and caring so deeply about my training. But more importantly, you truly cared about me, as a person. I felt like I had one-on-one conversations with you almost daily, to chat about science and life. You made sure I had every single one of my questions answered and had all the tools and resources I needed for the HEV project and for medical school applications. Because of you, I hold myself accountable for paying it forward to students who I mentor. I will continue to bring this attitude to residency, and when I am an attending. Everyone deserves to have a mentor like you. For that, I am forever grateful to you. Thank you, Tho!

To my thesis advisor, **Dr. Vivek Prabhakaran**, thank you for all of your trust and patience, as well as giving me full autonomy in pursuing my research interests. I could not have asked for a more supportive PhD mentor, and you have given me all I needed to be successful in my training and beyond. You embody what I hope to be, a physician scientist who excels at everything they do! Also a big thank you to **Nagesh Adluru** and **Veena Nair** who have not only been brilliant with their technical work in the lab but were also integral components of my graduate school experience and training from the get-go. I came into the lab with no neuroimaging background, and you both have been so patient and nurturing to my development as a neuroscientist.

To **Dr. Samuel Poore**, you were the first to take me in under your wing and gave me my first experience in the OR, where I completely fell in love with surgery and the OR. You always made me feel welcome to departmental events and your OR room and for that, I am deeply grateful. In the MD-PhD communities across the nation, you tend to hear how it is impossible to balance being a surgeon and being a PI. So it is awe-inspiring to see you not only prove them wrong, but how well you are excelling in your surgical practice, your mentorship to students, your basic science research lab, admin work, and your family life. You are the pinnacle of a great surgeon-

scientist, and you are everything that I aspire to be. Thank you!

To **Dr. Daniel Cho** and **Dr. Catharine Garland**, thank you allowing me the opportunity to start a clinical research project from the ground up. You have both been tremendously supportive of my ambitions, research ideas, and have generously provided me with one-on-one mentorship whenever I asked. Also a big thank you to Dr. Cho for advocating for medical student training opportunities. I cannot wait to continue my work in the CRANI lab.

I want to also extend a big thank you to my thesis committee: **Dr. John-Paul Yu, Dr. Beth Meyerand, Dr. Elizabeth Felton, Dr. Aaron Struck**, and **Dr. Nagesh Adluru** for providing me with encouragement and feedback throughout my PhD years. My work in the Prabhakaran lab would not be where it is today, without all of your support and mentorship. A big thank you for **Dr. Susanne Seeger**, my clinical mentor in the first two years of medical school who have been monumental to my development as a future physician.

Thank you to my MSTP family: **Dr. Anna Huttenlocher, Dr. Mark Burkard, Dr. John-Paul Yu, Dr. Elizabeth Felton**, **Chelsea Hanewall**, and **Nichole Monzon**. You have all been a major part of my training and none of this was possible without all of you. Big thank you to **JP**, you opened your doors for me to drop by any time to ask any and all questions that I can think of.

To **Dr. Kathy Foltz,** thank you for being the best advisor a student can ask for at UCSB. Despite your busy schedules, you always made time for me to talk about my motivations and aspirations, and you encouraged me at every step of the way. You were a champion for students; thank you for all that you do.

To **Dr. Bryanna Kunkel.** I was just one of thousands of students you had, but you still took the time to take me on a poster tour of ALL the research that was being conducted in the Chemistry department during your office hours. Thank you for igniting my passions for science during my first year at UCSB.

To my mother, **Li Gao**, and my father, **Genjiang Zhu**. You are both my biggest supporters in whatever I do. Thank you, Mom, you have sacrificed so much for me. You gave up your job as a managing director at a major bank in China, just so I can be provided a better education in the USA. You gave up your dreams so I can pursue mine. For that, I am forever indebted and grateful to you. Thank you, Dad, for keeping me grounded and teaching me about hard work and dedication. Your story of how you dug yourself out of poverty in rural China continues to inspire me and help me appreciate what I have. I love you both.

And finally, to **Zhifei Wang**, my wife. Fei, you are my greatest source of peace and comfort, and your love is a reminder that regardless of any unimaginable scenario life throws at us, that everything will be OK. That we would be OK. With all the uncertainty in this world and in our lives, I couldn't be happier that your love is a certain one. I love you more than words can possibly describe. Thank you for understanding the importance of what I do and what I hope to do, and for being the most accommodating person I can ever ask for.

Table of Contents

ABSTRACT

Epilepsy is the 4th most common neurological disorder. It is associated with a high risk of progressive cognitive and psychosocial dysfunction and presents a great burden on socioeconomic and healthcare costs. Temporal lobe epilepsy (TLE) is the most common form of focal epilepsy in adults and focal cortical dysplasia (FCD) is the most common form of refractory epilepsy in children. Current treatments include anti-seizure medications (ASMs), surgical interventions, neurostimulation, and the ketogenic dietary therapy. One third of patients do not respond to ASMs and surgical intervention frequently fail due to incomplete focus delineation and resection. Current conventional diagnostic and prognostic tools have limited applications in children and patients with disabilities, and they do not capture the complexity of the underlying functional and structural neural networks responsible for the seizures. Thus, identification of reliable neuroimaging biomarkers that can predict the likelihood of disease progression, drug resistance, or severity of neurological and psychological consequences is imperative. The purpose of this dissertation research is to investigate and characterize structural white matter abnormalities in patients with focal epilepsies, in hopes of identifying critical biomarkers to progress clinical management. Data from the Epilepsy Connectome Project (ECP) and the University of Wisconsin Health Hospital and Clinics clinical functional magnetic resonance imaging (MRI) was utilized for our studies. First, this dissertation investigated diffusion weighted imaging (DWI) MRI microstructural differences in fractional anisotropy (FA), mean diffusivity (MD), and radial diffusivity (RD) of clinical FCD patients. Second, graph theoretic measures were used to assess ECP whole brain connectome network abnormalities in TLE patients. Additionally, neurocognitive impairment was correlated with DWI metrics of FA, MD, and RD, as well as with DWI connectivity networks in the ECP connectome. Lastly, we associated neighborhood deprivation with the ECP white matter connectome to elucidate the impact of community-level socioeconomic disadvantage with disease status. Our findings demonstrate

widespread white matter microstructural abnormalities in the FCD patients, as well as global decreased cross-sectional areas of white matter connectivity networks in TLE patients. Furthermore, cognitive impairment in patients was also correlated with aberrant white matter microstructure and network differences. Taken together, this dissertation research elucidated the white matter changes in FCD and TLE, providing additional insights into the underlying pathophysiology of both focal epilepsy diseases.

CHAPTER 1

INTRODUCTION

Epilepsy is the 4th most common neurological disorder, with a prevalence of over 3.4 million in the USA and more than 46 million worldwide (1, 2). Clinically, it is defined by the International League Against Epilepsy as 1) having at least two unprovoked seizures within more than 24 hours apart, 2) one unprovoked seizure and a probability of further seizures similar to the general recurrence risk (at least 60%) after two unprovoked seizures, occurring over the next 10 years, and lastly 3) a diagnosis of an epilepsy syndrome (3). In addition, it is associated with a high risk in progressive cognitive and psychosocial dysfunction, and a great burden on socioeconomic and health-care costs (4-8). Current treatments include anti-seizure medications, surgical interventions, neurostimulation, and the ketogenic dietary therapy. Despite the myriad of anti-seizure medications available, 1/3 of the patients are considered drug resistant or refractory (intractable epilepsy) (9, 10). Surgical intervention offers seizure freedom in some patients with focal epilepsy; however, long-term surgical failures are common due to incomplete focus delineation and resection (11, 12). Conventional diagnostic tools using intracranial electrode recordings and task driven functional neuroimaging have limited applications in children and in patients with disabilities, which is prevalent in the epilepsy population. In addition, they do not capture the complexity of underlying functional and structural neural networks responsible for epilepsy. Thus, a neural circuit-based approach is indicated to provide a framework to investigate the influence of neural networks of focal epilepsy such as TLE in adults and FCD in children. Results and work from this thesis aim to characterize the structural and functional neuroplasticity with the goal of improving patient care for adult and pediatric patients with medically refractory focal epilepsy.

Temporal Lobe Epilepsy: Background and MRI Considerations

Temporal lobe epilepsy (TLE) is the most common form of focal epilepsy in adults (13). Often, TLE occurs in the form of mesial temporal lobe epilepsy secondary to a neurodegenerative process known as hippocampal sclerosis involving structures deep to the

temporal lobe including the hippocampus, parahippocampal gyrus, and the amygdala (14, 15). Other common etiologies may include infections, traumatic brain injuries, vascular anomalies, tumors, idiopathic, or cryptogenic (15). Although some patients with TLE undergo long-term remission, lifelong chronic TLE is debilitating and heavily associated with several cognitive, somatic, and psychiatric co-morbidities (5, 16, 17). Rapid cognitive impairment is also common, suggesting that its lifelong burden is associated with early brain and cognitive aging (18). While TLE surgery can reduce or control seizures in roughly 60%, patients with TLE still represents one of the largest proportions of those with intractable epilepsy (19, 20).

Historically, TLE and other partial epilepsies have been considered as relatively focal processes involving an epileptogenic zone (21-23), which is the specific region or location from which a patient's seizures arise. For decades, this concept has governed surgical management and the medical practice of drug-resistant partial epilepsy. However, in many cases, surgical resection of regions of seizure onset that was initially thought to be curative, is often met with seizure recurrence (11, 24, 25). Emerging evidence now illustrates through various EEG, structural, and functional MRI studies that TLE and other focal epilepsies may impact brain regions far beyond this epileptogenic focus (26-28), while providing evidence that TLE involves networks that is characterized by pathologies such as hyper-excitability and other seizure-related neural plasticity (29-32).

Early prediction of which patients will respond favorably to medications and whether they will respond favorably to surgery is imperative for the optimization of treatment and planning; however, current clinical methods for these predictions are inadequate (11, 24, 33). There are currently no reliable biomarkers that can predict the likelihood of disease progression, drug resistance, or to predict the severity of neurological or psychiatric consequences in patients with TLE. While previous studies have explored structural MRI biomarkers and fMRI connectivity studies (34-37), these studies were typically involved small patient samples and had highly variable results. This exposes that there is a fundamental lack of understanding of the

pathophysiological processes underlying epilepsy progression and remission, which impedes effective delivery of personalized medicine.

With the advent and availability of powerful imaging techniques, we can now quantitatively characterize these structural connections between brain regions that make up these epileptic networks (16, 34, 38). This provides new potential approaches for elucidating not only the pathophysiology, but also for treating and predicting refractory epilepsy in TLE (19, 20). Lately, diffusion tensor imaging (DTI) technique has been utilized to garner insight into the structural integrity of white matter tracts and its microstructures of TLE patients, revealing white matter structural abnormalities beyond just the epileptogenic zone (39).

Recent DTI studies have reported widespread bilateral reductions in fractional anisotropy (FA) and increases in mean and radial diffusivity (MD and RD) in subcortical white matter and was primarily related to reduce neurite density in TLE patients (40). Other studies have started to explore the interplay of focal seizure areas, such as the hippocampus, with its connectome-level effects using diffusion MRI connectomics, which their results revealed significant remodeling of connectome topology and structurally governed functional dynamics in TLE (41). While the concept of TLE as a network disorder is becoming widely accepted, there are few studies that have elucidated the structural connectome and the few that have typically involve small datasets. To our knowledge, no study has characterized the whole brain white matter connectome abnormalities in TLE patients compared to controls in a large scale and homogenous patient study.

The Epilepsy Connectome Project (ECP) is a large-scale dataset collection project of connectivity measurements of patients with idiopathic TLE (42-46). It was the first to develop and validate noninvasive state-of-the-art structural and functional imaging methods for characterizing the whole-brain connectome in a large-scale and non-lesional TLE patient study (42-48).

White matter connectome studies and DTI microstructural studies are both valuable

techniques for understanding the brain's white matter, but they serve different purposes and offer unique insights. In this dissertation, both studies are used in complement to gain a more comprehensive understanding of white matter structure and connectivity in the brain of patients with focal epilepsy.

Focal Cortical Dysplasia: Background and MRI Considerations

Focal cortical dysplasia (FCD) is a common form of intractable epilepsy in children (49). It is characterized by congenital malformations of the neocortex during development and is depicted by abnormal organizations in the cortical and subcortical regions (49). The prevalence of FCD is identified in up to 25% of patients with focal epilepsy (50) and 5% – 10% of patients with epilepsy also have FCD (51). Currently, the pathophysiology and etiology underlying FCD is unclear; however, previous studies indicated possible influence of environmental or genetic factors, infections, or perinatal injury (52). Because most patients with FCD do not respond to anti-seizure medications, surgery remains the predominant option of its treatment. Thus, in order to guide neurosurgical intervention, accurate and effective neuroimaging modalities are imperative to identify structural and functional irregularities and lesions (12, 53).

Historically, magnetic resonance imaging (MRI), positron emission tomography (PET), and single-photon emission computed tomography (SPECT) have been used for assessing FCD and other epilepsies for diagnosis and evaluating surgical indications (54, 55). Although much emphasis has been previously dedicated to gray matter regions, white matter abnormalities have long been identified and appreciated for their role in seizure pathology (56). More recently, diffusion tensor imaging (DTI) tractography has shown great promise in identifying malformations of cortical development through reconstructing the white matter tracts (56, 57). Specifically, it is widely used at the clinical front and in research to characterize abnormalities in white matter integrity and structure. Previous studies demonstrated DTI as a non-invasive and effective imaging tool of the white matter tracts for pre-operative planning in

FCD patients specifically (49, 58). Other previous work has assessed DTI abnormalities in FCD patients regarding abnormal connectivity, myelination, and microstructure (49, 53, 54, 58).

This thesis addresses the fundamental role of neural networks in the pathogenesis of FCD, through integration of advanced neuroimaging, clinical, and neuropsychological data that will inform insights into the structural and functional organization of epilepsy circuits.

Structural White Matter Magnetic Resonance Imaging

Magnetic Resonance Imaging (MRI) is a noninvasive imaging modality that has revolutionized the field of medical imaging (59). It operates on the natural magnetic properties of different tissues in our bodies. By subjecting the body to strong magnetic fields and radiofrequency pulses, MRIs targets the abundant hydrogen atoms from water (H_2O) and fat to generate detailed anatomical images (60). This thesis focuses on one important structural MRI technique: the diffusion weighted MRI.

Diffusion Weight Imaging: Diffusion Tensor Imaging

Diffusion Tensor Imaging (DTI) is a specific type mathematical modeling of DWI and is a widely popular neuroimaging tool among clinicians and researchers in characterizing the structural white matter of human subjects (61). The fundamental principle of DTI is based on how water molecules diffuse differently within tissues, which reveal information on the tissue architecture, integrity, and type (61, 62).

The output of DTI metrics is represented by 4 mathematical quantifications, which infer the direction and extent of water diffusion in the white matter tracts. Fractional anisotropy (FA) measures the degree of anisotropy of water molecules (63). Isotropic water molecules diffuse freely in any direction; however, when water molecules are limited to diffusion within a tube (axon), diffusion only occurs across this tube. Thus, this diffusion is considered anisotropic. The degree of this anisotropy can be assessed to elucidate the white matter tracts' axonal diameter,

fiber density, or myelin structure (63, 64). In the context of pathologies, a decreased FA of the white matter indicates increased isotropy of that tract, possibly due to reduced myelination or abnormal microstructural integrity.

There are three measures of DTI diffusivities that specifically measure the direction of molecule diffusion: mean diffusivity (MD), radial diffusivity (RD), and axial diffusivity (AD) (63). MD represents the average of the overall diffusion in all directions, RD represents diffusion of the two perpendicular directions in relation to the principal direction, and AD depicts the diffusion parallel to the principal direction, along the axonal tracts of the white matter (63). Typically, increased diffusivity measures indicate white matter structural abnormalities or compromise.

Diffusion Weight Imaging: Connectome

A DWI connectome focuses on mapping the axonal pathways, or tracts, that interconnect with different brain regions (65). The connectome approach provides a more global and detailed mapping of white matter networks, offering a more holistic perspective and insight into brain connectivity patterns. While DTI studies assesses the microstructural integrity of white matter tracts, DWI connectome studies connectome studies offer a much more comprehensive perspective of how white matter networks are structurally or anatomically connected (65). Thus, both studies are complementary in providing a comprehensive investigation into white matter abnormalities in neuropathological states, while the white matter connectome also carries functional implications (66-68). The integrity and efficiency of these pathways are crucial for the proper functioning of the brain, thus disruptions in white matter connectivity can provide insights into various neurological conditions and cognitive deficits.

In a connectome study, brain region end points are known as a node, and the white matter tracts between them are represented as edges (48, 69). White matter connectome data can be interpreted and analyzed using graph theory techniques to reveal network properties,

such as hubs, modularity, and small-worldness (47, 66). Work from this thesis delves into another technique called threshold free network-based statistics (TFNBS) (70). While traditional network analysis often involve the application of a threshold to the connectivity data to create binary networks (where edges are either present or absent), which ultimately may lead to biases in network properties. Setting an arbitrary threshold can result in the loss of valuable information (70). TFNBS eliminates the need of an arbitrary threshold by binarizing the connectivity data, considering the full range of connectivity strengths. It assesses the statistical significance of each connection across the entire distribution of connectivity strengths, avoiding the need to select a single threshold (70).

Thesis Summary

Temporal lobe epilepsy (TLE) is the most common type of focal epilepsy in adults and Focal Cortical Dysplasia (FCD) is the most common type of focal epilepsy in children. They are both associated with the largest group with medically refractory seizures in their respective populations (13). It has been previously established that focal epilepsy is localized to a seizure focus region called the epileptogenic focus (22, 23). For decades, this concept has guided clinical and surgical practice in targeted resection and ablation of the region as treatment (11, 25). While initially effective in achieving seizure freedom, many patients later saw a recurrence in these seizures (11, 24, 25). In addition to this, recent EEG and neuroimaging studies now demonstrate that focal epilepsy may affect regions beyond the epileptogenic zone, implicating broad network abnormalities in focal epilepsies (26-28).

Furthermore, despite the decades of research efforts, there is still a lack of reliable biomarkers that informs TLE and FCD disease progression, drug resistance, severity of cognitive and psychiatric co-morbidities, etc. The work in this thesis employs the Epilepsy Connectome Project (ECP), modeled after the Human Connectome Project (HCP), a large-scale multisite project

involving the University of Wisconsin Madison and the Medical College of Wisconsin (42-48). The ECP collected connectivity measurements in non-lesional TLE patients using diffusion-weighted magnetic resonance imaging (MRI) of structural connections. In addition, we also utilized the clinical fMRI FCD dataset from the University of Wisconsin Hospital Systems, which collected diffusion weighted MRI data as well as the structural neuroanatomical data. **The goal of this proposal is to characterize the structural brain plasticity and identify novel biomarkers in focal epilepsy patients using state-of-the-art neuroimaging methods. Overall, we hypothesize that FCD and TLE patients will exhibit distinct and discrete aberrant white-matter network connectivity and microstructure compared to that of healthy normal subjects.**

Specific Aims

Aim 1: Characterize diffusion tensor imaging based white matter microstructural abnormalities in patients with focal epilepsy.

Aim 2: Characterize diffusion-weighted MRI based white matter connectome abnormalities in patients with focal epilepsy.

Aim 3: Investigate the impact of cognitive impairment on white matter structure and connectivity in patients with focal epilepsy.

Ultimately, our studies have contributed to the overall understanding of the pathophysiology of focal epilepsy progression and remission, and provided more insight in identifying novel biomarkers that will hopefully inform novel clinical tools for diagnosis, formulate individualized management of patients via quantitative structural neuroimaging, improve prognosis, and provide tools for better pre-surgical planning.

CHAPTER 2

Application of Data Harmonization and Tract-Based Spatial Statistics Reveals White Matter Structural Abnormalities in Pediatric Patients with Focal Cortical Dysplasia

Daniel Y. Chu[1,2], Nagesh Adluru[1,3], Veena A. Nair[1], Anusha Adluru[1], Timothy Choi[1], Alanna Kessler-Jones[2,3], Kevin Dabbs[2], Jiancheng Hou[1], Bruce Hermann[2], Vivek Prabhakaran[1,2,4,5*], Raheel Ahmed[6*]

[1]Department of Radiology, University of Wisconsin-Madison, 1111 Highland Avenue, Madison, WI 53705, United States

[2]Department of Neurology, University of Wisconsin-Madison, 1111 Highland Avenue, Madison, WI 53705, United States

[3]Waisman Center, University of Wisconsin-Madison, 1500 Highland Avenue, Madison, WI 53705, United States

[4]Department of Medical Physics, University of Wisconsin-Madison, 1111 Highland Avenue, Madison, WI 53705, United States

[5]Department of Psychiatry, University of Wisconsin-Madison, 6001 Research Park Blvd, Madison, WI 53719, United States

[6]Department of Neurological Surgery, University of Wisconsin-Madison, 600 Highland Avenue, Madison, WI 53792, United States

*Co-principal authors

Published in *Epilepsy & Behavior*. PMID: 37011527; PMCID: PMC10371876.

Abstract

Our study assessed diffusion tensor imaging (DTI) metrics of fractional anisotropy (FA), mean diffusivity (MD), and radial diffusivity (RD) in pediatric subjects with epilepsy secondary to Focal Cortical Dysplasia (FCD) to improve our understanding of structural network changes associated with FCD related epilepsy. We utilized a data harmonization (DH) approach to minimize confounding effects induced by MRI protocol differences. We also assessed correlations between DTI metrics and neurocognitive measures of fluid reasoning index (FRI), verbal comprehension index (VCI), and visuospatial index (VSI). Data (n=51) from 23 FCD patients and 28 typically developing controls (TD) scanned clinically on either 1.5T, 3T, or 3T-wide-bore MRI were retrospectively analyzed. Tract-based spatial statistics (TBSS) with threshold-free cluster enhancement and permutation testing with 100,000 permutations were used for statistical analysis. To account for imaging protocol differences, we employed non-parametric data harmonization prior to permutation testing. Our analysis demonstrates that DH effectively removed MRI protocol-based differences typical in clinical acquisitions, while preserving group differences in DTI metrics between FCD and TD subjects. Furthermore, DH strengthened the association between DTI metrics and neurocognitive indices. FA, MD, and RD metrics showed stronger correlation with FRI and VSI than VCI. Our results demonstrate that DH is an integral step to reduce the confounding effect of MRI protocol differences during analysis of white matter tracts and highlights biological differences between FCD and healthy control subjects. Characterization of white matter changes associated with FCD related epilepsy may better inform prognosis and treatment approaches.

Introduction

Neuroimaging has enabled investigative analysis of brain networks yielding key insights into dynamics of neural network activity and an improved understanding of the structural and functional architecture of the brain. These analytical frameworks have been utilized for a broad range of clinical disorders including neurodegenerative (71, 72), neuropsychiatric, (73-75) and developmental disorders in adults and children (76, 77). Network analyses have also been leveraged to better understand the neurobiological basis of epilepsy, a chronic neurological disorder with high prevalence and public health burden (1). These findings have provided insights into the pathophysiological basis for disease generation and progression (54, 78, 79) and have improved our understanding of the network representation for neurocognitive and clinical phenotypes associated with epilepsy (56).

The majority of these studies comprise of single center data cohorts (51, 58, 80, 81). Whereas multi center imaging data sets improve recruitment and reduce bias from single center recruitment, pooling data sets creates methodological constraints and impacts generalizability, due to underlying differences in image acquisition protocols and scanners utilized for neuroimaging. Harmonized analytical methods have been applied for image processing in multicenter epilepsy cohorts (82). However, few studies have directly examined the effectiveness of data harmonization in addressing image acquisition differences within neuroimaging datasets for epilepsy (83). We therefore addressed the role of data harmonization to minimize the effects of confounding factors introduced by differences in MRI scanning parameters.

FCD is the most common etiology for medication refractory epilepsy in children and is identified in up to 25% of patients with focal epilepsy (50). Our primary aim was to determine the distributive neural network substrates for neurocognitive dysfunction, a principal co-morbidity for subjects with FCD related epilepsy. Our primary hypothesis was, that in epilepsy secondary to FCD, alterations within distributive structural network connectivity is associated with

neurocognitive dysfunction. We investigated white matter tract differences between pediatric subjects with medication refractory epilepsy secondary to FCD, in comparison to healthy controls, with respect to fractional anisotropy (FA), mean diffusivity (MD), and radial diffusivity (RD), using rigorous preprocessing techniques. Our secondary aim was to highlight the application of Combined association test (ComBat) method of data harmonization (84-86) on our data set of pediatric subjects with FCD. In addition to evaluating its effectiveness and robustness, we also hypothesized that application of ComBat harmonization would remove variations in DTI metrics between different MRI scanning parameters, while preserving the underlying biological variabilities. To emphasize and extend the real-world application of data harmonization, we utilized a real-world imaging dataset from a cohort of subjects undergoing routine clinical neuroimaging evaluation, as opposed to research scans obtained from homogenously curated healthy subjects.

Methods

Participants

Twenty-three pediatric patients with a diagnosis of FCD (15 males and 8 females) and 28 typically developing (TD) healthy controls (15 males and 13 females) were included in this study. The study inclusion criteria were children with epilepsy, aged 1-18 years with MR imaging evidence of a prototypical FCD lesion. The radiographic identification of FCD on MR imaging was based on characteristic features of cortical thickening, blurred grey-white matter junction, and abnormal signal intensity on T1 and T2 weighted images (87). Subjects with tandem radiographic lesions consistent with trauma, developmental or acquired conditions were excluded. The DTI scans for these FCD patients were performed between July 2013 and March 2020 and included patients under the age of 18. The control group made up of a subset from previous studies (88). The inclusion criteria of control groups consisted of healthy normally

developing children under the age of 18. The exclusion criteria for the control group included no histories of initial precipitating event (simple of complex febrile seizures), no seizures, no neurological disease, no loss of consciousness >5min, and no family history of first-degree relative with epilepsy or febrile convulsions. This study was carried out under the approval of the Institutional Review Board of the School of Medicine and Public Health, University of Wisconsin Madison.

MRI Image Acquisition and Data Preprocessing

Participants were scanned on either 1.5 T, 3 T, or 3 T-wide bore whole-body commercial MRI scanner (Sigma GE Healthcare, Wisconsin) at the University of Wisconsin. The DTI acquisition parameters were as follows: all healthy controls and FCD patients were scanned either with b = 800 s □mm^{-2} or b = 1000 s □mm^{-2} depending on the scanner location, each with a unique set of gradient directions optimized for DTI axial acquisition with repetition time (TR) = 9,000 ms, echo time (TE) = 76.6 ms, single average (NEX = 1), a reconstructed matrix size of 256 × 256, in-plane resolution = 1 mm x 1 mm, FOV = 120 mm, 75 axial slices with no gap between slices, slice thickness = 3 mm, excitation flip angle α = 90°, and 56 gradient encoded directions.

All diffusion data was preprocessed with the MRTrix3 (89), FSL (90), and ANTS (91) following DESIGNER guidelines (92). The specific steps of DTI processing are as follows: (1) motion correction and distortion of eddy current; (2) correction of head-motion for gradient direction vectors; (3) extraction of brain mask and image registration; (4) estimation of diffusion tensors at each voxel; (5) calculation of FA, MD, RD maps from the diffusion tensor maps.

Neuropsychological Testing

The Wechsler Intelligence Scale for Children Fourth or Fifth Edition (WISC-IV and WISC-V) (93) was administered to patients with epilepsy secondary to FCD and three primary index scores were examined including the fluid reasoning index (FRI), verbal comprehension

index (VCI), and visual spatial index (VSI) (mean=100, standard deviation=15). These summary index scores represent neurocognitive abilities in discrete domains and are reproducible across the pediatric age group. VCI measures the ability to understand and retain verbal information (crystallized intelligence); VSI measures the ability to understand spatial relationships and FRI measures the ability to reason and create new links (fluid intelligence). Within the FCD group, FRI, VCI, and VSI indices were obtained from 16 participants. Neuropsychological tests were administered as part of clinical care. In order to understand their association with white matter structure in FCD, the three cognitive metrics were correlated with significant DTI findings of this study as described below.

Statistical Analyses

Tract based spatial statistics (TBSS) (94) in MNI space with threshold free cluster enhancement (TFCE) and permutation testing (95) with 100,000 permutations was used for statistical analysis, controlling for age and sex. TBSS is a well-established and widely used voxel wise whole-brain analysis method, that helps investigate skeleton voxels within white matter tracts, and identifies group-level differences in microstructural network properties. It generates statistically significant clusters, which can be anatomically labeled using a tractography atlas (94). Analysis of covariance (ANCOVA) was employed to investigate group differences on each DTI metric and the statistical threshold for significance was considered at $p < 0.01$ after family-wise error correcting for multiple comparisons. The family-wise error correction is performed by comparing the TFCE scores to the null distributions (generated using the permutations) of the max (across the white matter skeleton voxels) statistic of the TFCE score.

The regional information of the statistically significant spatial clusters for each DTI metric was identified from the Johns Hopkin's University (JHU) White Matter Tractography Atlas from FSL (https://fsl.fmrib.ox.ac.uk/fsl/fslwiki/Atlases) (96, 97).

Data Harmonization

To account for DTI protocol differences, we employed non-parametric data harmonization using NeuroComBat (84) of the TBSS data in the MNI space prior to the permutation testing. NeuroComBat harmonization "combats the batch/protocol effects" by accounting for additive (on the bias) and multiplicative (on the variance) effects of the protocol on DTI outcomes using a linear model. These correction effects are the expected values of the empirically estimated Bayesian prior distributions either parametrically via Expectation Maximization or non-parametrically via importance sampling. Such a prior based approach is robust when there are small sample sizes per each protocol.

Data harmonization works by treating all protocols to preserve group effects. It moves all distributions to a common distribution that is equidistant to all distributions to achieve an unbiased mean distribution registration. Due to the lack of reference or ground truth, data harmonization is a reasonable approach in reducing biases from any particular protocol, which is akin to generating an unbiased population mean template image (reference frame/coordinate system) from a set of images (98, 99).

Specifically, data harmonization is based on a linear model with an offset/shift (γ_{iv}) and a slope/scale (δ_{iv}) as shown in the equation below for i^{th} protocol, j^{th} participant/scan, and v^{th} voxel.

$$y_{ijv} = c_v + \boldsymbol{X}_{ij}\boldsymbol{\beta}_v + \gamma_{iv} + \delta_{iv}\epsilon_{ijv}$$

where c_v is the overall mean for y for v^{th} voxel. $\boldsymbol{X}_{ij}$ is the design matrix of covariates of interest whose effects on v^{th} voxel ($\boldsymbol{\beta}_v$) we would like to maintain. $\epsilon_{ijv} \sim Normal(0,1)$ is the normal variability in the measurements without any protocol specific variability. The offset and slope variables are estimated using empirical Bayesian framework. This framework improves the variance of these estimates because it assumes these parameters are from a common distribution (per protocol) for all the voxels. That is, $\gamma_{iv} \sim Normal(mean_i, var_i)$ and

$\delta_{iv} \sim InvertedGamma(shape_i, scale_i)$. These site-specific mean, variance, shape, and scale parameters are estimated non-parametrically. The information from *all the voxels*, not just the participants from a single protocol, is used in estimating the shift and scale parameters at each voxel. The term involving $\boldsymbol{\beta_v}$ is added to the measures to preserve the effects of interest.

The distributions across voxels of the gamma and delta estimates for each protocol and DTI measure is illustrated in **Supplementary Figure 1**. Data from MR imaging protocols 2 and 3 are shifted and scaled relatively more compared to that of MR imaging protocols 1 and 4. These shifts and scales are estimated such that the distributions of the measures from the different protocols align to a common distribution. Spatial maps of the shift and scale effects of data harmonization for each of the measure (FA, MD, RD) and the four protocols is shown in **Supplementary Figure 2**. We have also included probability density estimates of the bivariate distributions of the shift and scale effects shown in **Supplementary Figure 3**. Additionally, our group has developed an interactive R application with simulated measurements and protocol effects using this study's parameters (https://nadluru.shinyapps.io/harmonization_demo/). A sample figure from this application is shown in **Supplementary Figure 4**.

Results

Participant Demographic Characteristics and Neuropsychological Scores

Table 1 summarizes the participant demographics and scan parameters. Of the 51 subjects participating in this study, 23 subjects are in the FCD group and 28 are in the TD healthy control group. There were no age and sex differences between the 2 cohorts. The FCD lesion was localized to the left hemisphere in 14 subjects (n = 14; 61%) and to the right hemisphere in 9 subjects (n = 9; 39%). The FCD lesion was localized most frequently to the frontal (n=15, 65%) and temporal lobes (n=5, 22%) respectively.

We identified four different sets of DTI scanning protocols for our cohort. The first

parameter set (MRI Protocol 1) consists of imaging obtained on a 1.5T scanner, with 26 volumes, 25 volumes over b > 0, and a b-value of 1000 s □mm^{-2}. The second parameter set (MRI Protocol 2) consists of imaging obtained on a 3T scanner, with 26 volumes, 25 volumes over b > 0, and a b-value of 1000 s □mm^{-2}. The third DTI parameter set (MRI Protocol 3) consists of imaging also obtained on a 3T scanner, but with 31 volumes, 30 of which are b > 0, and contains a b-value of 800 s □mm^{-2}. Lastly, the fourth DTI parameter set (MRI Protocol 4) consists of imaging obtained on a 3T-wide bore scanner, with 41 volumes, 40 volumes over b > 0, and a b-value of 800 s □mm^{-2}. All TD controls were scanned with MRI Protocol 1. The FCD group contains 3 subjects scanned under MRI Protocol 1, 6 subjects with MRI Protocol 2, 6 subjects in MRI Protocol 3, and 8 subjects in MRI Protocol 4. Mean WISC-IV and WISC-V index scores were FRI= 86 ± 15.39, VCI= 88 ± 15.76, and VSI= 87 ± 19.04 (**Table 1**).

	TD Controls	FCD Patients
Sample size	28	23
Sex (M/F)	15/13	15/8
Age (Years)	11.39 ± 2.38 [β]	11.06 ± 4.46
# Subjects with MRI protocol 1: (1.5T; 26 volumes; 25 # of b > 0; b-value = 1000 s □mm^{-2})	28	3
# Subjects with MRI protocol 2: (3T; 26 volumes; 25 # of b > 0; b-value = 1000 s □mm^{-2})	0	6
# Subjects with MRI protocol 3: (3T; 31 volumes; 30 # of b > 0; b-value = 800 s □mm^{-2})	0	6
# Subjects with MRI protocol 4: (3Tw; 41 volumes; 40 # of b > 0; b-value = 800 s □mm^{-2})	0	8
Fluid Reasoning Index (FRI) score	N/A	86 ± 15.39
Verbal Comprehension Index (VCI) score	N/A	88 ± 15.76
Visual Spatial Index (VSI) score	N/A	87 ± 19.04
Lobar distribution of FCD lesions [α]		
Frontal		15 (65%)
Temporal		5 (22%)
Parietal		2 (7%)

Table 1. Participant Demographics and Scanning Information. Demographic, DTI scanning protocol information, and neuropsychological scores for 51 subjects for the study cohort.
[α]: 1 subject had multi lobar distribution
[β]:There was no statistical differences in mean age between the two groups.

Data Harmonization

Relative mean differences in FA, MD and RD indices across significantly different clusters, on FCD and TD group comparisons, were computed before and after data harmonization. **Figure 1a** illustrates the effect of data harmonization on group differences between FCD and TD groups focusing on relative mean differences in FA, MD, and RD across significantly different clusters. The effects of harmonization on each DTI index are illustrated for both FCD and TD groups (**Figure 1b**). Within significant FA clusters, data harmonization removed FA differences caused by protocol discrepancies while preserving significant FA group differences, resulting in expected reduction of median inter-group differences from -15% to -13%. Likewise, following data harmonization there was a significant decrease in inter-group differences between FCD and TD groups, from 10% to 8% for MD, and from 15% to 11% for RD measures respectively. This demonstrates that data harmonization can improve statistical power in detecting underlying, significant group differences in FA, MD and RD measures after adjusting for protocol-based differences.

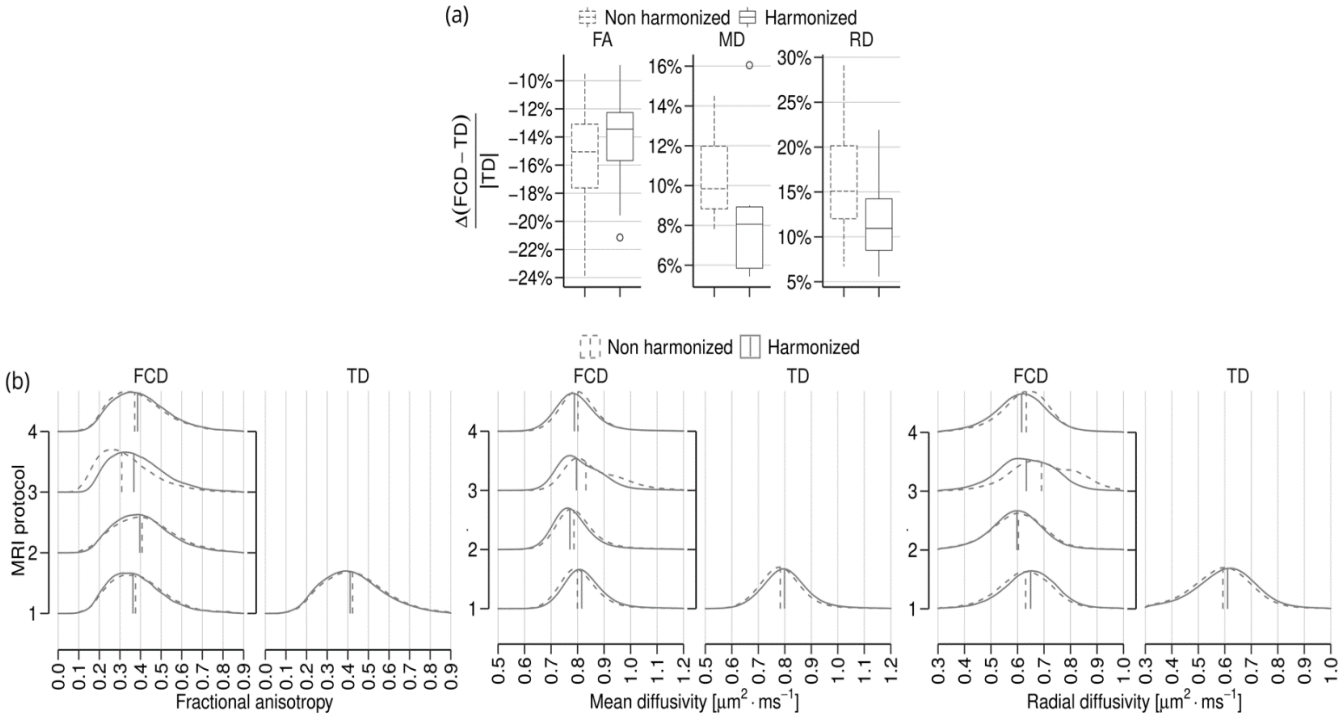

Figure 1. Application of Data Harmonization towards comparison of FA, MD, and RD indices between FCD and TD groups. **a)** All 3 DTI indices exhibited reductions in group differences between FCD and TD as a result of ComBat data harmonization. For all 3 DTI indices, data harmonization removed FA, MD, and RD inter-group differences attributable to protocol differences while preserving intrinsic significant inter-group differences; **b)** The direct effect of data harmonization, while preserving for age, sex, and group effects, for each DTI protocol for FA (left panel), MD (middle panel), and RD (right panel) are shown in these plots for FCD and TD groups. Following data harmonization, distributions of DTI values across different MRI protocols are more aligned, as visible by the closer median values, indicating reduction of protocol-based differences in DTI group comparisons.

Analysis of Diffusion Tensor Imaging Metrics

There were 17 FA clusters that were significantly different between FCD and TD groups. FA was decreased in the FCD group (median decrease 13.3%; range 8.89% - 21.15%), in comparison to the TD cohort. There were 9 MD clusters that were significantly different between FCD and TD groups. MD was increased in the FCD group in comparison to the TD group (median increase 8.0%; range 5.43% - 16.05%). RD comparison between FCD and TD showed 22 significantly different RD clusters. RD was increased in FCD group compared to the TD cohort (median increase 11.0%, range 5.59% - 21.91%). **Figure 2** illustrates cluster level histograms and density plots for age and sex adjusted FA, MD, and RD values for 3

representative clusters respectively, that are significantly different on FCD and TD group comparison after harmonization.

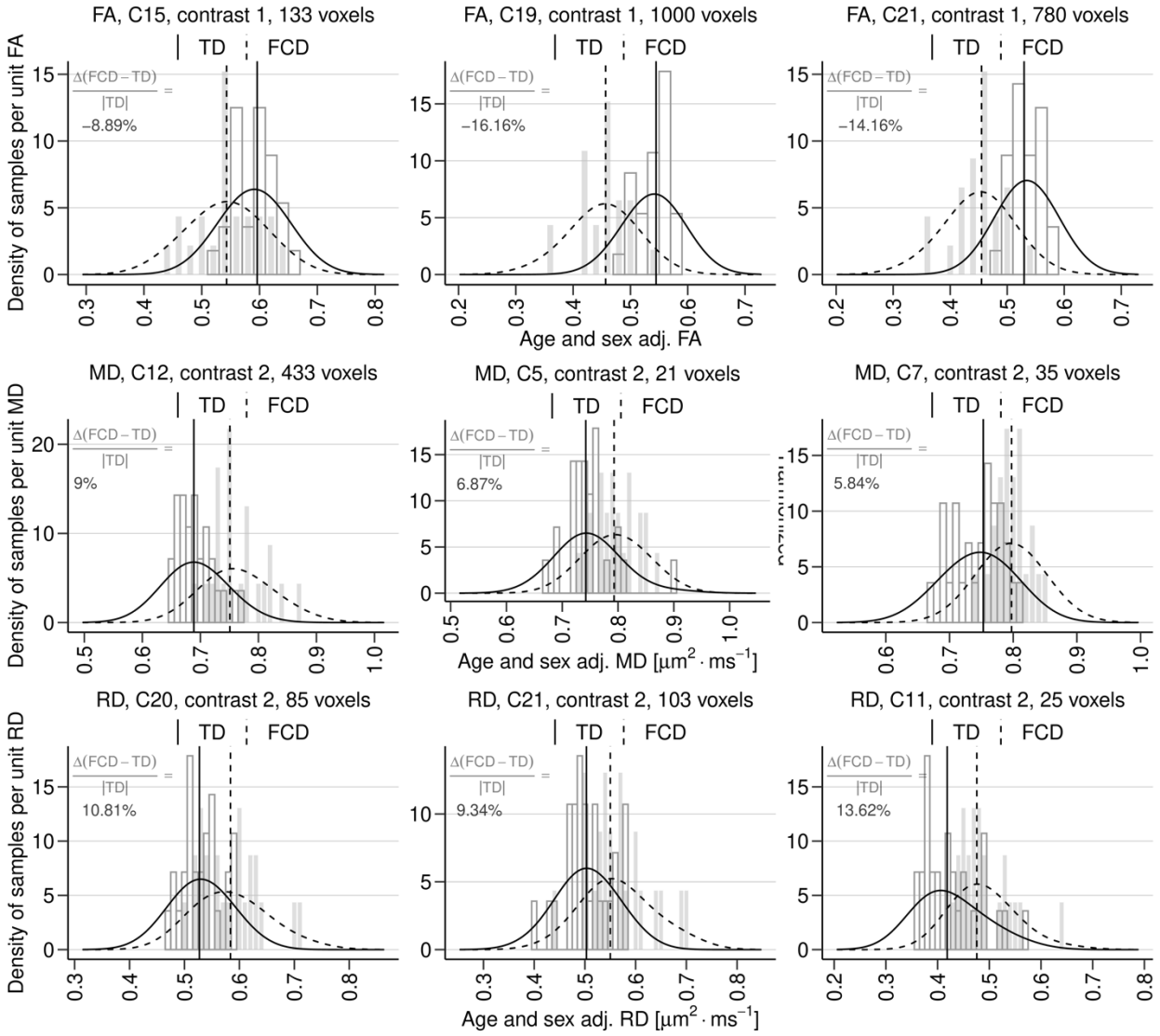

Figure 2. Graphical representation of differences in significant FA, MD, and RD Clusters between FCD and TD groups. The top 3 significant clusters with regions of the highest confidence of FA, MD, and RD are illustrated graphically in cluster-level histograms and density plots of the age and sex adjusted median. The significant FA clusters demonstrated a collective decrease among the 3 clusters in the FCD group when compared to the TD group. On the contrary, the significant MD and RD clusters both exhibited collective increase among the cluster age and sex adjusted measures. All 9 statistically significant clusters are shown for FCD and TD groups after data harmonization. Contrast 1 and 2 depict the directionality of the FCD median where contrast 1 exhibits a decrease in age and sex adjusted FA, MD, or RD and contrast 2 exhibits an increase in age and sex adjusted FA, MD, or RD.

Across statistically significant clusters of all harmonized FA, MD, and RD measures, there was a significant reduction in age and sex residualized anisotropy and a significant increase in diffusivity measures (**Figure 3**). The FA measure exhibited a decrease in median FA value from 0.53 in the TD group to 0.45 in the FCD group (15.1% reduction). The median MD value increased from 0.72 in the TD group to 0.76 in the FCD group (5.6% increase). Lastly, the median RD value increased from 0.50 to 0.57 (14% increase) between the FCD and TD groups respectively.

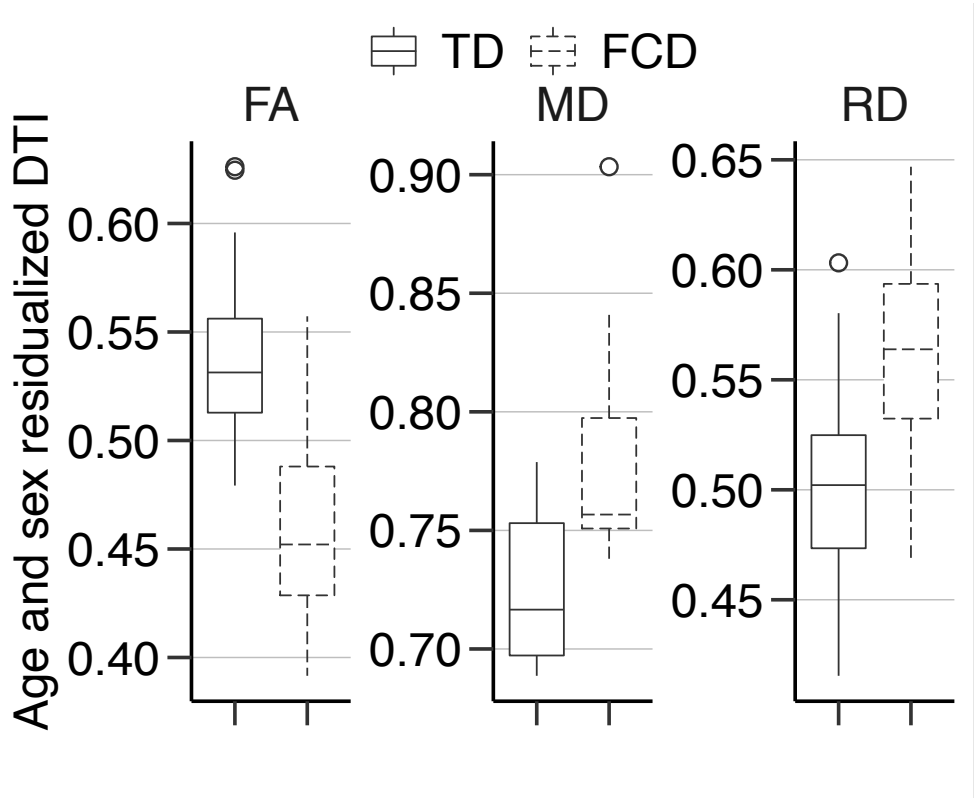

Figure 3. Summary of DTI Index Comparison between FCD and TD following Data Harmonization. FA, MD, and RD DTI measures were assessed between TD and FCD groups following data harmonization. A significant decrease in FA was noted on comparison of FCD to the TD group. A significant increase in MD and RD measures was observed in the FCD group compared to the TD group. MD and RD are in units of μm^2 □ ms^{-1}; FA does not have units.

Significant Cluster and Top White Matter Atlas Regions

In order to identify differences between the FCD and TD cohorts at the white matter tract level, the JHU White Matter Tractography Atlas via FSL was queried for the 48 clusters that were significantly different on FA, MD, and RD comparisons between the 2 groups. The atlas query provides a percent confidence, which is the average probability that a cluster belongs in a specific, labeled white matter tract within the atlas. **Supplementary Table 1** highlights the membership of DTI clusters for each metric in neuroanatomically labeled tracts according to the JHU White matter tractography atlas. The tracts are ranked by the average probability of membership.

Forceps minor, the left superior longitudinal fasciculus (SLF-L), and right SLF (SLF-R) white matter tracts showed the highest overlap with significant FA clusters with percentage confidence values of 64.1%, 43.5% and 40.4% respectively. The SLF-L, left inferior front-occipital fasciculus L (IFOF-L), and the left uncinate fasciculus (UF-L) were identified as the white matter tracts with the highest overlap with significant MD cluster with percentage confidence values of 62.2%, 52.3%, and 41.5% respectively. Lastly, the SLF-L, SLF-R, and IFOF-L white matter tracts were identified with the highest overlap with significant RD clusters with percentage confidence values of 71.3%, 46.6%, and 42% respectively. **Figure 4** illustrates the white matter tract regions, in anatomical space, with the highest confidence percentage for each DTI metric.

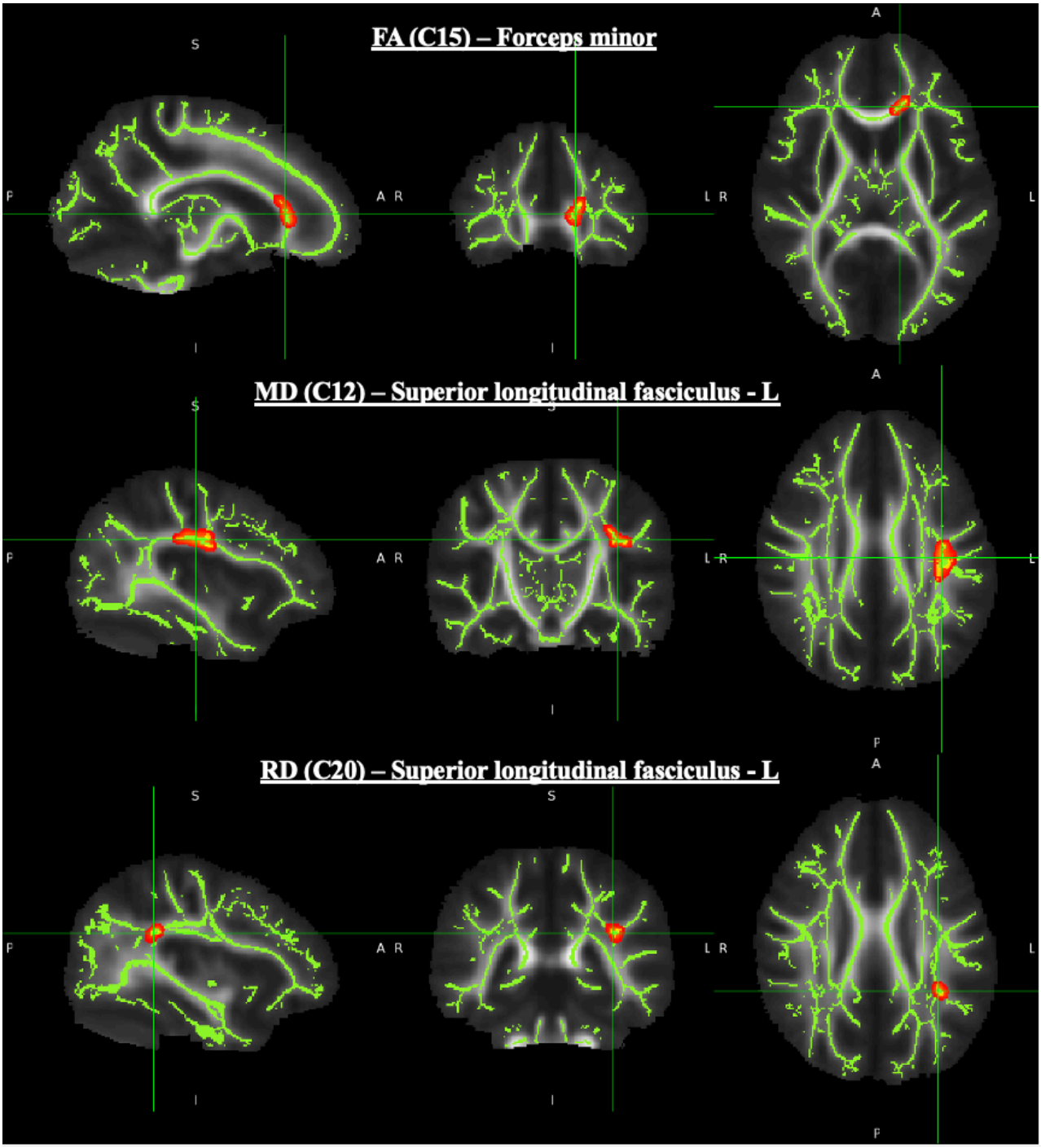

Figure 4. Spatial representation for membership of significant clusters within white matter tracts: Sagittal, coronal, and axial views of the cluster with the highest percent confidence for FA (C15, *top*), MD (C12, *middle*) and RD (C20, *bottom*) measures. See also Supplementary Table 1.

Significant Cluster and Top White Matter Atlas Regions

We tested the association between DTI metrics (FA, MD and RD) and neurocognitive scores (FRI, VCI, and VSI) using regression analyses, following data harmonization. **Figure 5** indicates the effect of data harmonization of DTI metrics to remove MRI parameter differences while preserving its association with neuropsychological indices. The harmonized and original findings for each DTI parameter are illustrated. Our results illustrate that following harmonization, the distributions and median DTI values for all NP indices, under each imaging protocol, are more aligned thus reducing the contribution of MRI protocol-based differences. **Figure 6** depicts plots of summary findings for correlation coefficients between neurocognitive indices and DTI metrics for both harmonized and original data. **Supplementary Table 2** details the quantitative values of these correlations.

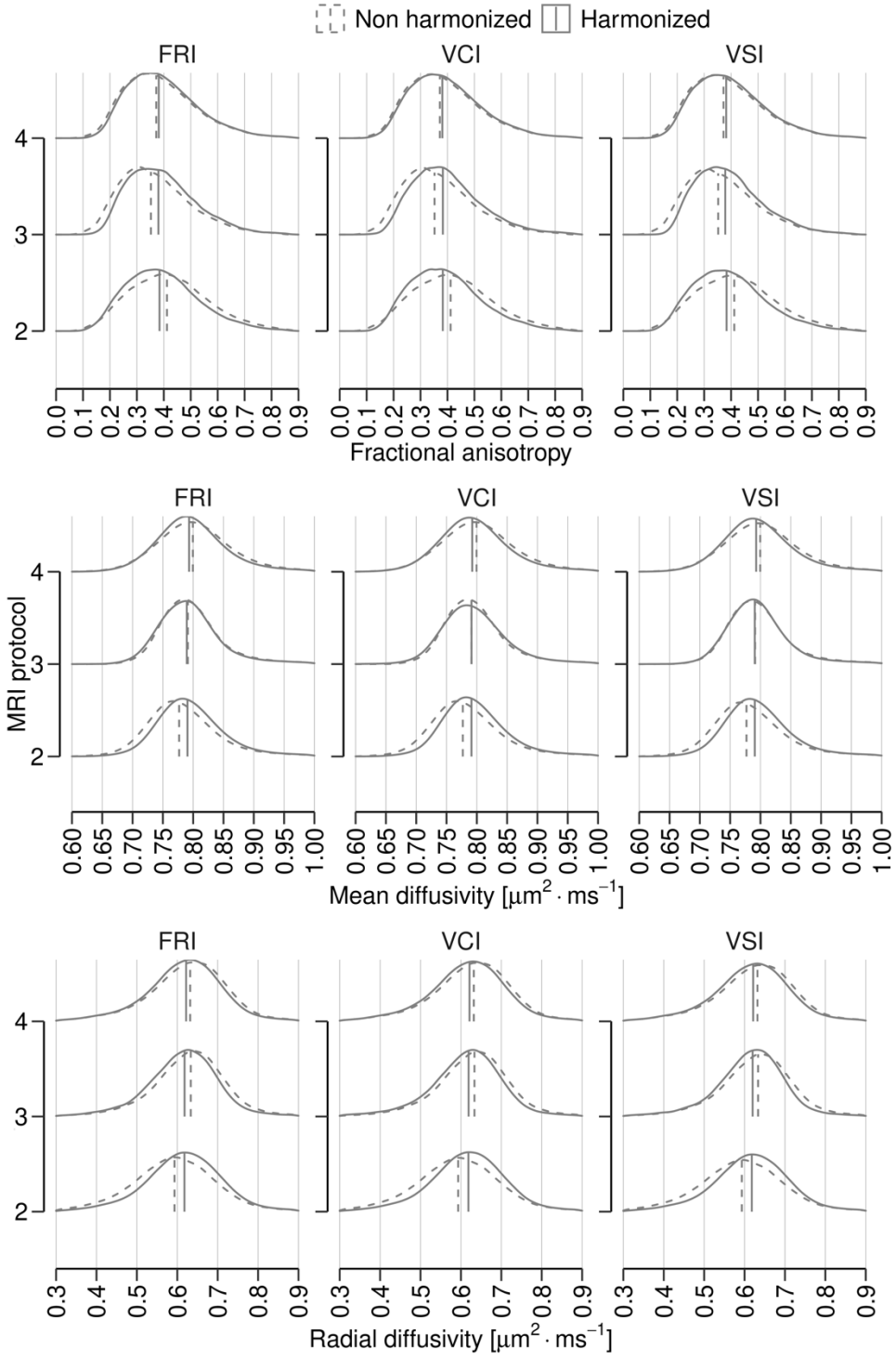

Figure 5. Harmonization of DTI metrics removes MRI protocol-based differences while preserving associations with NP measures. Illustration of the direct effect of data harmonization on preserving associations between FA, MD, and RD indices and neuropsychological measures. Following harmonization, the distributions and the median DTI values for each imaging protocol are more aligned, thus reducing the protocol-based differences between DTI measures.

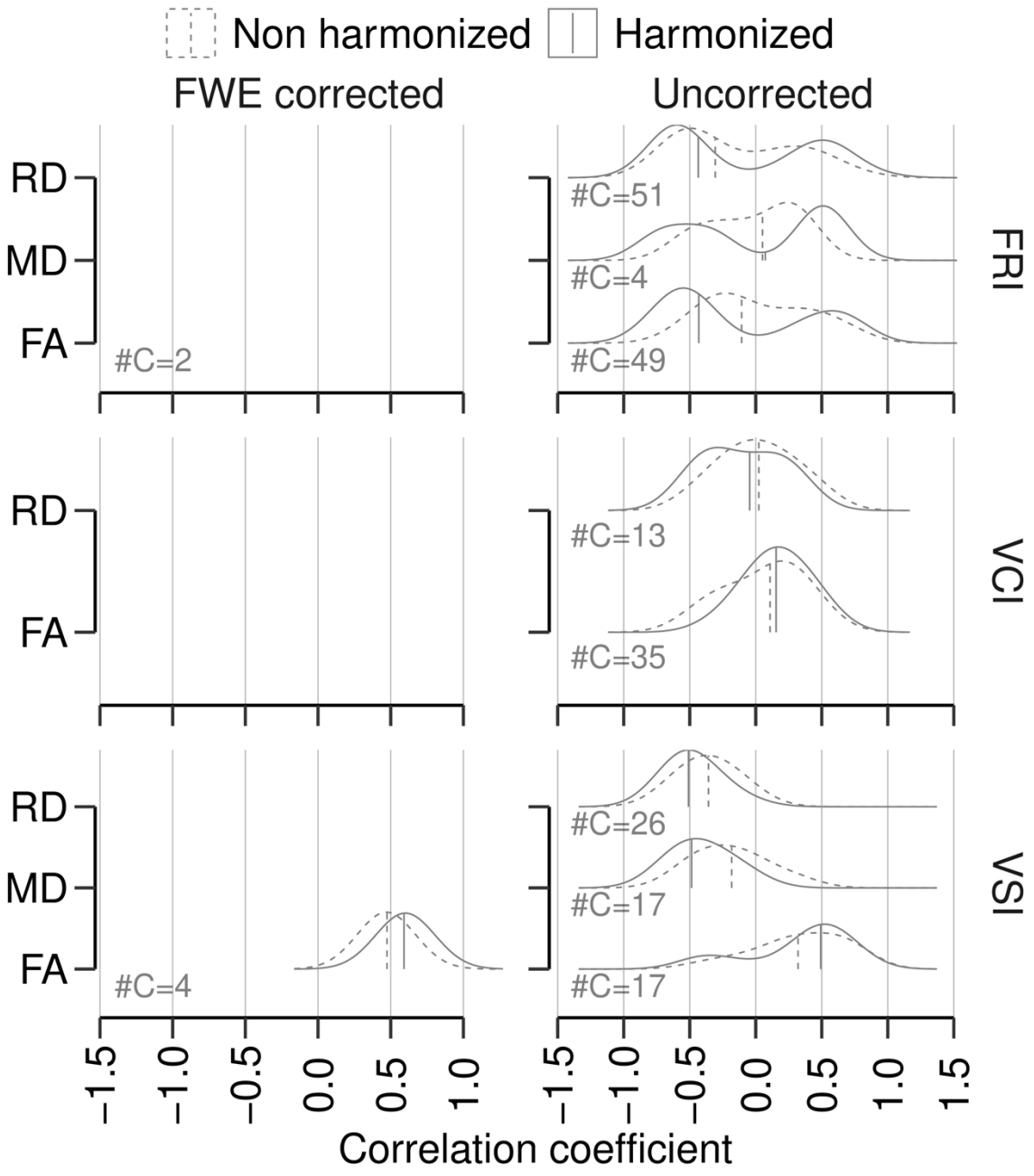

Figure 6. Correlations between pre and post data harmonization DTI indices with NP measures across significant clusters. Kernel density estimates (KDE) of the distributions of correlation coefficients between NP measures and DTI indices in clusters with $p \leq 0.05$ is displayed. The number of significant clusters and median values for each DTI index are depicted. Our analysis indicates that significant associations are evident in clusters with uncorrected p-values except for the association between FA and VSI, and FA and FRI. The KDE for FA and FRI for corrected p value is not shown because it has only two clusters. Representative associations can be viewed as linear models on the scatter plots in **Fig. 7**. The median values for each of the distribution are shown in Supplementary Table 2.

For FRI, there were 2 significant corrected FA cluster associations (harmonized median R-value of 0.67), 4 significant uncorrected MD cluster associations (harmonized median R-value of 0.07), and 51 significant uncorrected RD clusters (harmonized median R-value of -0.43). For VSI, there were 4 significant corrected FA cluster correlations (harmonized median R-value of 0.59), 17 significant uncorrected MD clusters (harmonized median R-value of -0.49), and 16 significant uncorrected RD clusters (harmonized median R-value of -0.51). Lastly, for VCI, there were 35 significant uncorrected FA cluster associations (harmonized median R-value of 0.15) and 15 significant RD clusters (harmonized median R-value of -0.05). The harmonized correlations yielded stronger associations compared to the non-harmonized in almost all correlations. **Figure 7** highlights the representative scatter plots of the top significant clusters of the associated white matter regions with the highest confidence for each DTI metric and cognitive index. The top JHU white matter tractography atlas regions of the significant DTI clusters and its association with FRI, VCI, and VSI are detailed in **Supplementary Table 3** along with their corresponding confidence percentage and their anatomical depictions are illustrated in **Figure 8**.

Overall, FA is positively correlated with all neurocognitive measures (FRI, VCI, VSI), while MD and RD are negatively correlated with the neurocognitive measures. Data harmonization strengthened the association of each DTI metric with each neurocognitive index in almost all cases. The only associations that survived statistical correction were FA-FRI and FA-VSI. Harmonization improved the correlation of FA-FRI from 0.50 to 0.67 after harmonization. Harmonization of FA-VSI strengthened the correlation coefficient value from 0.47 to 0.59.

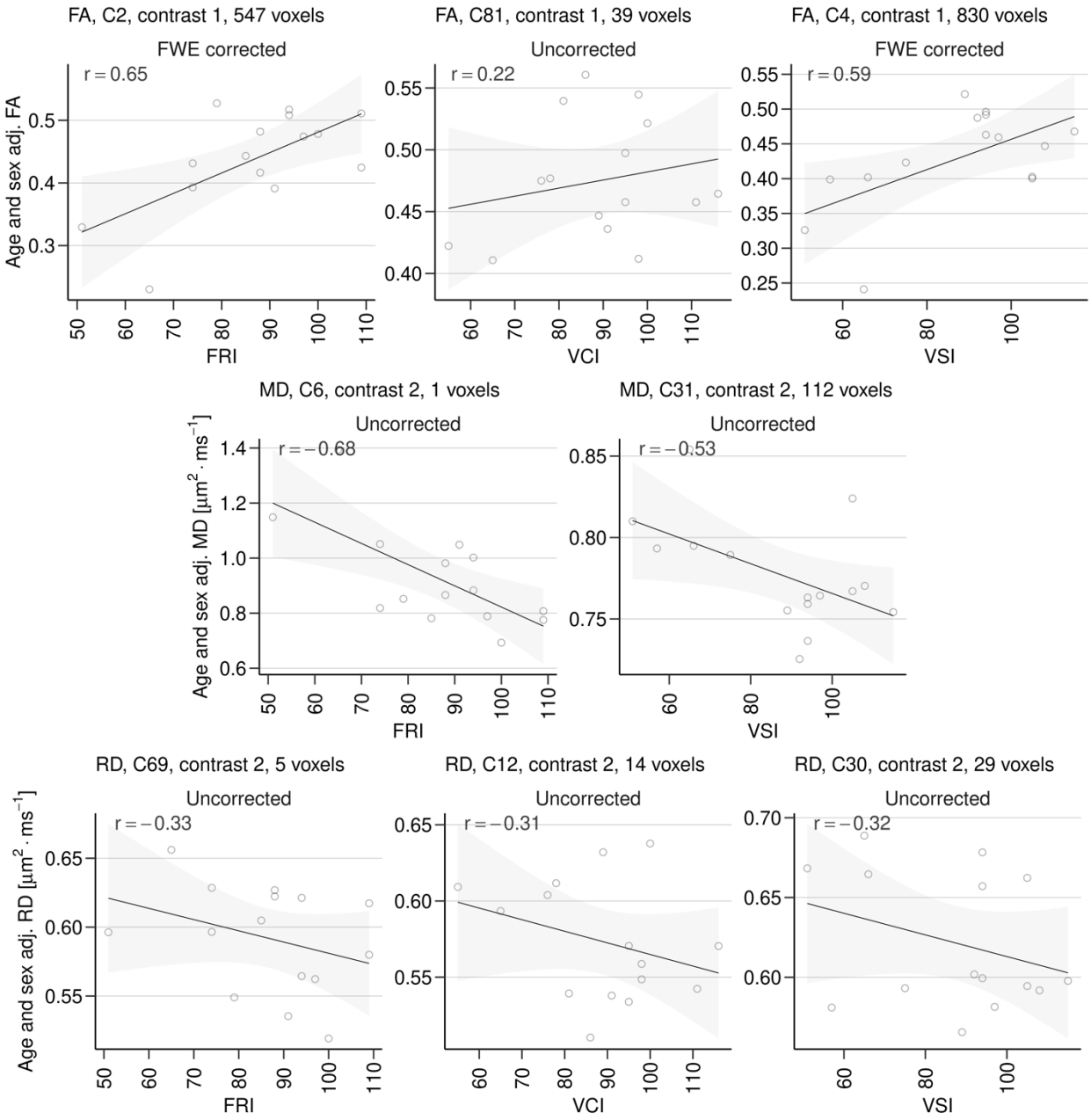

Figure 7. Correlations of FA, MD, and RD with Neuropsychological Indices FRI, VCI, and VSI in representative statistically significant representative clusters from TBSS. These correspond to the clusters shown in Supplementary table 3. Contrast 1 depicts a positive trend and contrast 2 depicts a negative trend.

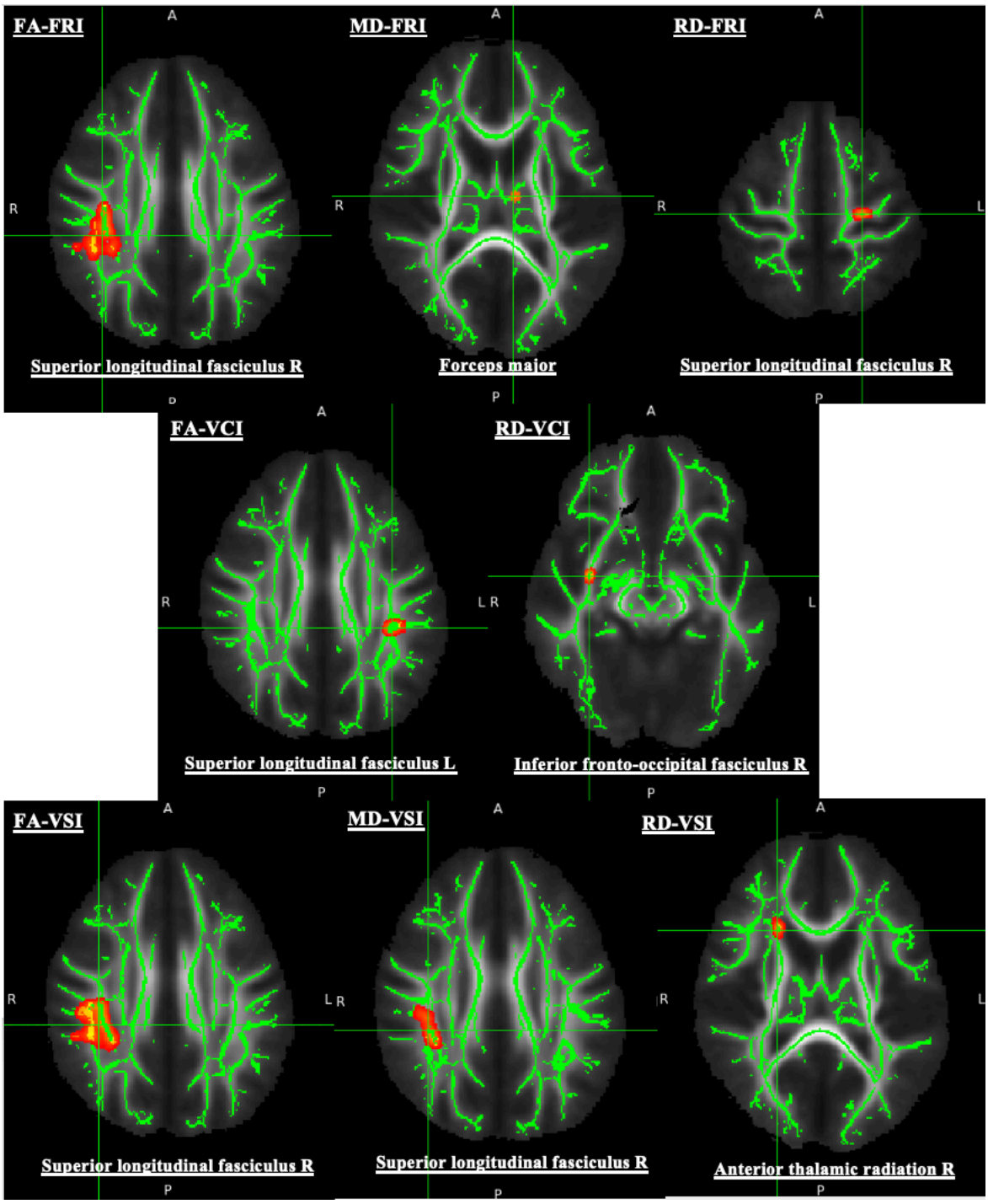

Figure 8. Top Correlated Regions of DTI Measures and Neurocognitive Factors: Anatomical axial depictions of top white matter regions found in significant clusters of DTI metrics correlated with FRI, VCI, and VSI.

Discussion

Our study goal was to improve our understanding of white matter tract changes associated with childhood onset epilepsy secondary to FCD and whether these changes are associated with neurocognitive dysfunction. We investigated white matter tract differences between patients with epilepsy secondary to FCD and typically developing (TD) healthy controls with respect to fractional anisotropy (FA), mean diffusivity (MD), and radial diffusivity (RD) indices, using rigorous preprocessing techniques. Within a cohort of FCD epilepsy subjects, our results indicate, for the first time, that application of data harmonization, eliminates confounding variations in DTI metrics due to different MRI scanning parameters, while highlighting intrinsic biological variabilities in white matter tracts. To our knowledge, data harmonization has not been applied towards analysis of white matter tractography changes in FCD and their association with FCD-related cognitive comorbidities.

The common step forward across research disciplines is the increasing demand for multi-site collaboration and NIH sanctioned sharing of datasets. Therefore, inter-scanner differences are a foreseeable and apparent obstacle in imaging studies. Data harmonization is a well-established and reliable method to address and eliminate these confounding methodological constraints to reveal true biological differences. Previous studies have evaluated the effectiveness of the Combined association test (ComBat) for data harmonization (84-86). In accordance with our results, Fortin et al. assessed the FA and MD DTI maps of 205 healthy participants and highlighted that ComBat preserved the biological variability and removed variations introduced by site and scanner differences (84). Zavaliangos-Petropulu et al. examined DTI metrics of 317 participants from the Alzheimer's Disease Neuroimaging Initiative and found that ComBat harmonization was effective in pooling data from 47 different scanning sites to detect consistent and robust associations (100). Additionally, Beer et al. found that ComBat harmonization provided better detection of longitudinal cortical thickness changes compared to non-harmonized data, illustrating the utility of the ComBat technique extends

beyond DTI studies (101). Our results demonstrate that data harmonization is an impactful analytical approach for analyzing heterogenous clinical datasets, through adjustment of parameter differences, thereby highlighting underling biological differences.

White Matter Structural Alterations

Our results demonstrate that despite the presence of a focal radiographic FCD lesion, systematic analysis of DTI reveals widespread microstructural alterations in white matter tracts. Across statistically significant clusters, FA decreased, while MD and RD increased. These findings may indicate underlying abnormalities in myelination of white matter tracts, degradation of myelin and axonal membranes within existing axons, or the reduced density of myelinated axons (58). Similar changes in DTI metrics have been demonstrated in previous studies (56, 102-107).

Consistent with earlier results, our analysis demonstrated that the most significant regional FA reductions, with the highest confidence, occurred within forceps minor and superior longitudinal fasciculus (58). Forceps minor has been implicated in executive function and superior longitudinal fasciculus has been demonstrated to be involved in language processing (108). Kim et al. illustrated lower FA values within the superior longitudinal fasciculus, and at the inferior fronto-occipital fasciculus and inferior longitudinal fasciculus respectively (109). Our study FA findings concur with these results. Moreover, our MD and RD results showed a significant increase within these tracts (**Figure 4)**.

Voxel by voxel comparison of DTI, using statistical parametric mapping has demonstrated regional changes in anisotropy and diffusivity in subjects with malformations of cortical development (MCD) (80). These changes were often evident beyond the focal MCD lesion identifiable on anatomical MR imaging. The likely reasons for reduced anisotropy include presence of heterotopic grey matter tissue at the grey-white matter interface, microdysgenesis and altered myelination within white matter tracts (80). On the other hand, changes in diffusivity are attributable to reduced cell density due to neuronal cell loss secondary to maldevelopment

due to secondary gliosis from ongoing disease. Lee et al. demonstrated significant FA reduction within fibers in ipsilateral hemispheres together with reduction in subcortical fibers (79). Reduced FA within subcortical white matter regions has also been demonstrated (79, 110) often adjacent to the FCD lesion (87). These studies, however, differ in their image acquisition protocols, MR scanner resolution (58, 80) and subject populations as well as disease heterogeneity (79, 87).

Few studies have explored FCD-associated white matter region correlations with increases in diffusivity MD and RD. However, DTI studies on TLE has well-documented evidence of significantly higher diffusivity in regions that are concordant with our study findings such as the uncinate fasciculus, the inferior fronto-occipital fasciculus, and the inferior longitudinal fasciculus (104).

White Matter Tract Changes Associated with Neurocognitive Dysfunction

Diffusion tensor imaging indices (FA, MD, RD) were more correlated with cognitive metrics of fluid reasoning (FRI) and visual spatial abilities (VS) than verbal comprehension (VCI), where the associations were minimal. We found MD to have moderately negative correlations with visuospatial indices. RD was also negatively correlated with fluid reasoning (FRI) and visual spatial ability (VSI). This directionality illustrates that decreased anisotropy and increased diffusivity are associated with lower cognitive scores. These results were expected and consistent with our hypothesis since increasing MD and RD (and decreasing FA) are indicative of decrement in structural integrity and white matter abnormalities. Our results further showed that FA was positively correlated with FRI and VSI.

Importantly, data harmonization improved the statistical sensitivity to almost all DTI-neuropsychological associations reflected in the increase in the magnitude of the correlation coefficients. Verbal comprehension yielded minimal associations with FA and RD. This is consistent with the fact that verbal comprehension is a receptive language function and is more likely to be affected with temporal localization of lesions. Within our study cohort, there was a

relatively low incidence (22%) of temporal localization for FCD lesions. The superior longitudinal fasciculus was the top JHU atlas region in all FA associations with neurocognitive indices, as well as MD with VSI, and RD with FRI. This finding, highlighting involvement of the SLF, is also consistent with the predominant frontal localization (65%) of FCD lesions within our cohort. Other top regions include forceps major (MD-FRI), inferior fronto-occipital fasciculus (RD-VCI), and anterior thalamic radiation (RD-VSI).

Currently, there is minimal literature exploring these specific neuropsychological factors in FCD and DTI specifically, though a previous study has reported impaired neuropsychological function in children with non-lesional localization-related epilepsy associated with white matter abnormalities (111). In addition, some specific regions we found correlated with lower FA and high MD and RD included regions that are important for memory processing, such as the uncinate fasciculus and the anterior thalamic radiation (102). Thus, investigations into executive function and memory in FCD will be beneficial to further correlate white matter tracts with abnormal DTI metrics.

Existing literature investigating the association of DTI metrics with neurocognitive indices is limited even in other neurocognitive disorders. Within a cohort of juvenile myoclonic epilepsy patients, a positive correlation was identified between structural connectivity indices and cognitive task performance (112). Madaan et al. reported a weak positive correlation between FA and VCI at the right uncinate fasciculus in children with mild traumatic brain injury (113). Suprano et al. utilized DTI to investigate the association between white matter microarchitecture and IQ scores in children and found that FA and axial diffusivity (AD) were significantly correlated with VCI in regions such as the forceps minor bundle of the corpus callosum and bilateral inferior fronto-occipital fasciculus (114).

Limitations

Our study cohort was limited to a modest sample size and precluded detailed analyses of specific subgroups based on lobar and hemispheric distribution of FCD lesions or verification

of FCD histological subtypes, based on histopathological analysis. These respective subgroups may have intrinsic biological network variations that can potentially impact interpretation of TBSS-based analysis of white matter differences between FCD subjects and healthy controls. The radiographic inclusion criteria of subjects with visible FCD lesions, did not take into account subjects with occult MR invisible FCD lesions. Our results demonstrate the presence of white matter structural alterations, but do not provide a causal etiology for the neurocognitive dysfunction that is evident in a significant proportion of FCD subjects. It is also unclear if the demonstrated changes are primarily related to cortical dysplasia or are secondary changes related to ongoing epilepsy or occur secondary to medication use. However, our current study demonstrated, that within a modest sample cohort, application of data harmonization effectively enabled correction for intra-site scanning parameter differences and allowed comparison of intrinsic biological differences between subjects with dysplasia and healthy controls.

Future studies utilizing whole brain connectome models, within larger cohorts, are planned to provide additional insights into network connectivity changes associated with cortical dysplasia and help elucidate the biological underpinnings of neuropsychological impairment, a major comorbidity of epilepsy (56, 88, 115).

Conclusions

Our results demonstrate the application of data harmonization on a heterogenous DTI imaging data set of subjects with epilepsy secondary to focal cortical dysplasia. Study results confirm the presence of widespread alterations in underlying white matter tracts in epilepsy that extend beyond the focal radiographic MR lesion. Data harmonization reduced the confounding effect induced by differences in MRI scanning parameters and highlighted underlying differences in white matter tracts between FCD subjects and normative healthy controls. Data harmonization also strengthened the association between DTI metrics and neurocognitive indices within the FCD cohort. Ongoing reproduction and validation of these structural

abnormalities in larger data sets will contribute towards a better understanding of the pathogenesis, prognosis and improved therapeutics for FCD related epilepsy.

Declaration of Interests

The authors declare that they have no known conflict of interests in terms of personal relationships or financial interests that have appeared to influence the research and work on this paper.

Acknowledgements

We are immensely grateful for the support from the Clinical and Translational Science Award (CTSA): Grant UL1TR002373, the AES Pre-doctoral Fellowship, the Medical Scientist Training Program Grant: T32 GM140935, UW Madison MSTP Radiology Fellowship, and the NIH grants R01NS

CHAPTER 3

Characterizing White Matter Connectome Abnormalities in Temporal Lobe Epilepsy Patients Using Threshold-Free Network-Based Statistics

Daniel Y. Chu[1,2], Nagesh Adluru[1,3], Veena A. Nair[1], Timothy Choi[1], Anusha Adluru[1], Camille Garcia-Ramos[2,4], Kevin Dabbs[2], Jedidiah Mathis[5], Andrew S. Nencka[6], Lisa Conant[5], Jeffrey R. Binder[5], Mary E. Meyerand[4], Andrew L. Alexander[3], Aaron F. Struck[2,7], Bruce Hermann[2], Vivek Prabhakaran[1,2,4,8]

[1]Department of Radiology, University of Wisconsin-Madison, 1111 Highland Avenue, Madison, WI 53705, United States

[2]Department of Neurology, University of Wisconsin-Madison, 1111 Highland Avenue, Madison, WI 53792, United States

[3]Waisman Center, University of Wisconsin-Madison, 1500 Highland Avenue, Madison, WI 53705, United States

[4]Department of Medical Physics, University of Wisconsin-Madison, 1111 Highland Avenue, Madison, WI 53705, United States

[5]Department of Neurology, Medical College of Wisconsin, 8701 Watertown Plank Rd, Milwaukee, WI 53226, United States

[6]*Department* of Radiology, Medical College of Wisconsin, 8701 Watertown Plank Rd, Milwaukee, WI 53226, United States

[7]William S Middleton Veterans Hospital, 2500 Overlook Terrace, Madison, WI 53705, United States

[8]Department of Psychiatry, University of Wisconsin-Madison, 6001 Research Park Boulevard, Madison, WI 53719, United States

Manuscript submitted and under review.

Abstract

Emerging evidence illustrates that temporal lobe epilepsy (TLE) involves network disruptions represented by hyper-excitability and other seizure-related neural plasticity. However, these associations are not well-characterized. Our study characterizes the whole brain white matter connectome abnormalities in TLE patients compared to healthy controls from the prospective Epilepsy Connectome Project (ECP) study. Furthermore, we assessed whether aberrant white-matter connections are differentially related to cognitive impairment and a history of focal-to-bilateral tonic-clonic (FBTC) seizures. Multi-shell connectome MRI data were pre-processed using the DESIGNER guidelines. The IIT Destrieux gray matter atlas was used to derive the 162x162 structural connectivity matrices (SCMs) using MRTrix3. ComBat data harmonization was applied to harmonize the SCMs from pre and post scanner upgrade acquisitions. Threshold-free network-based statistics (TFNBS) was used for statistical analysis of the harmonized SCMs. Cognitive impairment status and FBTC seizure status were then correlated with these findings. We employed connectome measurements from 142 subjects, including 92 patients with TLE (36 males, mean age = 40.1 ± 11.7 years) and 50 healthy controls (25 males, mean age = 32.6 ± 10.2 years). Our analysis revealed overall significant decreases in cross-sectional area (CSA) of the white matter tract in TLE group compared to controls, indicating decreased white matter tract integrity and connectivity abnormalities in addition to apparent differences in graph theoretic measures of connectivity and network-based statistics. Focal and generalized cognitive impaired TLE patients showcased higher trend-level abnormalities in the white matter connectome via decreased CSA than those with no cognitive impairment. Patients with a positive FBTC seizure history also showed trend-level findings of association via decreased CSA. Widespread global aberrant white matter connectome changes were observed in TLE patients and further characterization of these changes may ultimately identify novel biomarkers and elucidate TLE's impact on brain plasticity.

Introduction

Epilepsy is the 4th most common neurological disorder, with a prevalence of over 3.4 million in the USA and more than 46 million worldwide (1, 2). In adults, Temporal lobe epilepsy (TLE) is the most common form of focal epilepsy (13). Although some TLE patients undergo long-term remission, lifelong chronic TLE is debilitating and heavily associated with several cognitive, somatic, and psychiatric co-morbidities (16). Predicting which patients will respond favorably to surgery or anti-seizure medication is imperative for the optimization of treatment and planning; however, current methods for these predictions are inadequate. Currently, there are no reliable biomarkers for accurate assessment of treatment efficacy, disease progression, or the severity of neurological and psychiatric consequences in TLE patients. Previous literature with modest sample sizes reported variable results for MRI biomarkers, which expose a fundamental lack of understanding in the pathophysiological processes underlying epilepsy progression and remission (34-37).

Emerging evidence have demonstrated that TLE involves a series of networks that is characterized by pathologies such as hyper-excitability and other seizure-related neural plasticity (29-32). Recent DTI studies have reported widespread microstructural abnormalities in subcortical white matter and was primarily related to reduced neurite density in TLE patients (40), as well as microstructural abnormalities in the corpus callosum, cingulum, and external capsule (116). Other studies explored the interplay of focal seizure areas, such as the hippocampus, with its connectome-level effects using diffusion MRI connectomics, revealing significant remodeling of connectome topology and structurally governed functional dynamics in TLE (41). In contrast to DTI studies, DWI connectome studies map the entirety of white matter connections across the whole brain, providing a comprehensive overview of how different brain regions are structurally connected. Few studies have characterized the whole brain white matter connectome abnormalities in TLE patients compared to controls in a large-scale patient population.

The Epilepsy Connectome Project (ECP) is a large-scale dataset collection project of connectivity measurements of patients with sporadic TLE (43, 44, 47). In this present study, we utilized the ECP multi-shell connectome diffusion weighted MRI (ms-dMRI) data for the evaluation of structural connections and dynamic network interactions using graph theoretical descriptive analysis of topology to characterize the white matter connectome in TLE patients. Furthermore, we correlated the findings to cognitive impairment status and focal-to-bilateral tonic-clonic (FBTC) seizure history (previously known as generalized tonic-clonic seizures) in TLE patients. We hypothesize that TLE patients will reveal discrete white matter connectivity abnormalities in addition to apparent differences in graph theoretic measures of connectivity and network-based statistics compared to HCs. Ultimately, this study will identify novel MRI structural biomarkers and further substantiate the concept that TLE is a progressive network disorder, involving ongoing neural plasticity induced by seizure activity.

Methods

Participants

Participants are from the ECP, a multisite collaborative research project between the University of Wisconsin Madison and the Medical College of Wisconsin (MCW) conducted between 2016 and 2018. This prospective study was approved by the institutional review board (IRB) at the MCW, and all participants provided written informed consent.

The inclusion criteria for TLE patients required two of the following: 1) clinical semiology consistent with seizures of temporal lobe origin, 2) previous MRI consistent with mesial temporal sclerosis (MTS) or hippocampal atrophy, 3) EEG revealing temporal intermittent rhythmic delta or epileptiform activity over the temporal lobe(s), and 4) EEG monitoring video evidence of temporal lobe onset seizure. Diagnosis of TLE was overseen by epileptologists and potential cases were reviewed by the clinicians scrutinizing the previously mentioned clinical evidence

(structural brain MRI, interictal EEG, clinical semiology, and ictal-EEG monitoring for those who were admitted to epilepsy monitoring units), all available past and current medical records surrounding seizure care, management, and diagnosis. Contentious diagnoses were reviewed and discussed by all epileptologists of the study to reach a consensus. Patients were excluded if they had lesions other than MTS, active infectious, autoimmune, or inflammatory seizure etiology. Controls were healthy adults and exclusion criteria included history of learning disability, substance abuse, brain injury, psychiatric illnesses, and current vasoactive medication use. All participants had no MRI contraindications.

The majority of studies utilizing the ECP participants have investigated the resting-state functional connectivity and cortical surface morphometry, and only one study explored the DWI by utilizing machine learning tools to determine intrinsic TLE structural connectome phenotypes (43, 44, 47).

Data Acquisition

MRI images were acquired on a 3T GE MR750 scanners (General Electric, Waukesha, WI) using a Nova 32-channel head coil. T1-weighted structural images were acquired using a 3D gradient-echo pulse (MPRAGE) sequence (repetition time (TR) = 604 ms, echo time (TE) = 2.516 ms, inversion time = 1060 ms, flip angle = 8°, field of view (FOV) = 25.6 cm, 0.8 mm isotropic). T2-weighted structural images were acquired using a 3D fast spin-echo (CUBE) sequence (TR = 2500 ms, TE = 94.398 ms, flip angle = 90°, FOV = 25.6 cm, 0.8 mm isotropic). Diffusion weighted MRI (dMRI) data were acquired using the high-angular resolution diffusion imaging (HARDI) approach (117). The ECP dMRI acquisition uses multiband EPI (118) with slide acceleration factor 3 that includes a total of 4 runs, with 2 runs with 75-directions each, and opposite phase encoding polarity (AP and PA), and 2 runs with 76 directions each. The DWI images had the additional acquisition parameters: alternating b = 1000 s/mm^2 and b = 2000 s/mm^2, and 9 b = 0 volumes.

Data Processing and Statistical Analyses

Modern tools from the emerging field of network neuroscience were used for detailed network analysis of the structural connectivity pathways for better understanding of the plasticity changes in patients with TLE. Network neuroscience methods were able to quantify the organization of structural connections as edges, providing insights into network communication efficiency patterns (119, 120). In addition, we used robust statistical techniques such as threshold free network-based statistics (TFNBS) for predictive modeling (70). **Figure 1** provides an overview of the connectography reconstruction from connectome quality multi-shell DWI data. Preprocessing of the data followed DESIGNER guidelines, which included the removal or mitigation of artifacts such as noise, Gibb's ringing, distortion due to eddy currents, B_1-bias and EPI warping due to field inhomogeneities. The curated DWI data was deconvolved using constrained optimization with the shell and major tissue specific response functions to estimate fiber orientation distributions (FOD) at each voxel in the brain. Anatomical cortico-subcortical gray matter atlas regions identified using FreeSurfer reconstruction and parcellation of the gray matter are used to define the nodes in the neuronal networks. Underlying white matter fiber bundles connecting pairs of these nodes were used to define the edges. These networks can be represented using symmetric matrices, which encode the adjacency or connectedness of the nodes. The tractography was performed using tckgen command in MRtrix3. Fifteen million streamlines were generated by dynamic seeding in the whole brain using the FODs and a probabilistic algorithm (iFOD2) which performs second order integration over FODs. The step size was set to the default value of ½ the voxel size. The tract stopping criteria were also set to the defaults of 45° angular threshold for curving, minimum length of twice the voxel size, maximum length of 100 times the voxel size. The FOD amplitude cut off was set to 0.05. tcksift2 algorithm from MRtrix3 was used to filter the streamlines and compute the weights for each of the streamline that are used in computing the final edge weights in the networks. Fiber density estimates were heuristically shrunk based on the presence of gray matter using the fd_scale_gm option for

tcksift2. SIFT proportionality constant μ was also saved which is used to scale the network adjacency matrices. These networks can be represented using symmetric matrices, which encode the adjacency or connectedness of the nodes.

Parametric data harmonization using neuroComBat (121) of the connectivity matrices was employed to account for the DV25 to DV26 change, a major software of the GE MR scanner. This included a change from sagittal to axial acquisition. Harmonization addressed the batch/protocol effects by accounting for additive (on the bias) and multiplicative (on the variance) effects of the scanner software and slice direction in acquisition on connectivity outcomes using a linear model by preserving group, age, and sex effects. These correction effects are the expected values of the empirically estimated Bayesian prior distributions either parametrically via Expectation Maximization or non-parametrically via importance sampling. Such a prior based approach is robust when there are small sample sizes per each protocol. **Supplementary Figure 1** illustrates the effects of harmonization on the adjacency matrices (edge weights) before permutation testing.

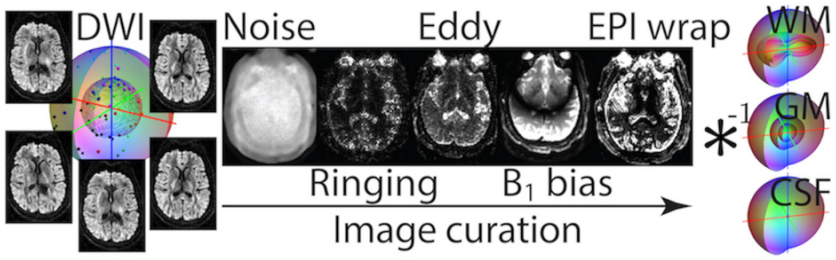

(a) Multi-shell connectome acquisition.

(b) DESIGNER guidelines.

(c) Spherical deconvolution.

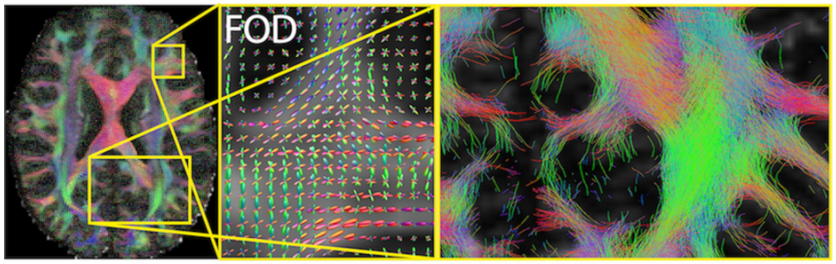

(d) Voxelwise fiber orientation distributions (FOD).

(e) Whole brain tractography.

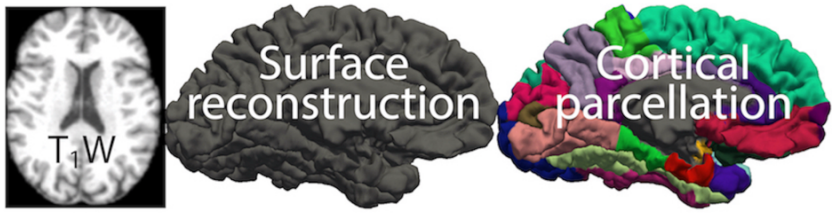

(f) FreeSurfer based cortico-subcortical parcellations from T1w images.

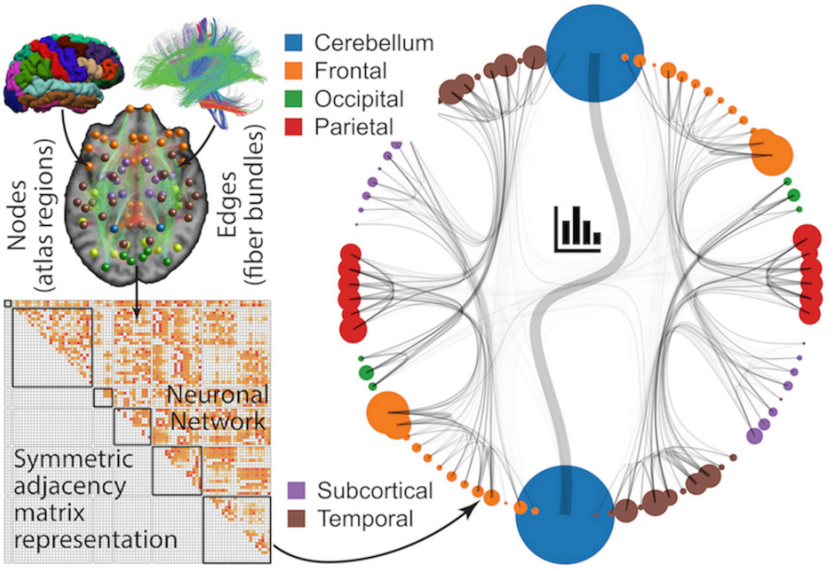

(g) Cortico-subcortical parcellations and whole brain tractography are used to estimate neuronal networks which are represented using adjacency matrices and can be visualized as chord diagrams.

Figure 1. Overview of the connectography reconstruction from connectome quality multi-shell DWI data. a-c) Preprocessing of the multi-shell data followed DESIGNER guidelines (92) which included the removal or mitigation of artifacts such as noise, Gibb's ringing, distortion due to eddy currents, B_1-bias and EPI wrapping due to field inhomogeneities using tools in FSL (90), ANTs (122), and MRTrix3 (89). **d-e)** The curated DWI data was deconvolved using constrained optimization with the shell and major tissue specific response functions to estimate fiber orientation distributions (FOD) at each voxel in the brain. **f)** Anatomical cortico-subcortical gray matter atlas regions identified using FreeSurfer reconstruction and parcellation of the gray matter used to define the nodes in the neuronal networks. **g)** Underlying white matter fiber bundles connecting pairs of these nodes were used to define the edges. These networks can be represented using symmetric matrices, which encode the adjacency or connectedness of the nodes.

The resulting connectographs were fed into the TFNBS that are described in **Figure 2.** General linear modeling (GLM) generated statistic graphs from connectographs, which were thresholded to cluster the nodes (70). The product of the size and maximum of the clusters were summed across the thresholds to obtain threshold-free cluster enhanced statistic graphs. Permutation testing with 5000 permutations was used to obtain null distributions for each connection or the maximum across the connections. Comparing each connection in the unthresholded statistic graph with 1) max-null or 2) connection specific null results in family-wise error corrected or uncorrected p-value graphs respectively. Statistically significant results at $p \leq 0.05$ were reported. Age and sex were used as nuisance variables in the GLM. Results were then correlated with cognitive impairment status and patient history of FBTC seizures.

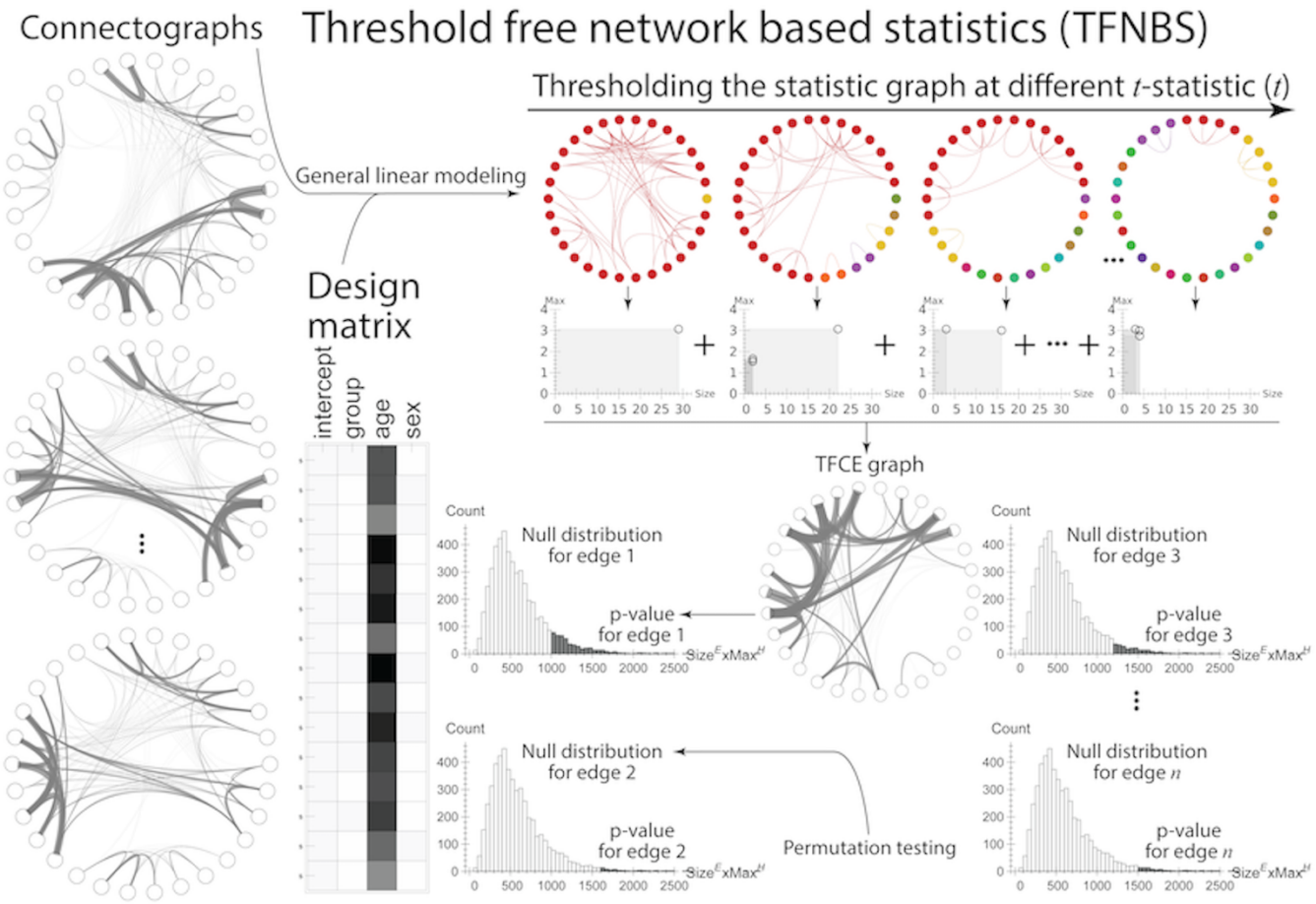

Figure 2. Overview of threshold-free network-based statistics (TFNBS). General linear modeling is used to get statistic graphs from connectographs. The statistic graphs are thresholded at different thresholds to cluster the nodes. The product of size and max of the clusters are summed across the thresholds to obtain threshold-free cluster enhanced statistic graph. The null distribution can be obtained for each connection or maximum across the connections using permutation testing. Comparing each connection in the unthresholded statistic graph with (1) max-null or (2) connection specific null, results in family wise error corrected or uncorrected p-value graphs respectively.

Results

Demographics of Study Participants

Multi-shell DWI connectome data were collected from 142 participants including 92 TLE patients (36 males, mean age = 40.1 ± 11.7 years) and 50 HCs (25 males, mean age = 32.6 ± 10.2 years) ranging from ages 18 to 60. The participant sociodemographic and clinical characteristics is shown in **Table 1**. The average years of education of the TLE patient group

and HC group is 14.6 ± 2.8 years and 16.1 ± 2.7 years respectively. The full-scale intelligence quotient (FSIQ) average score for the TLE group is 101.7 ± 13.8 and 113.4 ± 15.1 for HCs. In the TLE group, 62 patients have a positive FBTC seizure history, 21 patients have never experienced a FBTC seizure, and the remaining patients had an unknown FBTC history. Notable clinical characteristics of the TLE patients include 12.2 ± 20.3 mean lifetime FBTC seizures, mean age of seizure onset of 22.4 ± 14.2, mean disease duration of 18.0 ± 14.0, mean seizure frequency of 5.8 ± 10.6 per month, and mean number of anti-seizure medications of 1.77 ± 0.97. The seizure lateralization and diagnosis of TLE was determined by board-certified neurologists, in accordance with criteria defined by the International League Against Epilepsy, based on a matrix of interictal scalp electroencephalography (EEG) or intracranial video-EEG telemetry, seizure semiology, and neuroimaging evaluation. Forty-eight TLE patients have left lateralized seizures, 22 with right seizure lateralization, 10 bilateral, and 12 are unknown. In terms of cognitive impairment, 9 TLE patients (12%) had generalized cognitive impairment, 25 patients (33.3%) had focal cognitive impairment, and 41 patients (54.7%) had no cognitive impairment. The remaining patients had unknown cognitive impairment statuses. From the list of eligible ECP participants, 32 participants were excluded due to missing DWI data, poor quality control data, missing participant variables, or low number of links on harmonization matrices.

	TLE Patients (n=92)	Controls (HCs) (n=50)
Age (mean ± SD) *	40.1 ± 11.7	32.6 ± 10.2
Sex (M/F)	36/56	25/25
Education (mean ± SD) *	14.6 ± 2.8	16.1 ± 2.7
FSIQ (mean ± SD) *	101.7± 13.8	113.4 ± 15.1
FBTC (+/-)	62/21	N/A
Number of lifetime FBTC (mean ± SD)	12.2 ± 20.3	N/A
Age of Seizure Onset (mean ± SD)	22.4 ± 14.2	N/A
Disease Duration (mean ± SD)	18.0 ± 14.0	N/A
Seizure Frequency Per Month (mean ± SD)	5.8 ± 10.6	N/A
# of ASMs	1.77 ± 0.97	N/A
Seizure Lateralization (L/R/B/U)	45/19/10/18	N/A
Generalized cognitive impairment (n;%)	9; 12%	47
Focal cognitive impairment (n;%)	25; 33.3%	47
No cognitive imparment (n;%)	41; 54.7%	47

Table 1. Participant demographicsof

Note. –TLE = temporal lobe epilepsy. HC = healthy controls. SD = standard deviation. FSIQ = full-scale intelligence quotient. FBTC = generalized tonic-clonic. ASMs = anti-seizure medications. L = left; R = right; B = bilateral; U = unknown. *Significantly different between TLE and HCs ($p<0.05$).

Group Differences Between TLE vs. HC

The overall reconstructed connectography matrix of corrected, uncorrected, and the directionalities of the white matter tract cross-sectional areas (CSA) were generated in a symmetric adjacency network matrix. The IIT Destrieux gray matter atlas was used to drive the structural connectivity matrices of 162 x 162 nodes or edges originating from and organized into five regions of the brain: frontal, occipital, parietal, temporal lobes, and subcortical. The summary findings of both uncorrected and corrected number of significant connections or tracts ($p \leq 0.05$) between the HC and TLE group is depicted in **Figure 3**. The dominant directionality is revealed as decreased CSA in TLE patients when compared to that of healthy controls in both corrected and uncorrected results. Specifically after correction, TLE CSA is globally decreased across all brain regions when compared to HC CSA, inferring a general impact of TLE on the

DWI connectome via a reduction in white matter tract CSA. The top significant connections of decreased CSA in TLE patients have nodes between frontal-to-frontal tracts, frontal-to-parietal tracts, and frontal-to-temporal tracts.

A panel of 16 representative significant tract connections after multiple comparisons correction between TLE patients and HCs in the dominant directionality (decreased CSA) are more closely examined in **Figure 4**. The box plots in this figure describes these age and sex adjusted CSA differences between groups with the specific edges of these tracts displayed at the top of each graph. Our results showcase consistent significant reductions in TLE CSA across these 16 significant tracts when compared to HC CSA, indicating that these 16 connections may have been impacted by TLE via a decrease in white matter CSA.

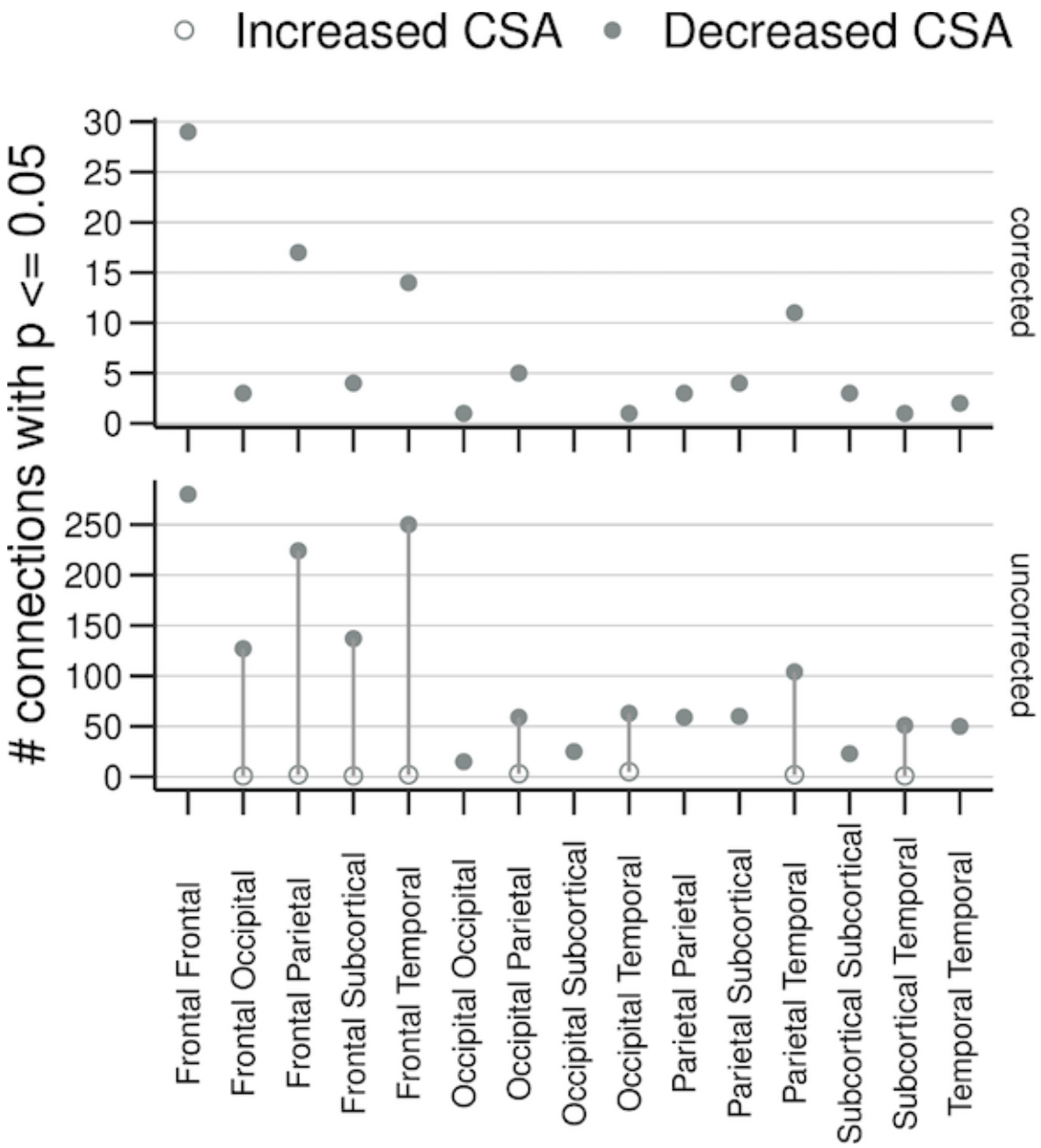

Figure 3. Summary Findings of TLE vs HC white matter connectome abnormalities. The white matter tracts are depicted by cross-sectional areas (CSA) in both directionalities. Overall, our results demonstrate that when comparing TLE vs HC DWI connectomes measures, decreased CSA is observed across the whole-brain in TLE patients, with the highest number of abnormal significant connections in the frontal-to-frontal region, the frontal-to-parietal region, and the frontal-to-temporal region. TLE = temporal lobe epilepsy; HC = healthy control; DWI = diffusion weighted imaging; CSA = cross-sectional area of the white matter.

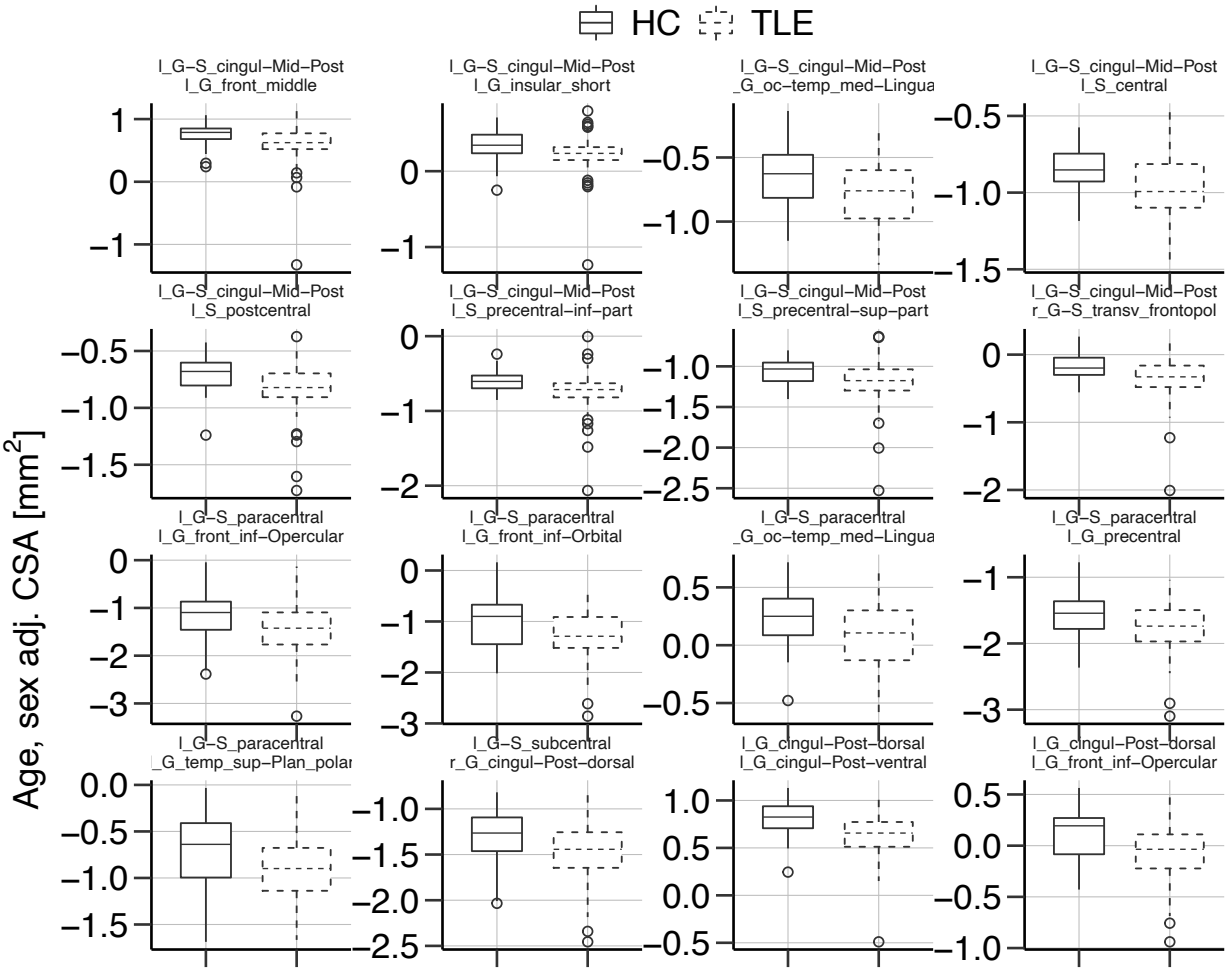

Figure 4. Representative TLE vs. HC White Matter Connectome Tract Cross Sectional Areas. Illustrated here are 16 representative analyses after multiple comparisons correction of TLE vs. HC DWI connectome abnormalities. The results indicate that TLE patients exhibit lower white matter tract age and sex adjusted expected CSA when compared to HCs. The originating nodes and region locations are noted above each box plot. TLE = temporal lobe epilepsy; HC = healthy control; DWI = diffusion weighted imaging; CSA = cross-sectional area of the white matter.

FBTC vs. non-FBTC in TLE Patients

Next, we assessed the effect of FBTC seizures on CSA of the white matter connectome in TLE patients. The summary findings of the uncorrected and corrected number of significant tracts ($p \leq 0.05$) between the TLE patients who had a FBTC seizure vs. TLE patients who have a negative FBTC seizure history are depicted in **Figure 5**. Our results indicate no survival after

significance after multiple comparisons correction; however, in the uncorrected results, the dominant contrast with the higher number of connections favors the direction where the FBTC group of TLE patients exhibited decreased CSA when compared to the non-FBTC group. These results demonstrate modest and trend-level findings of decreased CSA in the FBTC group of TLE patients compared to those who have never had a FBTC seizure. A much larger sample size will be needed to further elucidate whether FBTC seizures have a true impact on white matter connectome status and white matter tract integrity.

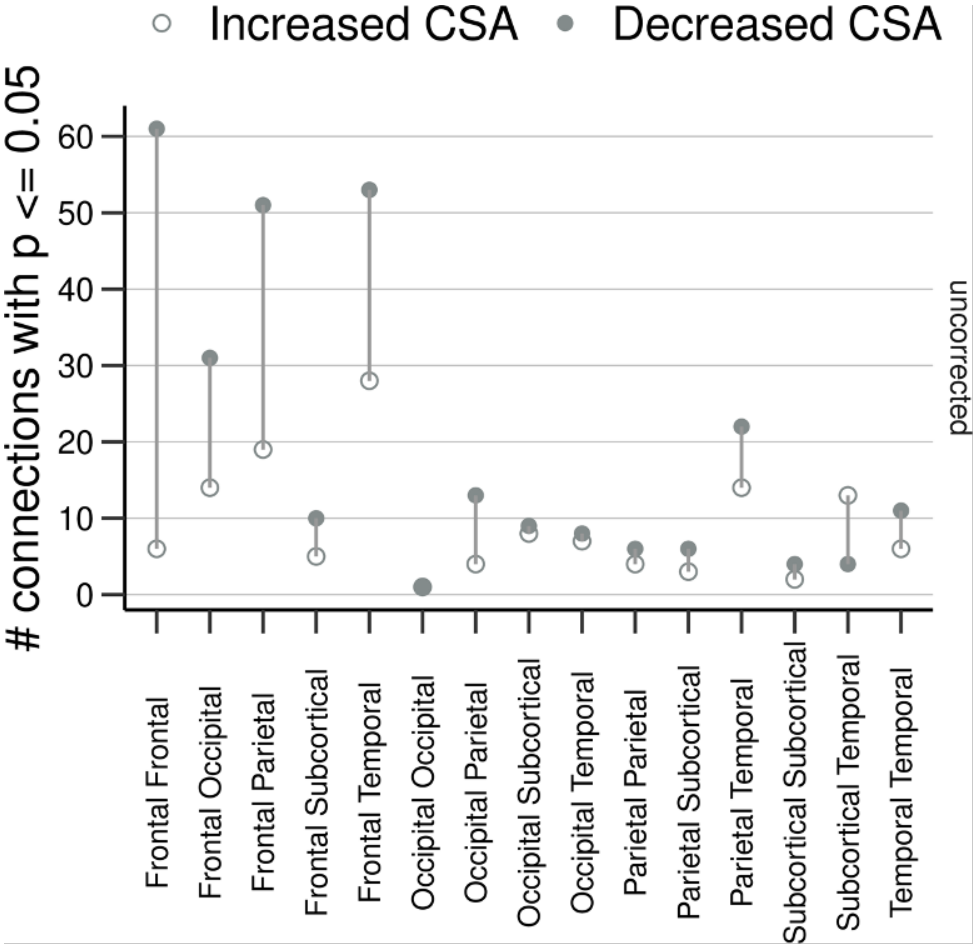

Figure 5. Summary Findings of FBTC vs. non-FBTC TLE Patients. Our results demonstrate that when comparing the DWI connectome of TLE patients with a positive history of FBTC seizures vs. those who never had a FBTC seizure, global decreased white matter tract CSA is observed in only the uncorrected analysis. Therefore, the differences appear to be modest and trend-level and will likely require a bigger sample size to confirm whether a positive FBTC seizure history has an impact in DWI connectome abnormalities. FBTC = generalized tonic-clonic; TLE = temporal lobe epilepsy; HC = healthy control; DWI = diffusion weighted imaging; CSA = cross-sectional area of the white matter.

Cognitive and Neuropsychological Considerations

Subject cognitive profiles and selected neuropsychological test scores were analyzed to correlate clinical variable signatures with DTI connectome data. Cognitive profiles were divided into three clusters of focal cognitive impairment, generalized cognitive impairment, and no cognitive impairment based on a previous study (123).

Our summary results of the uncorrected correlations of cognitive impairment and neuropsychological scores with the white matter connectome findings are illustrated in **Figure 6**. The focal cognitive impairment status and generalized cognitive impairment TLE patients yielded similar results exhibiting modest and trend-level findings of greater than 100 connections, all of which exhibited decreased CSA when compared to HCs. The highest number of white-matter tract correlations are similarly found in the frontal-frontal, frontal-temporal, and frontal-parietal regions. In TLE patients with no cognitive impairment, a smaller number of connections were revealed for decreased CSA when compared to HCs. In general, while all three cognitive statuses yielded decreased CSA in the TLE group compared to HCs, the cognitively impaired TLE groups demonstrated a modest trend where a higher number of significant tracts differences in the decreased CSA directionality compared to those who are not cognitively impaired, inferring that cognitive impairment may undermine the TLE white matter connectome structure and integrity. These clusters are further detailed in **Supplementary Figures 2**, **3**, and **4** showing representative TLE with focal, generalized, and no cognitive impairment vs. HC respectively.

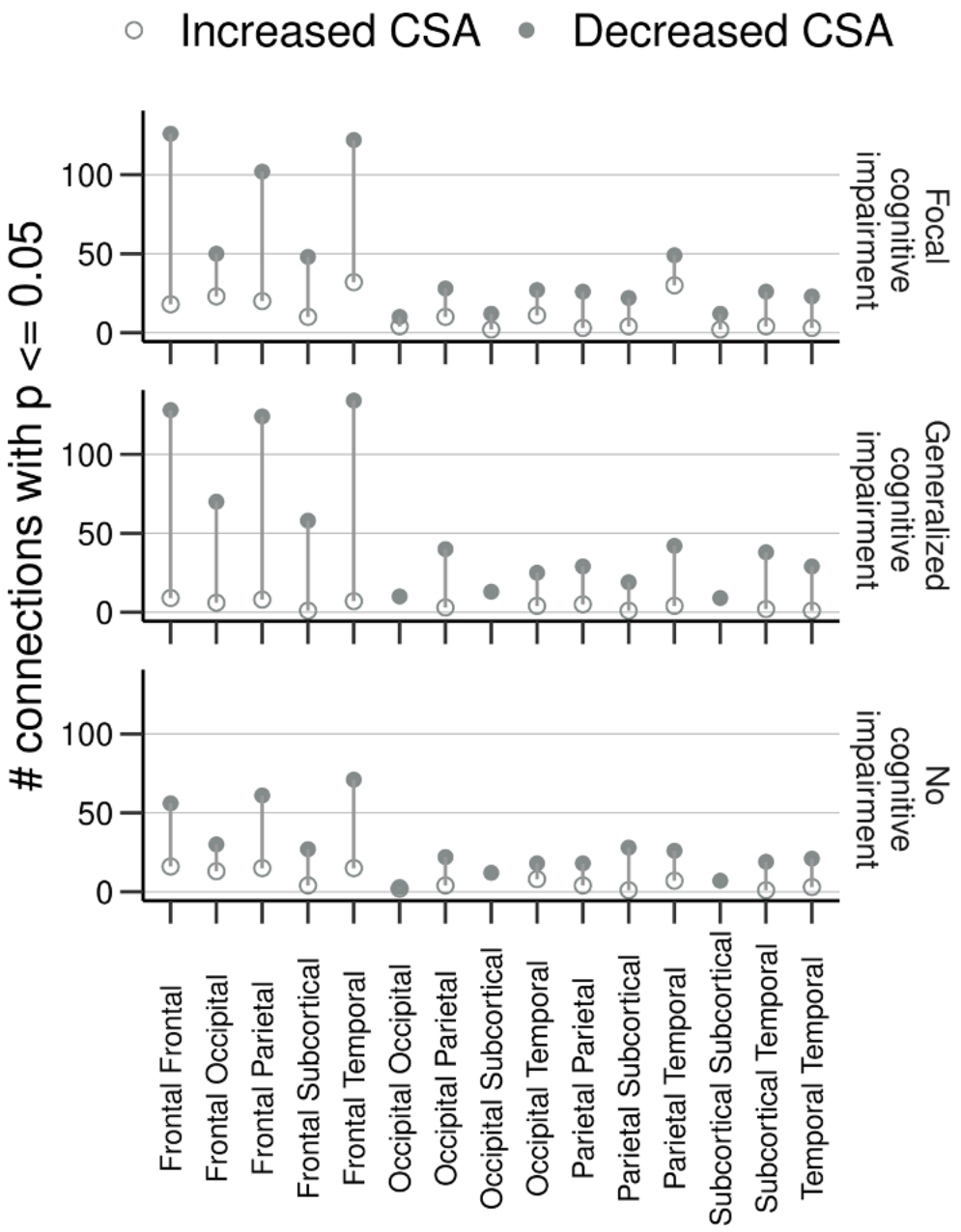

Figure 6. Summary of Cognitive Impairment Clusters in TLE Patients with White Matter Connectome Findings. The white matter connectome abnormalities of cognitive profiles were scrutinized in TLE vs. cognitively intact HCs. While these results did not survive correction, our uncorrected results demonstrated modest and trend-level findings in all 3 cognitive statuses in TLE patients vs. HC showcasing decreased white matter tract CSA as the dominant directionality. The clusters with cognitive impairments (both focal and generalized) reveal a greater number of significant abnormal white matter tract connections with decreased CSA compared to the cluster with no cognitive impairment. Similar to the TLE vs. HC whole brain analysis, the highest number of significant tracts are in the frontal-to-frontal region, the frontal-to-parietal region, and the frontal-to-temporal region across all cognitive profiles. A larger participant pool will be needed to confirm this trend.

Discussion

The present study investigates the structural DWI-based differences in connectivity networks in the white-matter of TLE patients and healthy controls using graph theory metrics. We further examined whether these differences were associated with a history of FBTC seizures and cognitive impairment status. A large-scale dataset from the ECP was utilized for this study. Datasets from the ECP will be released via the Connectome Coordination Facility (CCF) established at the Washington University in St. Louis. The CCF will become the long-term repository for the de-identified data and release at the earliest feasible time. Preprocessed DWI data are available from the senior author upon reasonable request. Associated scripts for data processing and analysis will be posted to GitHub upon publication of the manuscript.

Our study is one of the first few large-scale TLE DWI whole-brain connectome studies in characterizing white matter network connectivity abnormalities, and the ECP dataset is the first to provide connectome quality multi-shell DWI data with reverse phase encoded pair of acquisitions. The current investigation expands on our previous work in the lab on the ECP DWI dataset, revealing the association of patient neighborhood deprivation with white matter connectivity abnormalities (48), and showcasing that graph theory metrics were useful in predicting group membership, find intrinsic structural TLE phenotype differences, and associate results with cognitive and clinical measures via support vector machine analyses (47). Other previous literature exploring the TLE white matter connectome have revealed remodeling of connectome topology and structurally governed functional dynamics in 44 patients (41) and comparisons of connectome fingerprint to post-surgical seizure outcomes in 52 patients (124), and betweenness centrality analysis predicted post-surgical outcomes from pre-surgical evaluations in 47 patients (125).

Global connectome white matter networks of TLE vs. HC

Our study employs TFNBS, which is a direct extension of the threshold free cluster

enhancement (TFCE) used in tract based spatial statistics (TBSS) for correcting family-wise errors in multiple comparisons. The extension is based on the fact that for networks the neighborhood is determined by adjacency matrices and not the regular spatial 3D lattice. This gives unique advantages in that spatially non-local connections in the brain are considered when discerning statistically significant patterns. TFNBS is also unique when compared to the extensively used graph theoretic measures such as modularity, betweenness-centrality etc. TFNBS provides family-wise error corrected statistics at each of the connection level (i.e., it can provide statistical significance using the local network properties) while the graph theoretic measures provide statistics of the global network properties. The local approach offered by TFNBS is complementary to the global approach offered by graph theoretic measures and offers spatially specific biological interpretations that are not derivable using global approaches.

Our results highlight that global analysis of the white matter connectome differences between TLE patients and HCs reveal 97 significant connections after statistical correction with widespread reductions in TLE CSA. The top regions where the edges originate from, with the most significant tracts belong to the frontal to frontal, frontal to temporal, frontal to parietal, and temporal to parietal regions. Through these results, it is evident that TLE has impacted the connectivity networks of white matter, especially in the frontal and temporal regions of the brain. Recent studies have emphasized the importance of using whole-brain structural connectomes for understanding TLE and predicting seizure outcomes (66-68). In turn, our study investigated graph theoretic measures of ms-dMRI. Our results revealed widespread and global decreased CSA in TLE compared to healthy controls, which demonstrates its potential as a neuroimaging biomarker to identify and characterize TLE.

The Effect of FBTC History

Patients with FBTC seizures are more prone to cognitive impairment, premature mortality, psychiatric disorders and are at risk of several other disorders (126). These seizures may be severe, rapid, and involve the bilateral cortical, subcortical, and brainstem networks in

the brain. It is surprising that there is very limited literature on structural connectome associations with FBTC seizures. Therefore, we assessed the impact of FBTC seizures on the white matter connectome observed how the white matter network is affected in TLE patients with a history of FBTC seizures compared to TLE patients who never had a FBTC seizure. Our results indicate modest and trend-level differences in uncorrected significant tracts, none surviving multiple comparisons correction. The uncorrected results do demonstrate that overall, the FBTC group had decreased CSA when compared to the non-FBTC group. The majority of these tracts originated from frontal regions with the top edges stemming from frontal to frontal, frontal to parietal, and frontal to temporal. Future studies should reassess using a larger sample set.

Cognitive Impairment Status

Our study indicates that focal and generalized cognitive impairment showed very similar modest and trend-level associations with white matter connectome findings when compared to HCs. In comparison to the group with no cognitive impairment, both cognitively impaired groups have more than twice the number of significant tracts with decreased CSA. Interestingly, the number of significant connections is very similar between the focal and the generalized cognitively impaired groups. All groups had a greater number of significant tracts in the direction where CSA is decreased when compared to the controls, as opposed to increased CSA when compared to controls in the cognitive impairment clusters. A larger sample of cognitive impaired TLE patients can further clarify these findings.

Existing literature on DTI-based white matter connectomics of TLE patients have highlighted abnormalities in language and memory. Firstly, Kaestner et al. demonstrated that the structural connectome model was superior to models based on white matter microstructural or clinical features in predicting language impairment (127). Similarly, Munsell et al. showed that Boston Naming Test scores, a proxy for language performance, could be predicted using a model based on combined eigenvector node centrality (128). Network-based superficial white

matter analyses have shown abnormalities in graph theory metrics, such as decreased global efficiency, in language and memory-impaired subjects (129). Structural network topology revealed increased characteristic path length in a subgroup of TLE patients with the most pronounced cognitive impairments across multiple domains including memory and verbal comprehension (116). Altogether along with our results, it is evident that graph theoretic characterization of the white matter connectome serves as a useful biomarker for cognitive impairment in TLE. Future studies should identify additional biomarkers that are needed to discriminate between focal vs. generalized cognitive impairment.

Limitations

The sample size was modest for the cognitively impaired TLE patient analyses, so a future study with a greater number of participants will be beneficial to provide adequate power to the analysis. While there are some significant differences between the control and TLE group; however, our analyses corrected for the effect of age. The ECP, which aims to understand phenotypical heterogeneity in the more general population of TLE, contains a more representative sample of TLE patients than typically investigated in surgical series, only a subset of participants (35%) thus underwent the gold standard of ictal monitoring. Future studies may scrutinize the laterality effects in a completely ictally monitored cohort, but such cases may capture mostly the severe end of the epilepsy spectrum and is deemed unrepresentative of the general population of TLE. One pervasive problem in the study of TLE is the underlying heterogeneity of the disease and the lack of a definitive gold standard for diagnosis. Even with the best tools available, most patients with bitemporal lobe epilepsy required 41.6 days of EEG monitoring to detect such bilateral seizures, and some may require up to one year (130). Thus, we can never be sure of a “definitive” seizure laterality and TLE diagnosis. Additionally, drastic limiting of participant selection results in its own type of selection bias where results may be questionably extrapolated to the representative and less complicated TLE patient. The purpose of the ECP was to get a cross-sectional sampling of patients with TLE defined in the typically

clinical and pragmatic method with the help and oversight of epileptologists.

Acknowledgements

We are immensely grateful for the support from the American Epilepsy Society Pre-doctoral Fellowship, NIH T32 GM140935, UW MSTP Radiology Fellowship, and NIH grants U01NS093650, R01NS123378, R01NS105646, R01NS105646, R01NS111022, P50HD105353.

CHAPTER 4

Association of Neighborhood Deprivation with White Matter Connectome Abnormalities in Temporal Lobe Epilepsy

Daniel Y. Chu[1,2], Nagesh Adluru[1,3], Veena A. Nair[1], Timothy Choi[1], Anusha Adluru[1], Camille Garcia-Ramos[2,4], Kevin Dabbs[2], Jedidiah Mathis[5], Andrew S. Nencka[6], Carson Gundlach[1], Lisa Conant[5], Jeffrey R. Binder[5], Mary E. Meyerand[4], Andrew L. Alexander[3], Aaron F. Struck[2,7], Bruce Hermann[2], Vivek Prabhakaran[1,2,4,8]

[1]Department of Radiology, University of Wisconsin-Madison, 1111 Highland Avenue, Madison, WI 53705, United States

[2]Department of Neurology, University of Wisconsin-Madison, 1111 Highland Avenue, Madison, WI 53792, United States

[3]Waisman Center, University of Wisconsin-Madison, 1500 Highland Avenue, Madison, WI 53705, United States

[4]Department of Medical Physics, University of Wisconsin-Madison, 1111 Highland Avenue, Madison, WI 53705, United States

[5]Department of Neurology, Medical College of Wisconsin, 8701 Watertown Plank Rd, Milwaukee, WI 53226, United States

[6]*Department* of Radiology, Medical College of Wisconsin, 8701 Watertown Plank Rd, Milwaukee, WI 53226, United States

[7]William S Middleton Veterans Hospital, 2500 Overlook Terrace, Madison, WI 53705, United

States

[8]Department of Psychiatry, University of Wisconsin-Madison, 6001 Research Park Boulevard, Madison, WI 53719, United States

Published in *Epilepsia*. PMID: 3737641

Abstract

Social determinants of health, including the effects of neighborhood disadvantage, impact epilepsy prevalence, treatment, and outcomes. This study characterized the association between aberrant white matter connectivity in temporal lobe epilepsy (TLE) and disadvantage using a US census-based neighborhood disadvantage metric, the Area Deprivation Index (ADI), derived from measures of income, education, employment, and housing quality. Participants including 74 TLE patients (47 male, mean age=39.2) and 45 healthy controls (27 male, mean age=31.9) from the Epilepsy Connectome Project were classified into ADI-defined low and high disadvantage groups. Graph theoretic metrics were applied to multi-shell connectome diffusion weighted imaging (DWI) measurements in order to derive 162 x 162 structural connectivity matrices (SCMs). The SCMs were harmonized using neuroCombat to account for interscanner differences. Threshold-free network-based statistics were used for analysis and findings were correlated with ADI quintile metrics. A decrease in cross-sectional areas (CSA) indicate reduced white matter integrity. Sex and age-adjusted CSA in TLE groups were significantly reduced compared to controls regardless of disadvantage status, revealing discrete aberrant white matter tract connectivity abnormalities in addition to apparent differences in graph measures of connectivity and network-based statistics. When comparing broadly defined disadvantaged TLE groups, differences were at trend-level. Sensitivity analyses of ADI quintile extremes revealed significantly lower CSA in the most compared to least disadvantaged TLE group. Our findings demonstrate: 1) the general impact of TLE on DWI connectome status is larger than the association with neighborhood disadvantage; however, 2) neighborhood disadvantage, indexed by ADI, revealed modest relationships to white matter structure and integrity on sensitivity analysis in TLE. Further studies are needed to explore this relationship and determine if the white matter relationship with ADI is driven by social drift or environmental influences on brain development. Understanding the etiology and course of the disadvantage-brain integrity relationship may serve to inform care, management, and policy for patients.

Introduction

Social determinants of health, defined as the conditions in the environment in which persons are born, work, and live in, have been identified as having a significant effect on overall health and well-being (131) and implicated in several health disparities and inequities that continue to contribute disproportionately to the prevalence, care, and outcomes of several disease states (132). While research has explored metrics of socioeconomic status (SES) at the individual level (133-135), studies on the neighborhood-level disadvantage may provide contextual evidence to the conditions of their residential environment and its impact on health outcomes. These conditions may include the level of poverty, housing inequality, healthcare access, income, and level of education for each geographical region of interest. The area deprivation index (ADI) is one such measure of socioeconomic and neighborhood disadvantage that incorporates metrics of poverty level, housing, education level, and employment status based on zip codes of US neighborhoods (136). The ADI was created by the Health Resources and Services Administration and encapsulates the multifaceted nature of disparities at the community-level (136, 137).

In the context of epilepsy, interest is growing regarding how the framework of the social determinants of health and neighborhood disadvantage may impact its incidence, care, and outcomes. There is recognition in the importance of studying the effects of disparities in epilepsy, the existing literature demonstrates that socioeconomic deprivation increases the incidence and prevalence of epilepsy in both adults and children (138-141). A recent study utilizing the ADI metric, found that disadvantaged neighborhoods distinctly lacked access to level IV epilepsy centers (142),indicating the striking geographic influence on access and the quality of care considering that their availability has been described as essential to the proper management of epilepsy (143). Altogether, these studies contribute to the important work necessary to understand how disparities, such as neighborhood disadvantage, impact patients

with epilepsy. Further elucidation of these factors are imperative to inform and implement policy changes to address these disparities.

Temporal lobe epilepsy (TLE) is the most common form of focal epilepsy in adults, and recent diffusion tensor imaging (DTI) studies have consistently demonstrated abnormalities in white matter structure and connectivity (13, 116, 144, 145). Advanced neuroimaging studies can now evaluate these dynamic white matter networks and their interactions via multi-shell connectome diffusion-weighted MRI (67, 127, 129, 144, 146, 147). Currently, no studies have examined the impact and associations of neighborhood disadvantage on TLE white matter integrity in general and connectome status in particular. Identifying MRI structural biomarkers and their correlation with neighborhood disadvantage will further the understanding of how disparities may impact patients with epilepsy.

In the present study, we characterize the presence and degree of aberrant white matter connectivity in TLE patients compared to healthy controls (HCs) as a function of disadvantage using the US census-based neighborhood disadvantage metric, the ADI. We examine its association with diffusion weighted MRI findings from the Epilepsy Connectome Project (ECP) (43, 44, 46), a multi-institutional large-scale and homogenous patient study. We hypothesize that patients residing in disadvantaged neighborhoods as indexed by ADI are associated with aberrant white matter integrity and network in their DWI connectome status compared to patients from non-disadvantaged neighborhoods and healthy controls. Furthermore, we hypothesize that this effect will occur in the context of a generally adverse impact of TLE on DWI connectome status compared to healthy controls.

Methods

Study Participants

Multi-shell connectome diffusion weighted MRI measurements were employed from 119

participants, including 74 patients with TLE (29 males, mean age = 39.28 ± 11.71 years) and 45 healthy controls (23 males, mean age = 31.87 ± 10.14 years) from ages 18 to 60. All TLE patients and healthy controls were participants in the ECP, a multisite collaborative research project between the Medical College of Wisconsin (MCW) and the University of Wisconsin Madison (UW-Madison). All TLE patient and healthy control data were collected between March 2016 and December 2018.

The inclusion criteria for TLE patients required two of the following: 1) clinical semiology consistent with seizures of temporal lobe origin, 2) previous MRI consistent with mesial temporal sclerosis or hippocampal atrophy, 3) EEG revealing temporal intermittent rhythmic delta or epileptiform activity over the temporal lobe(s), and 4) EEG monitoring video evidence of temporal lobe onset seizure. Patients were excluded if they had lesions other than mesial temporal sclerosis (focal dysplasias and focal atrophy of other regions of the temporal lobe were excluded), active infectious, autoimmune, or inflammatory seizure etiology. Healthy controls were between the ages of 18 and 60. Exclusion criteria for the healthy controls included: Edinburgh Laterality (Handedness) Quotient less than +50; primary language other than English; history of any learning disability, brain injury or illness, substance abuse, or major psychiatric disorders (major depression, bipolar disorder, or schizophrenia); current use of vasoactive medications; and any medical contraindications to MRI.

Standard Protocol Approvals, Registrations, and Patient Consents

The ECP was reviewed and approved by the institutional review board (IRB) at the MCW, and all participants provided written informed consent. All experiments were performed in accordance with established guidelines and regulations.

Data Acquisitions

Magnetic resonance images were acquired on a 3T General Electric 750 scanners (Waukesha, WI) using a 32-channel head coil. T1-weighted structural images were acquired

with an MPRAGE sequencing the following parameters (repetition time (TR) = 604 ms, echo time (TE) = 2.516 ms, inversion time = 1060 ms, flip angle = 8°, field of view (FOV) = 205.6 cm, 0.8 mm isotropic). DWI was acquired using multiband echo planar imaging (EPI) with slide acceleration factor 3 that included a total of 4 runs, with 2 runs with 75-directions each, and opposite phase encoding polarity (AP and PA), and 2 runs with 76 directions each. The DWI images had the additional acquisition parameters: alternating b = 1000 s/mm^2 and b = 2000 s/mm^2, and 9 b = 0 volumes.

Data Processing and Statistical Analyses

Modern tools from the emerging field of network neuroscience were used for detailed network analysis of the structural connectivity pathways for better understanding of the plasticity changes in patients with TLE. These graph theoretical methods quantified the organization of structural connections as edges, providing insights into network communication efficiency patterns (66, 68, 119, 120, 148). Threshold free network-based statistics (TFNBS) were used for predictive modeling (70). **Figure 1** provides an overview of the connectography reconstruction from connectome quality multi-shell diffusion weighted imaging (DWI) data. Preprocessing of the data followed DESIGNER guidelines (92) which included the removal or mitigation of artifacts such as noise, Gibb's ringing, distortion due to eddy currents, B_1-bias and EPI wrapping due to field inhomogeneities using tools in FSL (90), ANTs (122), and MRTrix3 (89). The curated DWI data was deconvolved using constrained optimization with the shell and major tissue specific response functions to estimate fiber orientation distributions (FOD) at each voxel in the brain. Anatomical cortico-subcortical gray matter atlas regions identified using FreeSurfer reconstruction and parcellation of the gray matter used to define the nodes in the neuronal networks. Underlying white matter fiber bundles connecting pairs of these nodes were used to define the edges. These networks can be represented using symmetric matrices, which encode the adjacency or connectedness of the nodes.

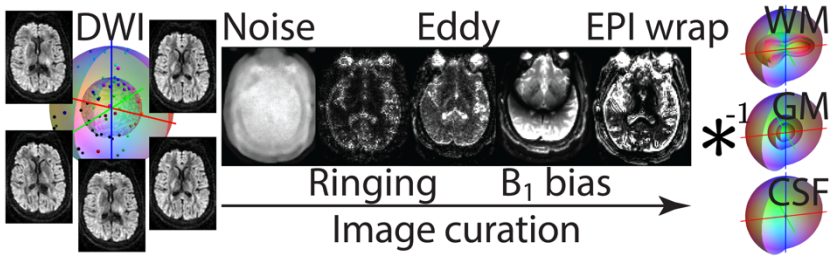

(a) Multi-shell connectome acquisition.

(b) DESIGNER guidelines.

(c) Spherical deconvolution.

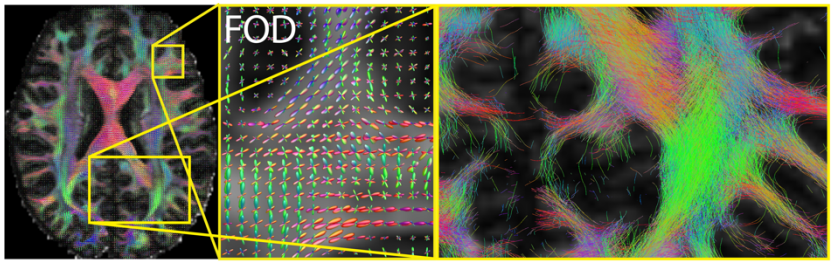

(d) Voxelwise fiber orientation distributions (FOD).

(e) Whole brain tractography.

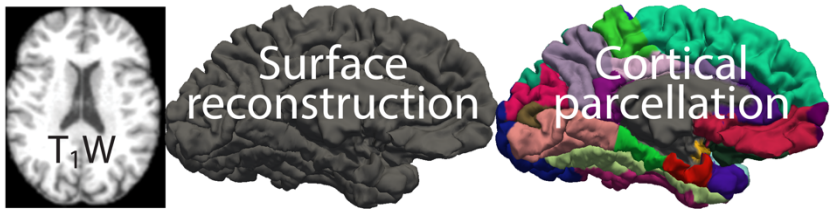

(f) FreeSurfer based cortico-subcortical parcellations from T1w images.

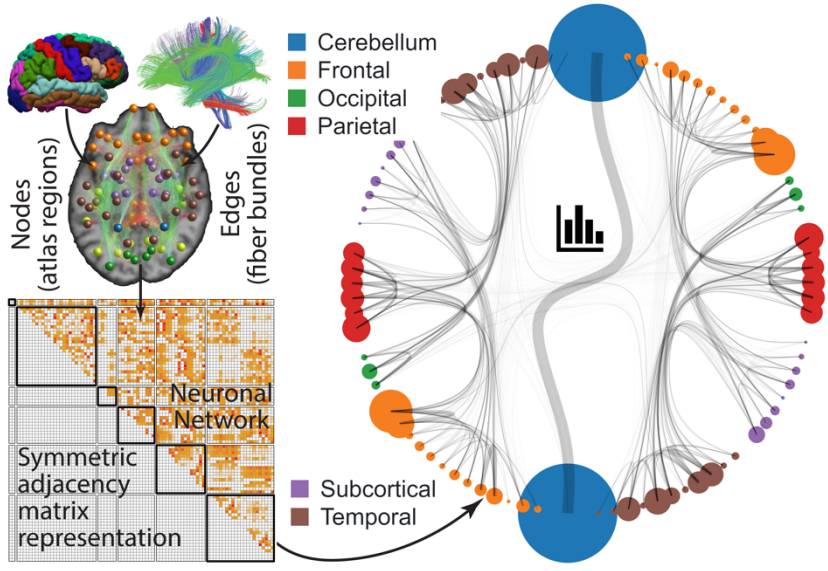

(g) Cortico-subcortical parcellations and whole brain tractography are used to estimate neuronal networks which are represented using adjacency matrices and can be visualized as chord diagrams.

Figure 1. Overview of the connectography reconstruction from connectome quality multi-shell DWI data. a-c) Preprocessing of the multi-shell data followed DESIGNER guidelines (92) which included the removal or mitigation of artifacts such as noise, Gibb's ringing, distortion due to eddy currents, B_1-bias and EPI wrapping due to field inhomogeneities using tools in FSL (90), ANTs (122), and MRTrix3 (89). **d-e)** The curated DWI data was deconvolved using constrained optimization with the shell and major tissue specific response functions to estimate fiber orientation distributions (FOD) at each voxel in the brain. **f)** Anatomical cortico-subcortical gray matter atlas regions identified using FreeSurfer reconstruction and parcellation of the gray matter used to define the nodes in the neuronal networks. **g)** Underlying white matter fiber bundles connecting pairs of these nodes were used to define the edges. These networks can be represented using symmetric matrices, which encode the adjacency or connectedness of the nodes.

Tractography was performed using the tckgen command in MRtrix3. Fifteen million streamlines were generated by dynamic seeding in the whole brain using the FODs and a probabilistic algorithm (iFOD2) which performed second order integration over FODs. The step size was set to the default value of ½ the voxel size. The tract stopping criteria were also set to the defaults of 45° angular threshold for curving, minimum length of twice the voxel size, maximum length of 100 times the voxel size. The FOD amplitude cut off was set to 0.05. The tcksift2 algorithm from MRtrix3 was used to filter the streamlines and compute the weights for each of the streamlines used in computing the final edge weights in the networks. Fiber density estimates were heuristically shrunk based on the presence of gray matter using the fd_scale_gm option for tcksift2. The spherical-deconvolution informed filtering of tractograms (SIFT) proportionality constant μ was also saved, which is used to scale the network adjacency matrices. These networks can be represented using symmetric matrices, which encode the adjacency or connectedness of the nodes. The edge weights in the networks represent cross-sectional areas (CSA) of the fiber bundles connecting pairs of regions/nodes. The CSA of a bundle of white matter fiber tracts is defined as the total sum of the iteratively optimized weights that represent the fidelity of fiber tracts compared to the measured diffusion signal. This optimization process represents a "semi-global" approach for tractography based connectivity estimation that takes into account the whole brain tractography and the local voxel level consistency between tracts passing through the voxel and the apparent fiber density estimated from the FOD within the voxel. This approach enables improved quantitative comparison of

connectivity between different regions as well as between different subjects in a study and can thus give a “metric” for comparing connectivity estimates in statistical analysis and thus enable more reliable directionality of the results.

To account for the DV25 to DV26, a major software of the GE MR scanner, which also included a change from sagittal to axial acquisition, parametric data harmonization using neuroComBat (121) of the connectivity matrices was employed. NeuroComBat harmonization “combats the batch/protocol effects” by accounting for additive (on the bias) and multiplicative (on the variance) effects of the scanner software and slice direction in acquisition on connectivity outcomes using a linear model by preserving group, age, and sex effects. These correction effects are the expected values of the empirically estimated Bayesian prior distributions either parametrically via Expectation Maximization or non-parametrically via importance sampling. Such a prior based approach is robust when there are small sample sizes per each protocol. **Supplementary Figure S1** illustrates the effects of harmonization on the adjacency matrices (edge weights) before permutation testing.

The resulting harmonized connectographs were fed into the threshold free network-based statistics (TFNBS) described in **Figure 2.** General linear modeling (GLM) generated statistic graphs from connectographs, which were thresholded to cluster the nodes (70). The product of the size and maximum of the clusters were summed across the thresholds to obtain threshold free cluster enhanced statistic graphs. Permutation testing with 5000 permutations was used to obtain null distributions for each connection or the maximum across the connections. Comparing each connection in the unthresholded statistic graph with 1) max-null, or 2) connection specific null resulted in family-wise error corrected or uncorrected p-value graphs respectively. SNR differences between DWI acquisition protocols can cause biases, but the SNR was good enough to reasonably estimate the shift and scale effects.

Altogether, these methods took advantage of the precision offered by connectome quality multi-band ms-dMRI in reconstructing the network representations of the brain (149-

152). Statistically significant results at p ≤ 0.05 (uncorrected and corrected) are reported via white matter tract CSA. Age and sex represented nuisance variables in the GLM.

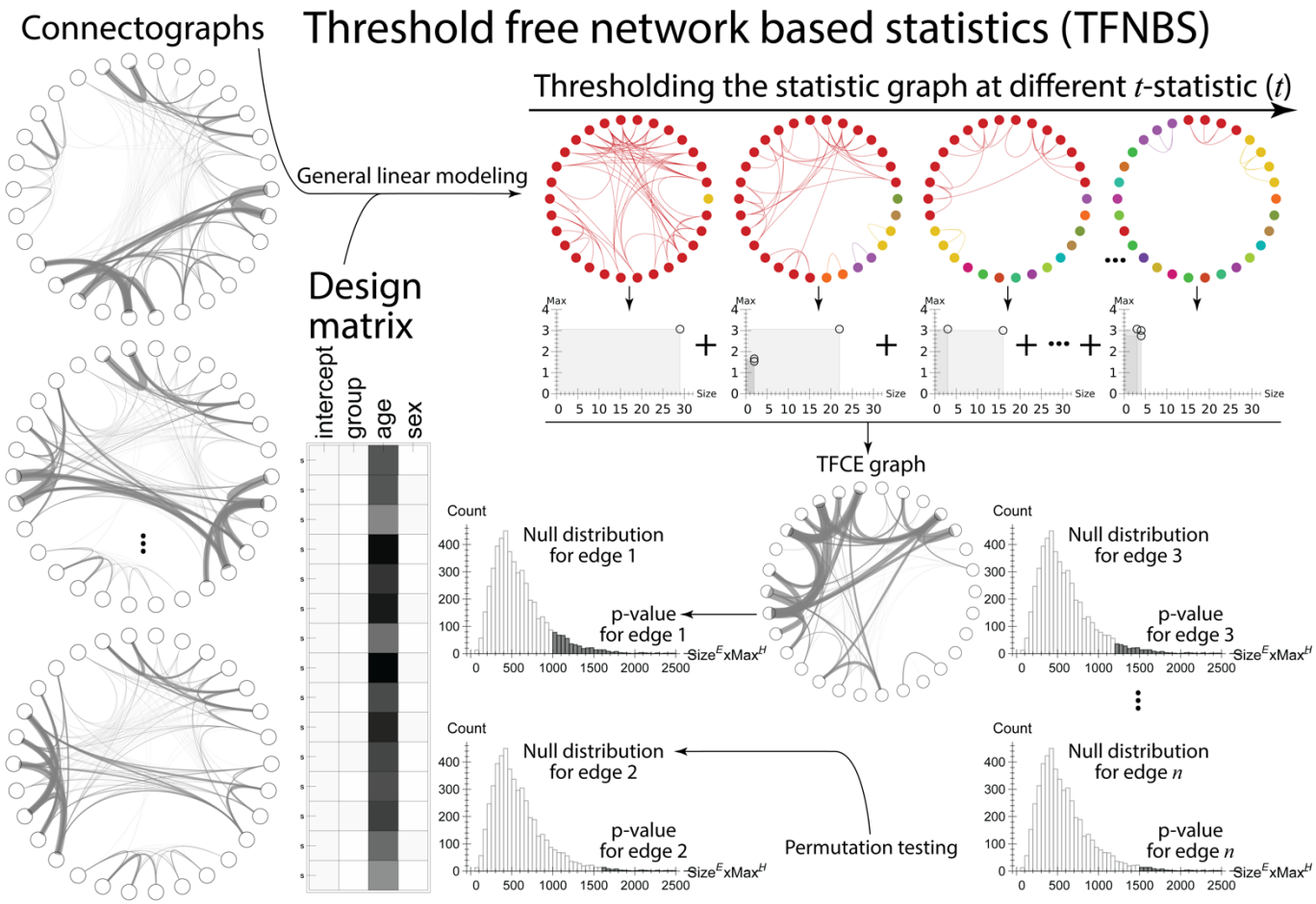

Figure 2. Overview of threshold free network-based statistics (TFNBS). General linear modeling is used to get a statistic graph from connectographs. The statistic graph is thresholded at different thresholds to cluster the nodes. The product of size and max of the clusters are summed across the different thresholds to obtain threshold free cluster enhanced (TFCE) statistic graph. That is $TFCE(cluster, E, H) = \sum_{t=min-thresh}^{t=max-thresh} size(t)^E \times \max(t)^H$, where E tunes the influence of cluster size or extent, and H tunes the influence of cluster max or height. The null distribution of TFCE values can be obtained for each connection or maximum across the connections (max-null) using permutation testing. Comparing each connection in the unthresholded statistic graph with (1) max-null or (2) connection specific null, results in family wise error corrected or uncorrected p-value graphs respectively.

Neighborhood Disadvantage

We examined the association between the ADI and multi-shell connectome diffusion weighted MRI measurements. The ADI uses American Community Survey (ACS) Five Year Estimates in its construction. For example, the 2018 ADI used the ACS data for 2018, which is a 5-year average of ACS data obtained from 2014-2018 (137). This window corresponds well with the timeframe for the current TLE and control sample (March 2016 to December 2018). Please also see https://www.neighborhoodatlas.medicine.wisc.edu/.

The ADI uses 17 US Census-based indicators to characterize socioeconomic disparities via census block groups based on zip codes. The metrics encompass measures of income, education, employment status, housing quality, access to health care resources, and other factors. The full list of ADI indicators has been presented previously in open-access publications (137, 153). Similar to comparable investigations, the distributions of census block group ADI scores of the TLE and control participants were grouped into quintiles from 1 to 5 based on Wisconsin statewide distributions (153, 154). A higher ADI indicates more disadvantage with the 5^{th} quintile signifying the most disadvantaged neighborhoods and the 1^{st} quintile score indicating the least disadvantaged neighborhoods.

The distribution of participants across ADI quintiles was uneven with some quintiles containing small number of participants. To maximize sample size for disadvantage assessment, ADI quintiles 1 and 2 were combined to reflect participants residing in less disadvantaged neighborhoods and ADI quintiles 4 and 5 were combined to reflect participants residing in the most disadvantaged areas, omitting the small number of participants in quintile 3 which was neither advantaged nor disadvantaged. **Table 1** summarizes the ADI grouping and basic participant demographics. Subsequent sensitivity analyses directly compared the ADI extremes of quintile 1 (least disadvantaged group) to quintile 5 (most disadvantaged group).

Groups	TLE Low Disadvantage (Quintiles 1+2)	TLE High Disadvantage (Quintiles 4+5)	HC Low Disadvantage (Quintiles 1+2)	HC High Disadvantage (Quintiles 4+5)
N	47	27	32	13
Male/Female	18/29	11/16	16/16	7/6
Mean Age	39.7 ± 11.51	37.7 ± 11.68	33.5 ± 9.91	28.0 ± 5.82
Education[a,b,c] (Years)	15.75 ± 2.83	13.37 ± 2.20	16.81 ± 2.72	14.86 ± 2.75
Race[d,e,f] (W/B/A/NA/O)	44/1/1/1/0	23/1/0/1/2	26/0/3/3/0	9/1/1/2/0
Age of Epilepsy Onset[g] (Years)	22.31 ± 13.46	23.16 ± 15.76	-	-
Disease Duration[h] (Years)	17.45 ± 13.25	15.99 ± 14.55	-	-
# of ASMs[i]	1.49 ± 0.93	2.15 ± 0.95	-	-
Frequency of Seizures[j] (# seizures per month)	4.43 ± 9.26	8.17 ± 13.04	-	-
Seizure Lateralization[k] (L/R/Bi/U)	21/11/5/10	18/4/2/3	-	-

W, White; B, Black; A, Asian; NA, Native American; O, other; L, left; R, right; Bi, bilateral; U, unknown.

[a] Significantly different between TLE low disadvantage and TLE high disadvantage (p=0.000332)
[b] No significant group differences between TLE low disadvantage and HC low disadvantage (p=0.098)
[c] No significant group differences between TLE high disadvantage and HC high disadvantage (p=0.056)
[d] No significant group differences between TLE low disadvantage and TLE high disadvantage (p=0.34)
[e] No significant group differences between TLE low disadvantage and HC low disadvantage (p=0.29)
[f] No significant group differences between TLE high disadvantage and HC high disadvantage (p=0.27)
[g] No significant group differences between TLE low disadvantage and TLE high disadvantage (p=0.81)
[h] No significant group differences between TLE low disadvantage and TLE high disadvantage (p=0.68)
[i] Significantly different between TLE low disadvantage and TLE high disadvantage (p=0.005)
[j] No significant group differences between TLE low disadvantage and TLE high disadvantage (p=0.17)
[k] No significant group differences between TLE low disadvantage and TLE high disadvantage (p=0.33)

Table 1. Participant Sociodemographic and Clinical Characteristics

Data Availability Statement

Datasets from the ECP will be released via the Connectome Coordination Facility (CCF) established at the Washington University in St. Louis. The CCF will become the long-term

repository for the de-identified data and release at the earliest feasible time. Preprocessed DWI data are available from the senior author upon reasonable request. Associated scripts for data processing and analysis will be posted to GitHub upon publication of the manuscript.

Results

Demographics of Study Participants

Multi-shell DWI connectome data were collected from 119 participants including 74 TLE patients (29 males, mean age = 39.28 ± 11.71 years) and 45 HCs (23 males, mean age = 31.87 ± 10.14 years) ranging from ages 18 to 60. Initially, the ECP contained 174 participants with 120 TLE patients and 54 HCs. **Supplementary Figure S2** illustrates the study further exclusionary workflow of participants with missing DWI data, residential addresses needed for ADI indexing, and participants with ADI quintile score of 3. Participant sociodemographic and clinical characteristics are provided in **Table 1**. The more disadvantaged group (quintiles 4 and 5) contained 40 participants, 27 with TLE and 13 HCs. The less disadvantaged group (quintiles 1 and 2) contained 79 total participants, 47 with TLE and 32 HCs.

Association of Neighborhood-Level Disadvantage with Diffusion Weighted Connectome

The IIT Destrieux gray matter atlas was used to derive the structural connectivity matrices of 162 x 162 nodes or edges originating from and organized into five cortical regions: frontal, occipital, parietal, temporal, and subcortical. The summary relationship between ADI and DWI connectome abnormalities is illustrated in **Figure 3.** As noted, quintiles 4 and 5 represent the more disadvantaged group and quintiles 1 and 2 represent the less disadvantaged. The age and sex-adjusted CSA was analyzed as a measure of structural integrity of the white matter tract connectome and the significant number of connections were reported for both corrected and uncorrected results. The two-way interaction analyses demonstrates significant differences via decreased CSA when comparing less disadvantaged TLE groups to more disadvantaged

HC groups (**Figure 3a)**, and widespread and enhanced significant differences via decreased CSA when comparing more disadvantaged TLE vs. less disadvantaged HC groups **(Figure 3b)**. The corrected results comparing the more versus less disadvantaged TLE groups (**Figure 3c**) revealed trend level differences ($p<0.10$). The uncorrected results demonstrated a significantly decreased number of connections (decreasing CSA) in the more compared to less disadvantaged TLE group (**Figure 3c**). Moreover, the more disadvantaged TLE group also exhibited a significantly greater number of abnormal connections (lower CSA) compared to the more disadvantaged HCs after correction (**Figure 3d**). For the disadvantaged TLE group the majority of abnormal connections involved edges originating from the frontal lobe to other cortical and subcortical regions. Similarly, the less disadvantaged TLE group also demonstrated abnormal connections, albeit fewer, via decreased CSA compared to the less disadvantaged HC group (**Figure 3e)**. Altogether, results from figures 3b and 3c demonstrate a general impact of epilepsy on the DWI connectome. **Figure 3f** shows one increased CSA connection in the frontal to parietal between in the disadvantaged HC group when compared to the non-disadvantaged HC group.

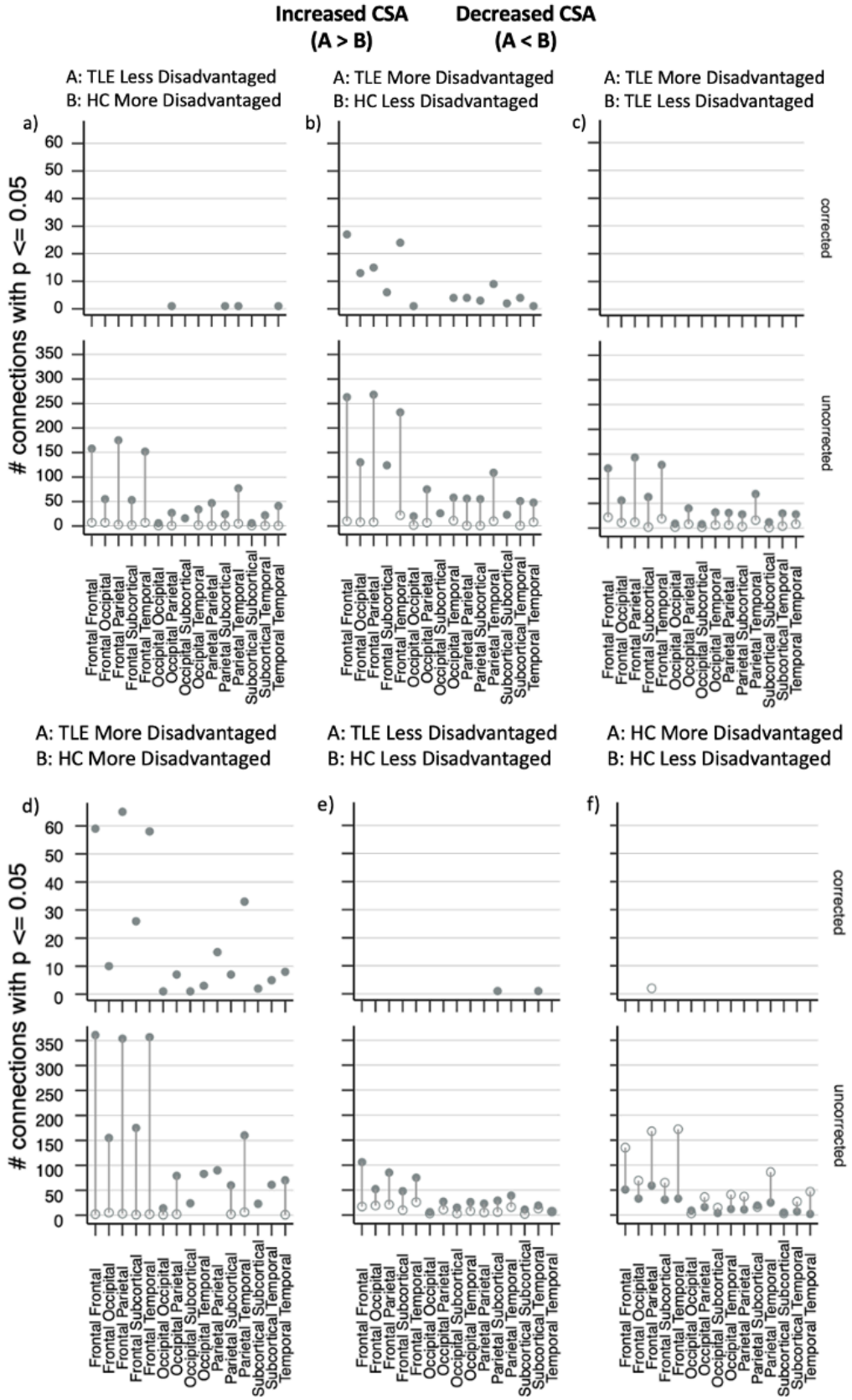
Increased CSA
(A > B)
Decreased CSA
(A < B)
A: TLE Less Disadvantaged
B: HC More Disadvantaged
A: TLE More Disadvantaged
B: HC Less Disadvantaged
A: TLE More Disadvantaged
B: TLE Less Disadvantaged
a)
b)
c)
connections with p <= 0.05
corrected
uncorrected
A: TLE More Disadvantaged
B: HC More Disadvantaged
A: TLE Less Disadvantaged
B: HC Less Disadvantaged
A: HC More Disadvantaged
B: HC Less Disadvantaged
d)
e)
f)
Frontal Frontal
Frontal Occipital
Frontal Parietal
Frontal Subcortical
Frontal Temporal
Occipital Occipital
Occipital Parietal
Occipital Subcortical
Occipital Temporal
Parietal Parietal
Parietal Subcortical
Parietal Temporal
Subcortical Subcortical
Subcortical Temporal
Temporal Temporal

Figure 3. Summary of Area Deprivation Index and its Association with White Matter Connectome Abnormalities in TLE Patients. a) The less disadvantaged TLE group showcases four significant differences compared to more disadvantaged HC group via decreased CSA. **b)** The more disadvantaged TLE group demonstrates enhanced differences when compared to less disadvantaged HC group via decreased CSA. **c)** The more disadvantaged and less disadvantaged ADI TLE groups exhibit white matter structural abnormality reflected by lower CSA across all analyses only within the uncorrected results. Thus, the differences appear to be modest and trend-level and will likely require bigger sample sizes. **d)** The more disadvantaged population of the TLE vs. HC demonstrates more enhanced and pronounced differences in the disadvantaged TLE when compared to the disadvantaged HCs via decreased CSA, suggesting a general impact of epilepsy. For TLE patients with upper ADI, the majority of the abnormal connectivities involve edges from frontal lobe and other regions. **e)** The less disadvantaged population of the TLE vs. HC shows similar, but fewer differences via decreased CSA compared to the more disadvantaged TLE vs. more disadvantaged HC. **f)** The more disadvantaged population of HC vs. less disadvantage) HC group shows one significant corrected white matter abnormality via increased CSA in the frontal to parietal region, likely due to noise due to effect size. CSA = cross-sectional area of the white matter.

Figure 4 presents a representative uncorrected white matter connectome CSA association showing that more disadvantaged TLE patients exhibited significantly lower white matter tract age and sex-adjusted expected CSA compared the less disadvantaged TLE group. Similarly, **Supplementary Figure S3** and **Supplementary Figure S4** provide representative corrected white matter connectome CSA association comparing more disadvantaged TLE vs. HC and less disadvantaged TLE vs. HC respectively. These figures also demonstrate the consistently reduced age and sex-adjusted expected CSA in TLE compared to HC. Permutation testing with 5000 permutations was used to correct for multiple comparisons by generating the null distribution of max-statistics.

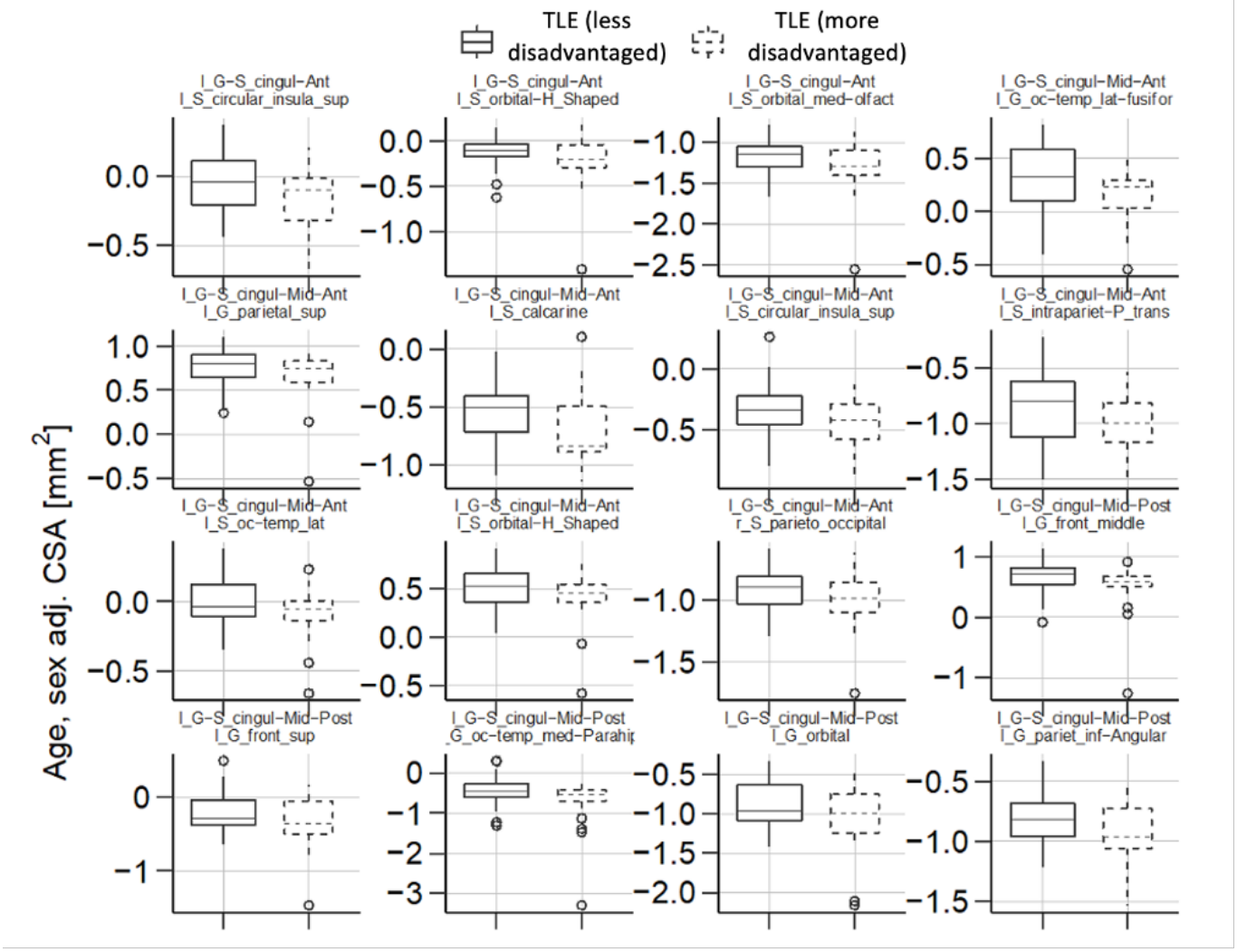

Figure 4. Representative Less Disadvantaged TLE vs. More Disadvantaged TLE ADI Analyses. Depicted are 16 representative analyses showing less disadvantaged ADI TLE patients vs. more disadvantaged TLE patients. The results indicate that TLE patients who are more disadvantaged exhibit lower white matter tract age and sex adjusted expected CSA when compared to those who are less disadvantaged. The originating nodes and region locations are noted above each box plot. Lower = less disadvantaged ADI groups; Upper = more disadvantaged ADI groups; CSA = cross-sectional area of the white matter.

Sensitivity Analysis of Neighborhood-Level Disadvantage with Diffusion Weighted Connectome

Figure 5 depicts the results of the sensitivity analysis limited to the extreme ADI quintile groups (quintile 1 vs. quintile 5). After correction, the more disadvantaged compared to less disadvantaged TLE group (**Figure 5a**) demonstrated significantly decreased age and sex-

adjusted CSA involving edges from the temporal to parietal regions and the temporal to occipital regions. Additionally, the more disadvantaged TLE patients demonstrated significantly more abnormalities compared to the more disadvantaged HCs (**Figure 5b**) via decreased CSA across the whole-brain with the highest number of connections involving edges in frontal to frontal, frontal to parietal, and frontal to temporal. The less disadvantaged TLE group compared to the less disadvantaged HC group (**Figure 5c**) also has fewer differences when compared to more disadvantaged counterparts with widespread decreased CSA in the uncorrected analysis and two connections after correction in the temporal to subcortical and parietal to subcortical regions. However, there is also one connection with increased CSA in the parietal to temporal region. When comparing the most disadvantaged to the least disadvantaged HCs, white matter tracts exhibit increased CSA globally (**Figure 5d).**

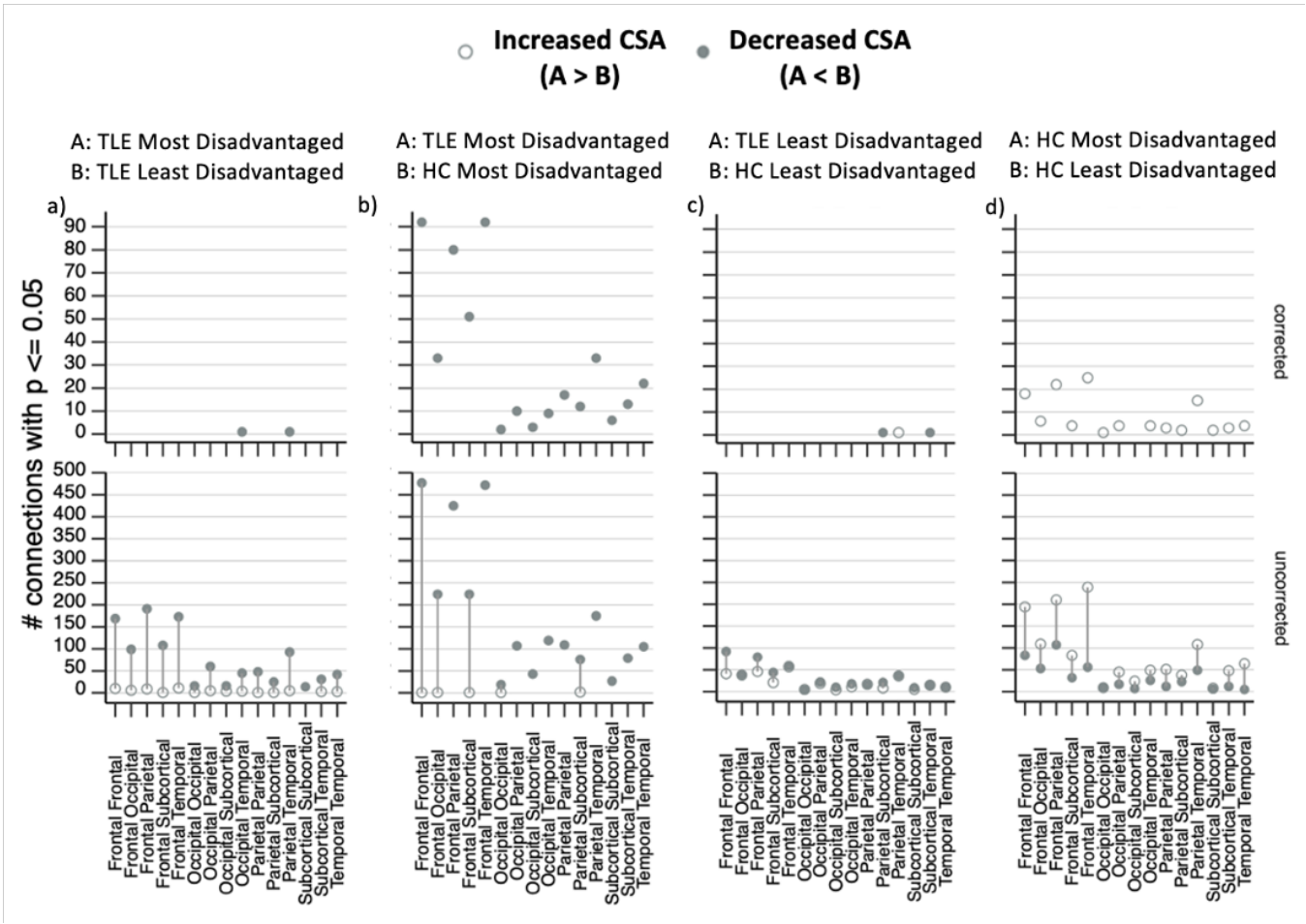

Figure 5. Sensitivity Analysis of Area Deprivation Index and its Association with White Matter Connectome Abnormalities in TLE Patients. The quintile extremes of the most disadvantaged group was compared to the least disadvantaged ADI group for these sensitivity analyses. **a)** The most disadvantaged ADI TLE exhibited white matter structural abnormality reflected by lower CSA when compared to least disadvantaged ADI TLE group. This sensitivity analysis showcases that more disadvantaged TLE patients did have significant abnormal white matter structure and connectivity compared to the least disadvantaged, especially of the tracts in the temporal to occipital and temporal to parietal regions. **b)** The most disadvantaged population of the TLE vs. HC demonstrate pronounced differences in the disadvantaged TLE when compared to the disadvantaged HCs. **c)** The less disadvantaged population of the TLE vs. HC shows similar, but fewer differences via decreased CSA compared to the most disadvantaged TLE vs. most disadvantaged HC and one difference via increased CSA. **d)** The more disadvantaged population of HC vs. less disadvantaged HC group shows a more pronounced effect from Figure 3D via increased CSA differences across the whole brain. CSA = cross-sectional area of the white matter.

Discussion

This study investigated the relationship between a geospatial metric of neighborhood disadvantage (ADI) and white matter integrity assessed by multi-shell connectome DWI data and graph theory analyses. While previous studies have predominantly addressed whether and how disparities impact seizure management and outcomes (138), here we extend the inquiry of neighborhood-level disadvantage to its association with white matter connectivity and structure by means of connectome DWI and graph theory analysis.

Sociodemographic and Clinical Variables of ECP Participants

In summary of **Table 1**, the only significant clinical variable group differences that was found between low and high disadvantage TLE groups was the number of ASM, where the high disadvantage TLE group had a significantly higher number of ASMs. All other epilepsy measures investigated exhibited no significant group differences between low and high disadvantage including mean age of epilepsy onset, mean disease duration, frequency of seizures per month, and seizure lateralization. The greater number of ASMs in the high disadvantage group may infer a more complicated and difficult epilepsy course, although caution is indicated given challenges to such a view. A recent study reported that clinical markers of epilepsy severity were only marginally associated with drug load (155) and that patients seem to accumulate drugs due to the chronicity of epilepsy. Overall, the drug load remained largely unexplained. The findings nevertheless call for scrutinizing multidrug therapies in patients with long-lasting epilepsies.

There were no significant racial/ethnic group differences between TLE low disadvantage vs. TLE high disadvantage, TLE low disadvantage vs. HC low disadvantage, or TLE high disadvantage vs. HC high disadvantage. For education, there were no significant differences between TLE low disadvantage vs HC low disadvantage and TLE high disadvantage vs HC high

disadvantage; however, there was a significant difference between TLE low disadvantage vs TLE high disadvantage showing that high disadvantaged group had fewer mean years of education compared to the low disadvantaged group. This is probably expected due to the that education is a metric encompassing 3 of the 17 census variables that the ADI captures (137).

Neighborhood Disadvantage Association in TLE with Diffusion Weighted Connectome

The findings illustrate associations between discrete white matter tract abnormalities and increased disadvantage as indexed by the ADI. Specifically, CSA was decreased within the more disadvantaged compared to less disadvantaged TLE group. While the initial corrected results were at trend level (**Figure 3c**), corrected sensitivity analyses of the ADI quintile extreme groups revealed significantly decreased CSA in the most compared to the least disadvantaged ADI group (**Figure 5a**). These analyses expand the understanding of deprivation effects in TLE which to date have focused on epilepsy incidence/prevalence, care and outcomes—to a reflection of the impact of ADI on brain health, specifically white matter integrity. Our sensitivity analysis revealed two significant connection differences reflected in decreased CSA in the edges within the temporal to parietal and temporal to occipital regions (**Figure 5a**).

In addition, the findings also inform the more general impact of TLE on white matter health through findings demonstrating that even the low (and high) disadvantage TLE participants exhibited more white matter abnormality compared to both the low (and high) disadvantaged controls respectively, reflected in the decreased age and sex adjusted expected CSA in the disadvantaged TLE groups compared to their respective control groups (**Figure 3d and 3e)**. Consistent with expectations based on the existing DTI literature, these findings indicate that TLE exerts a general adverse impact on DWI connectome status regardless of neighborhood adversity (144, 147). Furthermore, two-way interaction analyses demonstrating both ADI and TLE diagnoses impact shows that more disadvantaged TLE groups had widespread significant connections that exhibited decreased white matter CSA (**Figure 3b)**, while less disadvantaged TLE group still showed four significant differences with decreased

CSA when compared to the more disadvantaged HC group (**Figure 3a).** These findings are consistent with the general notion that TLE is a network disorder involving regions beyond the epileptogenic zone, evidenced by aberrant white matter tracts with nodes originating from widespread regions of the brain, while providing some evidence that ADI may be associated and further contribute with white matter structural abnormalities.

Specifically, previous literature on TLE structural connectome and white matter connectome reported notable reduced distant connectivity across several brain regions (144). Bonilha et al. (2015) showcased the valuable utility of the structural brain connectome in assessing TLE seizure outcomes after temporal lobectomy (67). Additionally, several studies have demonstrated the impact of the white matter connectome as a predictive biomarker of language, cognitive dysfunction, and memory impairment in TLE (127, 129, 146). The present study is the first to assess the association of neighborhood disadvantage as a function of ADI on the white matter connectome in TLE.

While the field of neighborhood disadvantage research is growing, there is still limited existing literature across several disease states particularly within epilepsy. Given the identified enhanced network abnormalities in high disadvantage TLE participants, it could be anticipated that these network abnormalities may mediate salient cognitive and/or behavioral abnormalities in TLE. Further areas open for investigation include ADI's relationship with cognition or potential behavioral complications, such as depression or anxiety, in epilepsy.

Neighborhood Disadvantage in Other Populations

Previous studies have linked ADI to outcomes in other populations. Boorgu et al (2022) reported an association between higher ADI and poorer neurological outcomes in a multi-center study of MS patients (156). Higher ADI (greater disadvantage) has also been associated with progression to dementia and cognitive decline as well as lower cerebral and hippocampal volume in cognitively unimpaired adults (153, 154, 157). In cognitively aging individuals, higher ADI has been linked with poorer performance on tests of executive function, verbal learning,

and memory (158). In typically developing youth, Rakesh et al (2021) found ADI to be associated with lower resting state functional connectivity both within and between networks such as the default mode, auditory, ventral attention networks in the adolescent brain (159).

If the assessment of neighborhood disadvantage is extended to include measures other than ADI, additional studies highlight associations with numerous neurological conditions. Pase et al (2022) reported that better memory and lower dementia risk scores were correlated with less neighborhood disadvantage in the Australian Healthy Brain Project cohort (160). In addition, greater disadvantage has been associated with primary pathological features of AD including neurofibrillary tangles and amyloid plaques (161). In young adults, Bell et al (2021) utilized a very similar model to ADI found that neighborhood disadvantage based on census block groups was negatively correlated with quantitative anisotropy on DTI, suggesting that white matter microstructure disruptions were more prevalent in adults with lower SES (162). Neighborhood disadvantage has also been associated with a higher risk of incident ischemic stroke in white individuals (163). There are plethora of studies linking neighborhood disadvantage with significant correlations to various neurological disorders and findings suggest that socioeconomic factors may play a role in the development and adaptation of the human brain.

Clinical Implications

Understanding the relationship of geospatial metrics of neighborhood disadvantages as a risk indicator and its impact on epilepsy may inform proper care, treatment delivery, and policy for underserved and disadvantaged patients. The ADI metric of neighborhood disadvantage captures additional variables that many of the individual level measures do not in existing literature. Further investigation of neighborhood-level deprivation effects on white matter integrity may advance understanding of the network abnormalities that underlie cognitive and behavioral comorbidities of epilepsy. The present study highlights evidence of a relationship between high neighborhood disadvantage and aberrant white matter tract structure and

connectivity in TLE patients. Disadvantage information for patients is readily attainable using only the patients' residential address (137). Thus, the accessibility of this information can serve as a meaningful tool for clinicians for decision making for disadvantaged patients and public health officials for policies aimed at reducing disparities for at-risk populations (137).

Limitations and Future Directions

This study has limitations. First, our sample size was modest within some ADI groups. Larger participant pools will provide greater power to detect statistical significance such as in the trends observed here. Second, this investigation was cross-sectional and prospective studies examining ADI associations with white-matter connectomes and other measures of brain integrity are essential to gain insight into the origin and progression of identified compromised brain integrity over time. Third, the ADI is composed of 17 census metrics from four categories and the relative explanatory power of these metrics and categories, as well as the comparative explanatory power of ADI compared to traditional clinical epilepsy variables (e.g., age of onset, laterality of TLE, antiseizure medication effects) on connectome status will be informative going forward. Fourth, the ADI is based on the participants' *current* area of residence. Why (e.g., independent or reflective of social drift) and how the duration of exposure to disadvantage on brain integrity requires examination. Finally, it should be remembered that the ADI is a reflection of advantage/disadvantage within a geographic area reflected by zip code. There may be variation across individuals within any target geographic area.

While the association reported here is provocative, establishing a causal link requires further work. Social and environmental factors could affect epilepsy progression/severity and influence the risk of associated comorbidities including cognitive, academic and psychiatric complications. This could occur through multiple mechanisms including but not limited to a lack of access to quality medical care, increased exposure to pollutants and toxins, poor nutrition, increased stress, and many other well-known limitations inherent in disadvantaged areas. Thus, work to identify causal factor(s) and their modifiability will require much work. Conversely, the

direction of causality could include the so-called “social drift model” where known complications of epilepsy (e.g., decreased education, unemployment, depressed income, psychiatric comorbidity) could lead to life in disadvantaged neighborhoods. These need not be mutually exclusive as some but not all patients could follow one of the two pathways. But again it is important to note that epilepsy has been found to be more prevalent among individuals in lower (more disadvantaged) socio-economic groups, independent of social drift and other known epilepsy risk factors (139, 140, 164).

Challenges to understanding the underlying causal links may be mitigated in a study with a large sample size that investigates the longitudinal changes of neighborhood indexes in relation to epilepsy onset, but the causal link may still be difficult to establish as some epilepsy patients have a strong family history that may predispose them not only to the genetics of the illness but also degraded neighborhood indexes.

Finally, while we focus here on disadvantage in human populations, an arguably relevant and important literature is that concerned with advantaged or enriched environments in animal populations. This longstanding highly developed literature has extended into epilepsy, demonstrating that antecedent exposure to enriched environments slows the development of epilepsy after an initial insult, and favorably modifies severity, course and associated comorbidities, including animal models of TLE as reviewed by Löscher and Stafstrom (2023) (165). The effects of environmental enrichment may affect the behavior of animals before, during, and after the induction of epilepsy. These effects have been observed in a variety of experimental models including chemoconvulsant-induced status epilepticus leading to chronic epilepsy, kindling, and mutant models. The favorable influences of environmental enrichment include reduced seizure frequency and progression, modification of circuit functions and plasticity, and reduction of anatomic alterations associated with repeated seizures (166). Findings that environment can impact many core features of experimental epilepsy is intriguing and arguably supports the general thesis that investigation of advantaged and in our case

disadvantaged environments in humans with epilepsy is an important path to pursue.

Acknowledgements

We are immensely grateful for the support from the AES Pre-doctoral Fellowship, T32 GM140935, UW MSTP Radiology Fellowship, and NIH grants U01NS093650, R01NS123378, R01NS105646, R01NS105646, R01NS111022, P50HD105353. In remembrance of Steven Whitman, PhD—friend, colleague, mentor and tireless advocate of the social determinants of health.

Conflicts of Interest/Ethical Publication Statement

None of the authors has any conflicts of interest to disclose. We confirm that we have read Epilepsia's position on issues involved in ethical publication and affirm that this report is consistent with those guidelines.

CHAPTER 5

DISCUSSION

Of the 3.4 million patients with epilepsy in the United States, over 35% will be deemed intractable and fail to achieve adequate seizure control with anti-seizure medications (10, 167). Patients with focal epilepsy represent a significant proportion of those with intractable epilepsy and are associated with high risks of cognitive and psychosocial co-morbidities (19, 20). Other management include surgical intervention, neurostimulation, and ketogenic dietary therapy. Epilepsy surgery can offer seizure freedom in only half of the patient population, but commonly fail due to incomplete focus delineation and resection.

Current methods in predicting the clinical course of medication or surgical treatment of focal epilepsies are inadequate. There are no reliable biomarkers that can currently predict disease progression, drug resistance, or the severity of cognitive and psychiatric comorbidities in patients with focal epilepsy. Therefore, work from this thesis strives to identify biomarker candidates via structural MRIs. Specifically this work characterized white matter microstructural abnormalities via DTI and the whole brain white matter connectivity networks via DWI connectome of patients with focal epilepsies. Our datasets included the clinical FCD patients and ECP TLE patients; both datasets are clinically representative demonstrating phenotypical heterogeneity in the general population of their respective disease states.

Diffusion Tensor Imaging Microstructural Abnormalities

Chapter 2 investigated white matter tract changes associated with childhood onset focal epilepsy secondary to FCD and were associated with neurocognitive dysfunction. We investigated white matter tract microstructural differences between patients with epilepsy secondary to FCD and typically developing (TD) healthy controls with respect to fractional anisotropy (FA), mean diffusivity (MD), and radial diffusivity (RD) indices, using rigorous preprocessing techniques. Furthermore, the study applies data harmonization via ComBat to eliminate methodological constraints, such as differences in DTI scanning parameters, to reveal true biological differences. Results demonstrated widespread microstructural alterations in white

matter tracts depicted by decreased FA, and increased diffusivities MD and RD across statistically significant clusters. Data harmonization was impactful for analyzing heterogenous clinical datasets, through adjustment of parameter differences, thereby highlighting underlying biological differences. Consistent with previous literature (109), FA reductions were most prominent in forceps minor, implicated in executive function, and the superior longitudinal fasciculus, involved in language processing. Additionally, MD and RD results revealed significant increases within these same tracts, giving further evidence of its abnormalities in our FCD cohort. While few studies have explored FCD-associated white matter region correlations with increases in MD and RD, DTI studies have well-documented evidence of significantly higher diffusivity in regions that are concordant with our study findings including the uncinate fasciculus, the inferior fronto-occipital fasciculus, and the inferior longitudinal fasciculus (104).

White Matter Connectome Network Abnormalities

Chapter 3 and 4 characterized the global white matter connectome abnormalities in patients with TLE of the whole brain, and associated TLE white matter connectome findings with neighborhood deprivation via ADI, respectively. Our study is the first large-scale TLE DWI connectome study providing connectome quality multi-shell DWI data with reverse phase encoded pair of acquisitions. This study employed TFNBS, a local approach offered by TFNBS is complementary to the global approach offered by graph theoretic measures and offer spatially specific biological interpretations. Our results highlighted that global analysis of the white matter connectome differences between TLE patients and HCs reveal 97 significant connections after statistical correction with widespread reductions in TLE CSA. The top aberrant edges originate from frontal to frontal, frontal to temporal, frontal to parietal, and temporal to parietal regions. Furthermore, this study showcased modest and trend-level differences in white matter connectome between TLE patients with a history of FBTC seizures vs. those who never had a FBTC seizure. The uncorrected results do demonstrate that overall, the FBTC group had decreased CSA when compared to the non-FBTC group but did not survive multiple

comparisons correction.

Chapter 4 investigated the relationship between a geospatial metric of neighborhood disadvantage (AD) and white matter network connectivity assessed by multi-shell connectome DWI data and graph theory analyses. The findings illustrate associations between discrete white matter tract abnormalities and increased disadvantage as indexed by the ADI. Specifically, CSA was decreased within the more disadvantaged compared to less disadvantaged TLE group. While the initial corrected results were at trend level, corrected sensitivity analyses of the ADI quintile extreme groups revealed significantly decreased CSA in the most compared to the least disadvantaged ADI group. These analyses expand the understanding of deprivation effects in TLE which to date have focused on epilepsy incidence/prevalence, care and outcomes—to a reflection of the impact of ADI on brain health, specifically white matter integrity. Our sensitivity analysis revealed two significant connection differences reflected in decreased CSA in the edges within the temporal to parietal and temporal to occipital regions. Importantly, the findings also inform the more general impact of TLE on white matter health through findings demonstrating that both low and high disadvantage TLE participants showcased more white matter abnormalities compared to both the low (and high) disadvantaged controls respectively, reflect in the decreased age and sex adjusted expected CSA in the disadvantaged TLE groups compared to their respective control groups. Consistent with expectations based on the existing DTI literature, these findings indicate that TLE exerts a general adverse impact on DWI connectome status regardless of neighborhood adversity (144, 147). Furthermore, two-way interaction analyses demonstrating both ADI and TLE diagnoses impact shows that more disadvantaged TLE groups had widespread significant connections that exhibited decreased white matter CSA, while less disadvantaged TLE group still showed four significant differences with decreased CSA when compared to the more disadvantaged HC group**.** These findings are consistent with the general notion that TLE is a network disorder involving regions beyond the epileptogenic zone, evidenced by aberrant white matter tracts with nodes originating from

widespread regions of the brain, while providing some evidence that ADI may be associated and further contribute with white matter structural abnormalities.

Neurocognitive Association in Focal Epilepsies

In Chapter 2, white matter microstructural changes (via FA, MD, and RD) were associated with neurocognitive dysfunction. Study participants took assessments with cognitive metrics including fluid reasoning index (FRI), visual spatial index (VSI), and verbal comprehension index (VCI). Our results found MD to have moderately negative correlations with VSI. RD was also negatively correlated with FRI and VSI. Lastly, FA was positively correlated with FRI and VSI. These directionalities illustrate that decreased anisotropy and increased diffusivity are associated with lower cognitive scores, which is consistent with our hypothesis as increasing MD and RD (and decreasing FA) are indicative of aberrant structural integrity. Currently, there is minimal literature exploring these specific neuropsychological factors in FCD and DTI specifically, though a previous study has reported impaired neuropsychological function in children with non-lesional localization-related epilepsy associated with white matter abnormalities (111). In addition, some specific regions we found correlated with lower FA and high MD and RD included regions that are important for memory processing, such as the uncinate fasciculus and the anterior thalamic radiation (102). Thus, investigations into executive function and memory in FCD will be beneficial to further correlate white matter tracts with abnormal DTI metrics.

In Chapter 3, our study assessed cognitive impairment status with white matter connectome status in TLE patients. Results indicate that focal and generalized cognitive impairment showed very similar modest and trend-level associations with white matter connectome findings when compared to controls. In comparison to the no cognitive impairment group of TLE patients, both cognitively impaired TLE groups exhibited more than twice the number of significant tracts with decreased CSA. Existing literature on DTI-based white matter connectomics of TLE patients have highlighted abnormalities in language and memory. Firstly,

Kaestner et al. demonstrated that the structural connectome model was superior to models based on white matter microstructural or clinical features in predicting language impairment (127). Similarly, Munsell et al. showed that Boston Naming Test scores, a proxy for language performance, could be predicted using a model based on combined eigenvector node centrality (128). Network-based superficial white matter analyses have shown abnormalities in graph theory metrics, such as decreased global efficiency, in language and memory-impaired subjects (129). Structural network topology revealed increased characteristic path length in a subgroup of TLE patients with the most pronounced cognitive impairments across multiple domains including memory and verbal comprehension (116). Altogether along with our results, it is evident that graph theoretic characterization of the white matter connectome serves as a useful biomarker for cognitive impairment in TLE. Future studies should identify additional biomarkers that are needed to discriminate between focal vs. generalized cognitive impairment.

Limitations and Future Directions

The FCD study was limited to a modest sample size and precluded detailed analyses of specific subgroups based on lobar hemispheric distribution of FCD lesions or verification of FCD histological subtypes based on histopathological analysis. Thus, these subgroups may have intrinsic biological network variations that can potentially impact interpretation of TBSS-based analysis between FCD and control white matter microstructure differences. Our results did not provide. Causal etiology for the neurocognitive dysfunction that was observed in a significant proportion of FCD patients. It is also unclear whether changes were primarily related to the cortical dysplasia or are secondary due to changes of ongoing epilepsy or medication use.

The ECP DWI connectome study had several limitations. The sample size was modest for the cognitively impaired TLE patient analyses, so a future study with a greater number of participants will be beneficial to provide adequate power to the analysis. While there are some significant differences between the control and TLE group; however, our analyses corrected for

the effect of age. The ECP, which aims to understand phenotypical heterogeneity in the more general population of TLE, contains a more representative sample of TLE patients than typically investigated in surgical series, only a subset of participants (35%) thus underwent the gold standard of ictal monitoring. Future studies may scrutinize the laterality effects in a completely ictally monitored cohort, but such cases may capture mostly the severe end of the epilepsy spectrum and is deemed unrepresentative of the general population of TLE. One pervasive problem in the study of TLE is the underlying heterogeneity of the disease and the lack of a definitive gold standard for diagnosis. Even with the best tools available, most patients with bitemporal lobe epilepsy required 41.6 days of EEG monitoring to detect such bilateral seizures, and some may require up to one year (130). Thus, we can never be sure of a “definitive” seizure laterality and TLE diagnosis. Additionally, drastic limiting of participant selection results in its own type of selection bias where results may be questionably extrapolated to the representative and less complicated TLE patient. The purpose of the ECP was to get a cross-sectional sampling of patients with TLE defined in the typically clinical and pragmatic method with the help and oversight of epileptologists.

The ECP DWI ADI study also has limitations. The sample size was modest within some ADI groups. Larger participant pools will provide greater power to detect statistical significance such as in the trends observed here. Second, this investigation was cross-sectional and prospective studies examining ADI associations with white-matter connectomes and other measures of brain integrity are essential to gain insight into the origin and progression of identified compromised brain integrity over time. Third, the ADI is composed of 17 census metrics from four categories and the relative explanatory power of these metrics and categories, as well as the comparative explanatory power of ADI compared to traditional clinical epilepsy variables (e.g., age of onset, laterality of TLE, antiseizure medication effects) on connectome status will be informative going forward. Fourth, the ADI is based on the participants’ *current* area of residence. Why (e.g., independent or reflective of social drift) and how the duration of

exposure to disadvantage on brain integrity requires examination. Finally, it should be remembered that the ADI is a reflection of advantage/disadvantage within a geographic area reflected by zip code. There may be variation across individuals within any target geographic area. Challenges to understanding the underlying causal links may be mitigated in a study with a large sample size that investigates the longitudinal changes of neighborhood indexes in relation to epilepsy onset, but the causal link may still be difficult to establish as some epilepsy patients have a strong family history that may predispose them not only to the genetics of the illness but also degraded neighborhood indexes.

Conclusions

Taken together, this dissertation contributes to the understanding of the underlying structural white matter plasticity in patients with focal epilepsy and further substantiates the concept that TLE is a progressive network disorder involving ongoing neural plasticity induced by seizure activity. Both the TLE and FCD datasets comprise of a heterogeneous but clinically representative group of patients, with the goal of understanding phenotypic heterogeneity in the more general populations as opposed to the refractory or surgical cases. Through novel methods of data harmonization and TFNBS, we elucidated aberrant white matter differences in microstructure and integrity, as well as abnormalities in white matter network connectivity. We also correlated cognitive impairment with these measures, implicating that cognition is an integral component of epilepsy burden. Furthermore, we establish that patients with more neighborhood disadvantage, using the area deprivation index, are correlated with greater abnormalities in white matter connectivity, indicating that socioeconomic disparities must be accounted in terms of clinical management and care. The work outlined in this dissertation lays the foundation for many future experiments. Future resting-state fMRI studies elucidating the functional networks can be correlated with the white matter structural connectome findings. Furthermore, surface based cortical morphometry studies incorporating gyrification, sulcal depth, fractal dimensionality, gray matter volume, and cortical thickness can provide additional

structural insights into focal epilepsy plasticity, as well as surface-based connectome studies. Understanding the etiology, the pathophysiology, and the structural plasticity of the focal epileptic brain may serve to inform care, management, and policy for our patients.

APPENDICES

Appendices A – C

Appendix A

Supplemental Materials for Chapter 2:

Application of Data Harmonization and Tract-Based Spatial Statistics Reveals White Matter Structural Abnormalities in Pediatric Patients with Focal Cortical Dysplasia

Supplemental Tables 2.1-2.3

Supplemental Figures 2.1-2.4

DTI Measure	Cluster #	JHU White Matter Tractography Atlas	Confidence (%)
FA	C15	Forceps minor (Fm)	64.125
FA	C19	Superior longitudinal fasciculus L (SLF-L)	43.533
FA	C21	Superior longitudinal fasciculus R (SLF-R)	40.383
MD	C12	Superior longitudinal fasciculus L (SLF-L)	62.185
MD	C5	Inferior fronto-occipital fasciculus L (IFOF-L)	52.333
MD	C7	Uncinate fasciculus L (UF-L)	41.500
RD	C20	Superior longitudinal fasciculus L (SLF-L)	71.333
RD	C21	Superior longitudinal fasciculus R (SLF-R)	46.571
RD	C11	Inferior fronto-occipital fasciculus L (IFOF-L)	42.000

Supplementary Table 1. Representative statistically significant clusters with group differences. The membership of these clusters in neuroanatomically labeled tracts according to the JHU White Matter Tractography Atlas is shown ranked by the average probability of the membership.

DTI Metric	Cognitive Indices	Corrected vs. Uncorrected p value	Harmonized vs. Original DTI	Correlation Coefficient
FA	FRI	Corrected	Harmonized	0.67
FA	FRI	Corrected	Original	0.5
FA	VCI	Uncorrected	Harmonized	0.15
FA	VCI	Uncorrected	Original	0.32
FA	VSI	Corrected	Harmonized	0.59
FA	VSI	Corrected	Original	0.47
MD	FRI	Uncorrected	Harmonized	0.07
MD	FRI	Uncorrected	Original	0.05
MD	VSI	Uncorrected	Harmonized	-0.49
MD	VSI	Uncorrected	Original	-0.18
RD	FRI	Uncorrected	Harmonized	-0.43
RD	FRI	Uncorrected	Original	-0.31
RD	VCI	Uncorrected	Harmonized	-0.05
RD	VCI	Uncorrected	Original	0.02
RD	VSI	Uncorrected	Harmonized	-0.51
RD	VSI	Uncorrected	Original	-0.36

Supplementary Table 2. Neuropsychological testing correlations with DTI metrics. This table details the harmonized and original median correlation coefficients of associations of neuropsychological testing of FRI, VCI, and VSI with each DTI metric (FA, MD, and RD). Correlation between cognitive function and FA-FRI and FA-VSI respectively, survived multiple comparisons correction. The other correlations are included to demonstrate trend-level relationships between cognitive function and individual DTI indices.

DTI Measure	Cognitive Index	Cluster #	JHU White Matter Atlas Tractography	Confidence (%)
FA	FRI	C02	Superior longitudinal fasciculus R	45.42
FA	VCI	C81	Superior longitudinal fasciculus L	69.90
FA	VSI	C04	Superior longitudinal fasciculus R	43.76
MD	FRI	C6	Forceps major	15.00
MD	VSI	C31	Superior longitudinal fasciculus R	67.70
RD	FRI	C69	Superior longitudinal fasciculus R	44.00
RD	VCI	C12	Inferior fronto-occipital fasciculus R	54.50
RD	VSI	C30	Anterior thalamic radiation R	37.67

Supplementary Table 3. Representative statistically significant clusters with association with neuropsychological index measures. The membership of these clusters in neuroanatomically labeled tracts according to the JHU White Matter Tractography Atlas is shown ranked by the average probability of the membership.

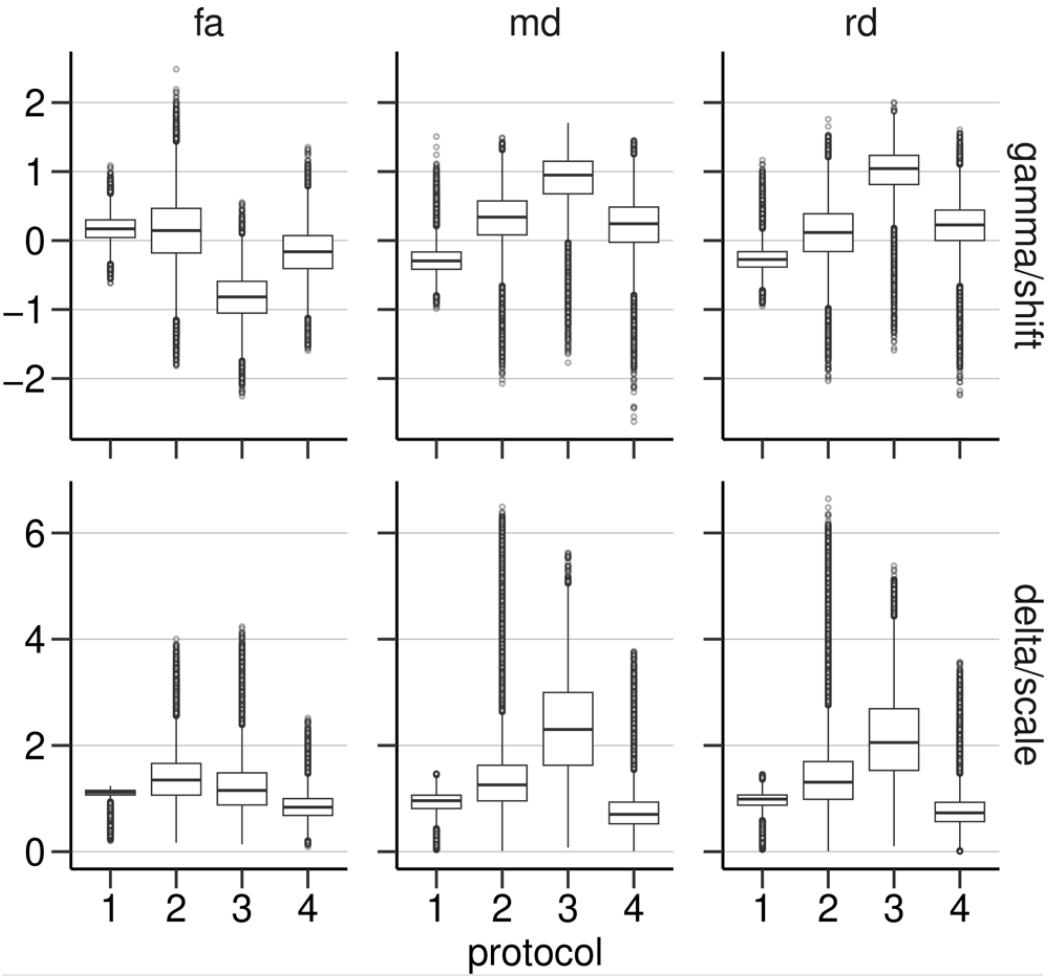

Supplementary Figure 1. Distributions of Offset/Shift/gamma and slope/scale/delta parameters estimated at each voxel for each protocol and DTI measure. Data from MR imaging protocols 2 and 3 is visualized to shift and scale relatively more compared to that of MR imaging protocols 1 and 4. These shifts and scales are estimated such that the distributions of the measures from the different protocols align to a common distribution (similar to images being aligned to an unbiased population average). Differences in DTI include MRI field strength (1.5T vs. 3T vs. 3T-weighted), b-values (800 s · mm^{-2} vs. 1000 s · mm^{-2}), number of volumes (26 vs. 31 vs. 41) and number greater than b>0 (25 vs. 30 vs. 40). Please also see Supplementary Figure 4.

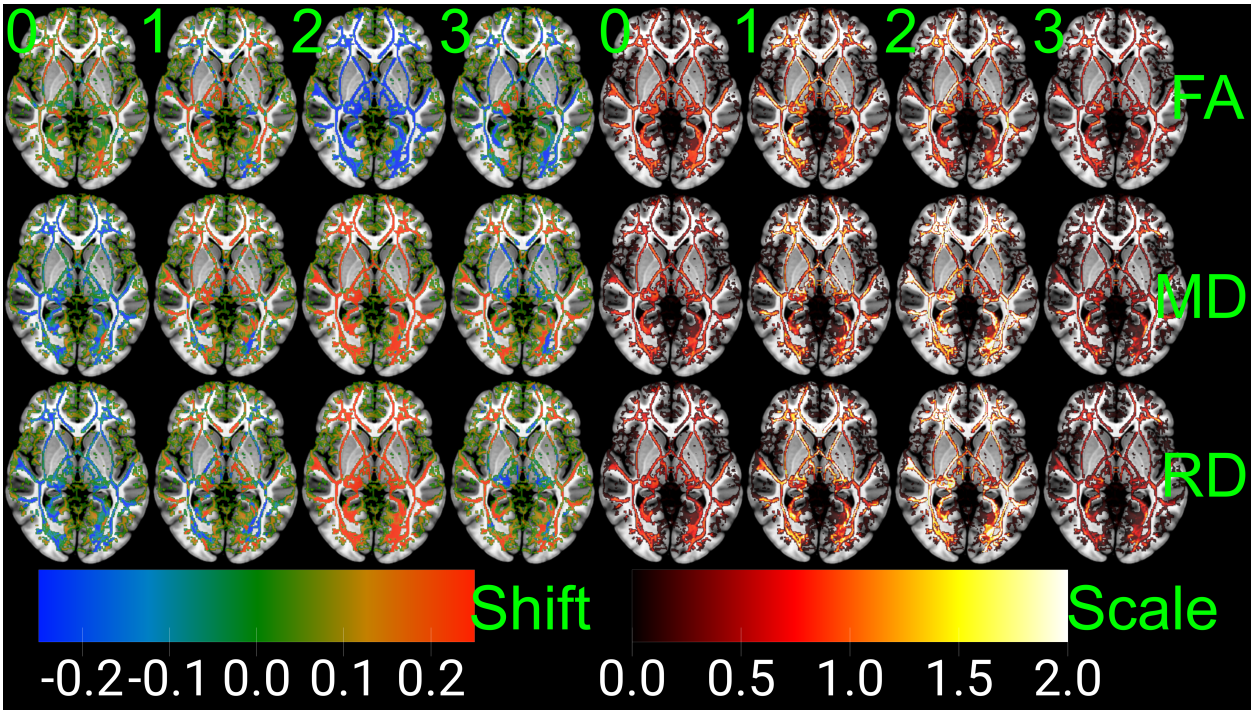

Supplementary Figure 2. Axial slices showing the shift and scale effects estimated for each of the DTI measures (FA, MD, RD) and each of the four protocols. Since the harmonization was performed on the data from the skeleton voxels of the white matter (pre-processing step in the tract based spatial statistics (TBSS)), the effects are shown for those voxels. Similar to the box plots in **Supplementary Figure 1,** we can observe that data from MRI protocols 2 and 3 get shifted and scaled relatively more compared to MRI protocols 1 and 4. We can also observe that for protocol 1 there are shifts in both directions (>0 and <0) across the voxels for FA, more so compared to the other protocols and measures. This pattern can also be observed in **Supplementary Figure 3** (second column, first and third rows).

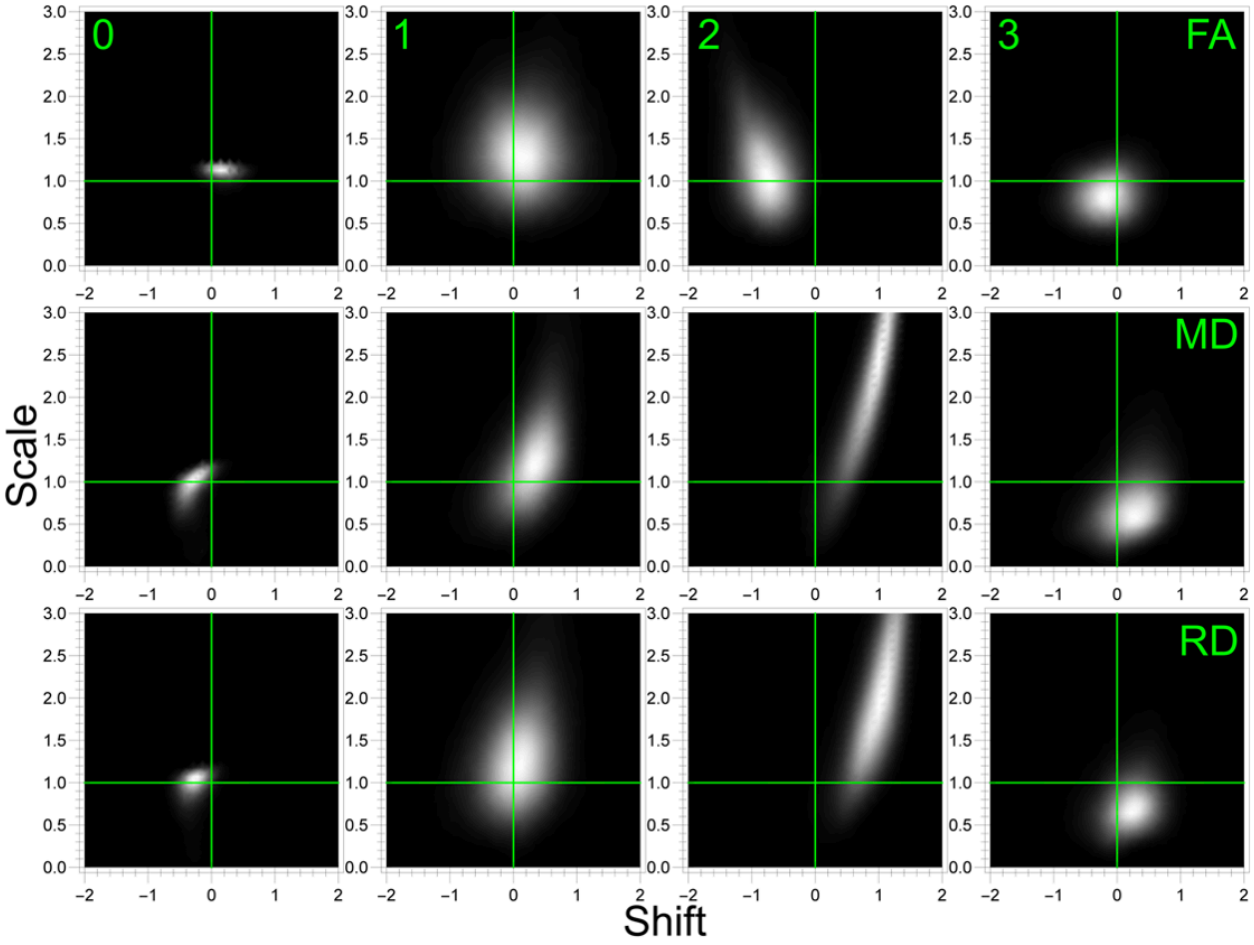

Supplementary Figure 3. Probability density plots for the bivariate distribution of shift (additive) and scale (multiplicative) effects estimated from data harmonization. The plots are shown for each of the DTI measures and the protocol. The no effect contour lines are shown in green. We can observe that the effects are bigger for protocols 2 and 3 and more so for MD and RD.

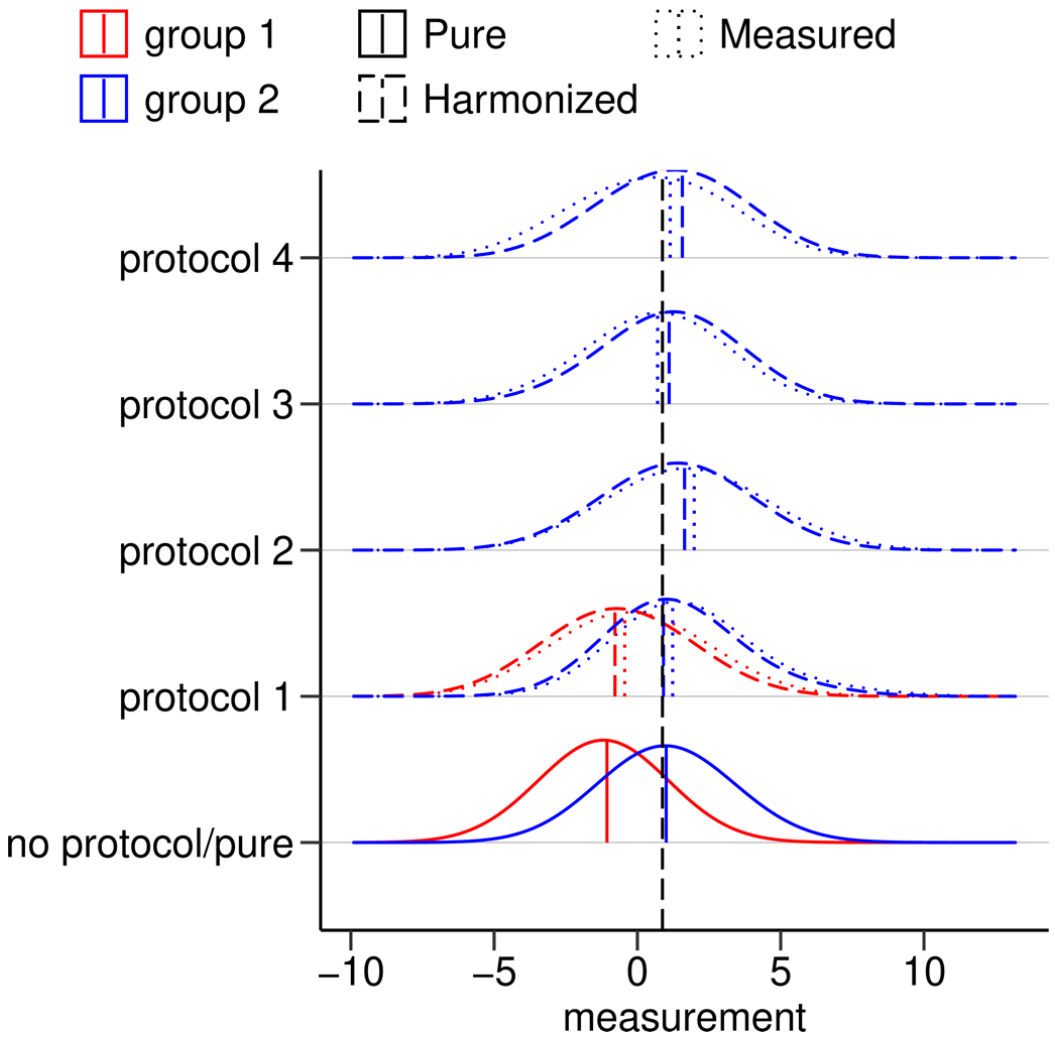

Supplementary Figure 4. Simulated data harmonization and protocol effects.
To help provide a graphic illustration of the approach, we have developed an interactive R application (https://nadluru.shinyapps.io/harmonization_demo/) with simulated measurements and protocol effects with a setup of groups and protocols similar to that in the study. The figure illustrates distributions of measures for two groups with and without protocol (no protocol/pure) effects simulated with setup modeled after the present study. Harmonized data are shown using dashed lines and measured (non-harmonized) data are shown using dotted lines. The median values are shown using vertical lines. The black dashed vertical line shows the median across the protocols.

We can observe that the harmonization aligns the distributions from different protocols to a common one, as can be seen by black median line aligning with the other dashed medians as closely as possible *while maintaining the group effect of interest*.

We can also observe, as can be seen by the gap between red and blue median lines, *the group effect being maintained while protocol effects get normalized by harmonization*.
Users of this simulated R application can select different parameters, like the number of voxels, participants, mean and variance of the groups, the protocol effects and see the effect of those on the harmonization output.

Appendix B

Supplemental Materials for Chapter 3:

Characterizing White Matter Connectome Abnormalities in Temporal Lobe Epilepsy Patients Using Threshold-Free Network-Based Statistics

Supplemental Figures 3.1-3.4

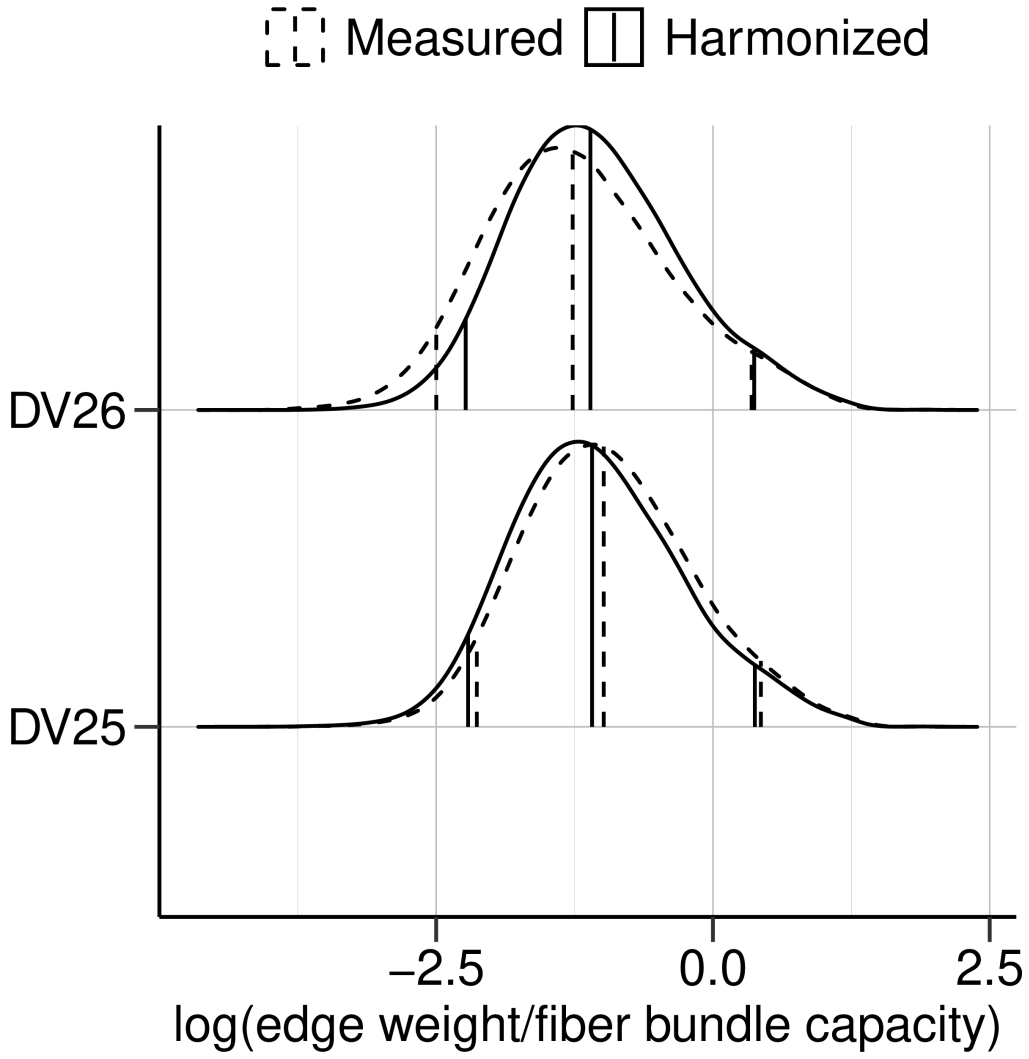

Supplementary Figure 1. Pre and Post Data Harmonization. The distributions of the log-transformed edge weights (fiber bundle capacities) before and after the software update (from DV25 to DV26). We can notice that the data harmonization aligns the two distributions to a common distribution as evidenced by the aligned quantiles.

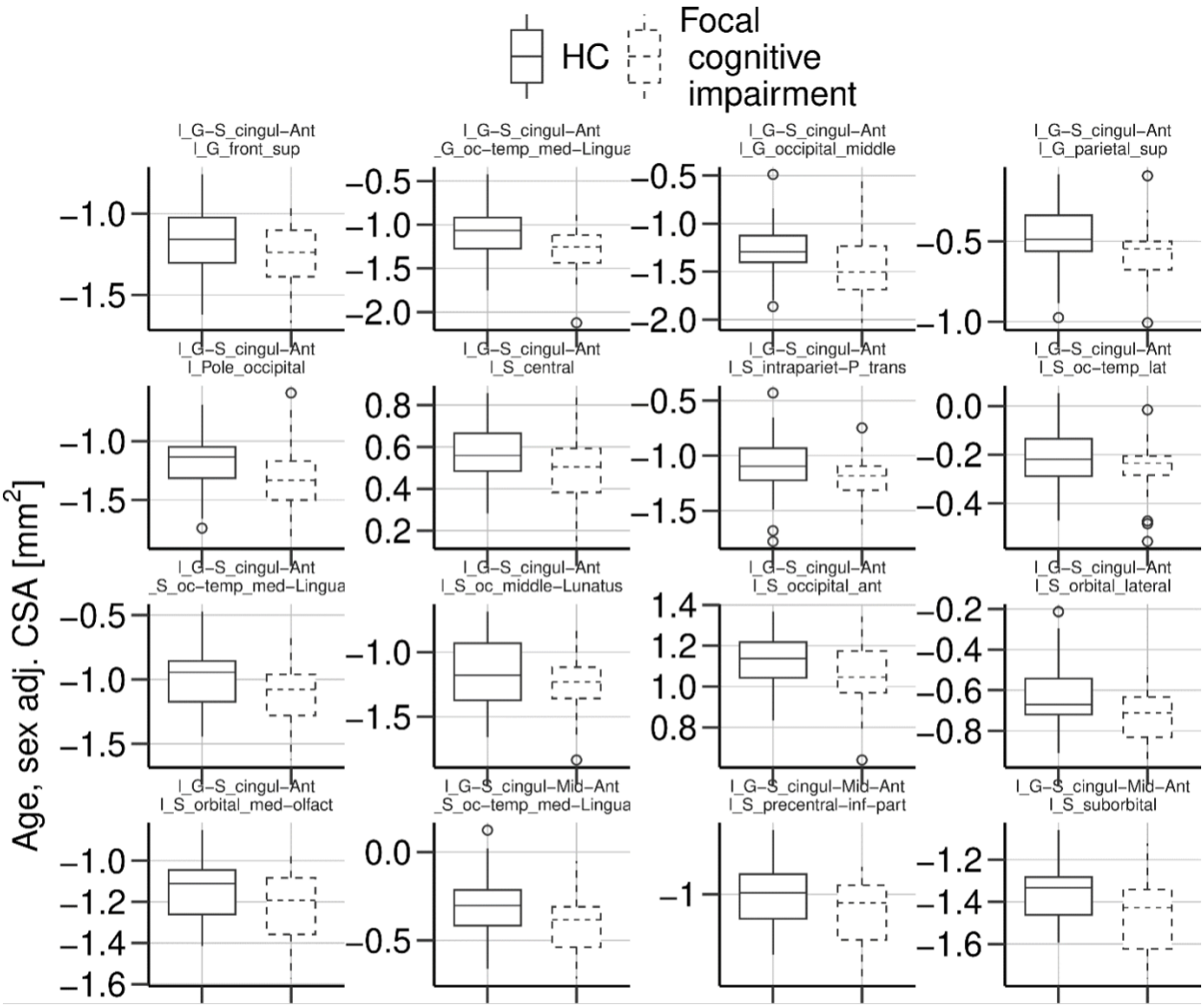

Supplementary Figure 2. Representative TLE with Focal Cognitive Impairment vs. HC White Matter Connectome Tract Cross Sectional Areas. Illustrated here are 16 representative analyses after multiple comparisons correction of TLE with focal cognitive impairment vs. HC DWI connectome abnormalities. The results indicate that TLE patients with focal cognitive impairment exhibit lower white matter tract age and sex adjusted expected CSA when compared to HCs. The originating nodes and region locations are noted above each box plot. TLE = temporal lobe epilepsy; HC = healthy control; DWI = diffusion weighted imaging; CSA = cross-sectional area of the white matter.

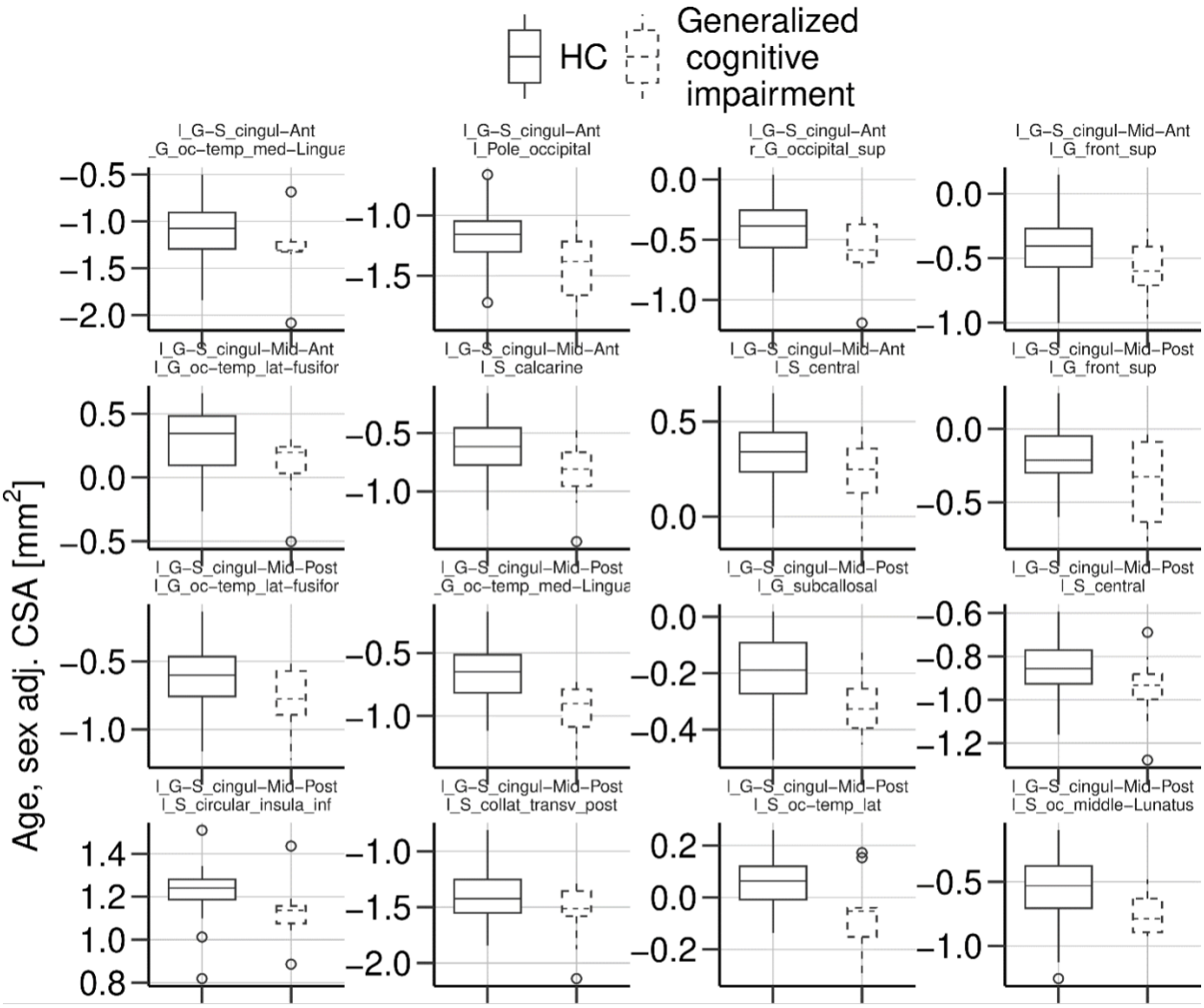

Supplementary Figure 3. Representative TLE with Generalized Cognitive Impairment vs. HC White Matter Connectome Tract Cross Sectional Areas. Illustrated here are 16 representative analyses after multiple comparisons correction of TLE with generalized cognitive impairment vs. HC DWI connectome abnormalities. The results indicate that TLE patients with generalized cognitive impairment exhibit lower white matter tract age and sex adjusted expected CSA when compared to HCs. The originating nodes and region locations are noted above each box plot. TLE = temporal lobe epilepsy; HC = healthy control; DWI = diffusion weighted imaging; CSA = cross-sectional area of the white matter.

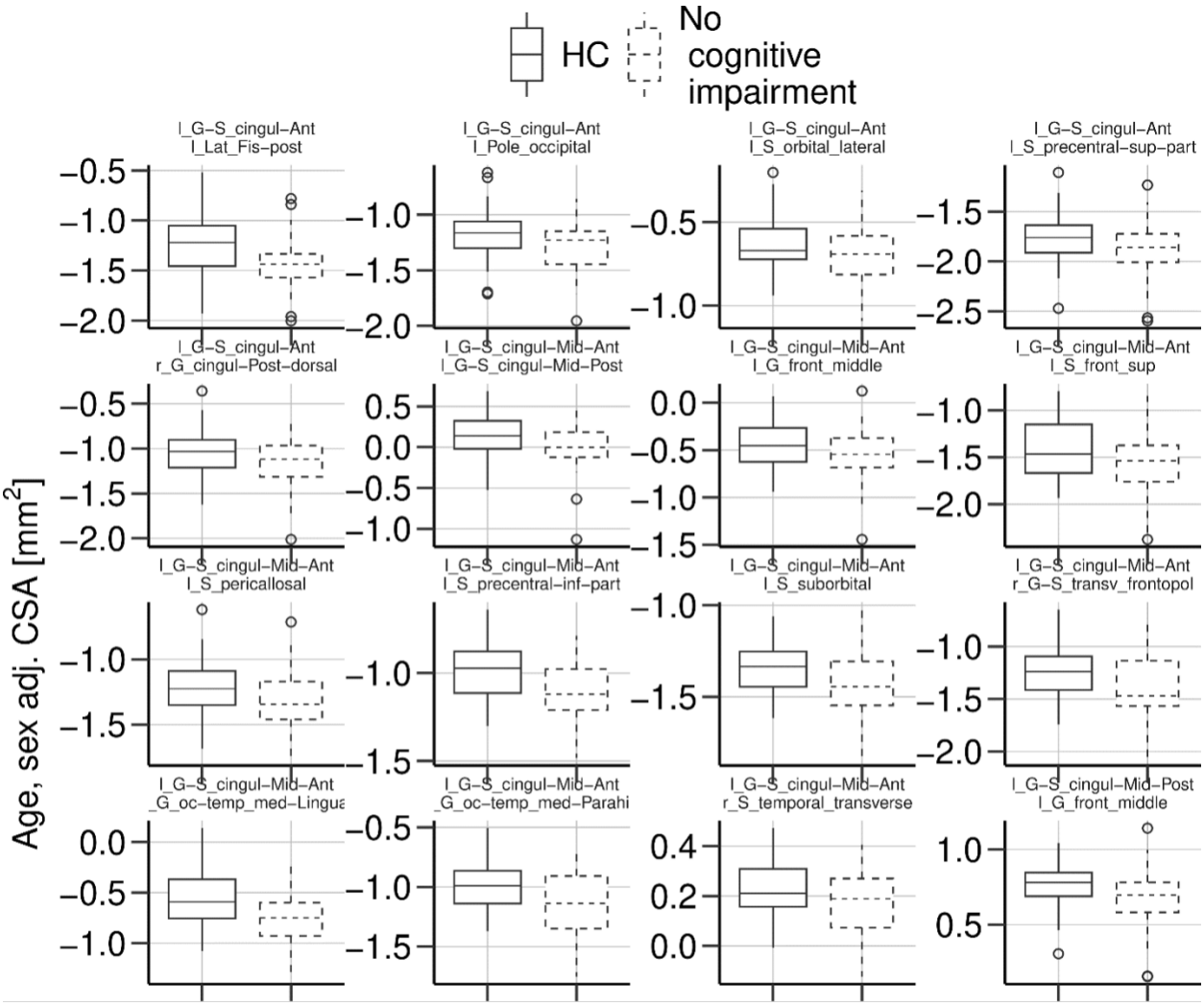

Supplementary Figure 4. Representative TLE with No Cognitive Improvement vs. HC White Matter Connectome Tract Cross Sectional Areas. Illustrated here are 16 representative analyses after multiple comparisons correction of TLE who are cognitively intact vs. HC DWI connectome abnormalities. The results indicate that TLE patients with no cognitive impairment exhibit lower white matter tract age and sex adjusted expected CSA when compared to HCs. The originating nodes and region locations are noted above each box plot. TLE = temporal lobe epilepsy; HC = healthy control; DWI = diffusion weighted imaging; CSA = cross-sectional area of the white matter.

Appendix C

Supplemental Materials for Chapter 4:

Association of Neighborhood Deprivation with White Matter Connectome Abnormalities in Temporal Lobe Epilepsy

Supplemental Figures 4.1-4.4

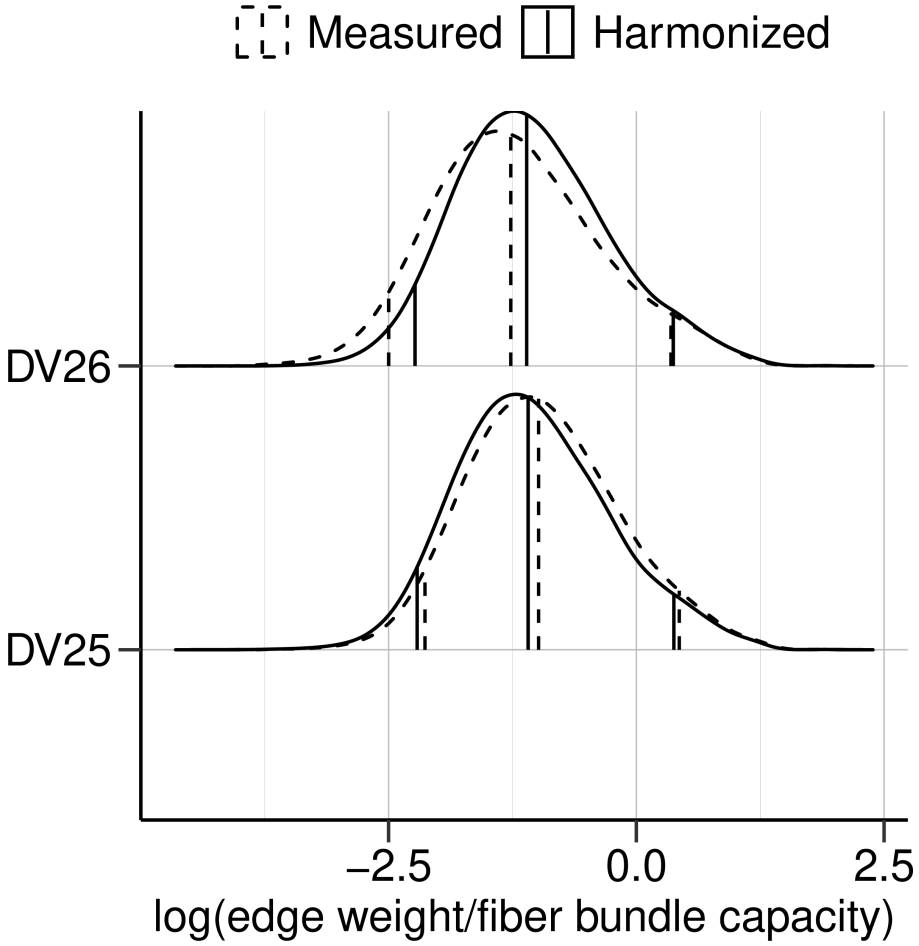

Supplementary Figure S1. Pre and Post Data Harmonization. The distributions of the log-transformed edge weights (fiber bundle capacities) before and after the software update (from DV25 to DV26). We can notice that the data harmonization aligns the two distributions to a common distribution as evidenced by the aligned quantiles.

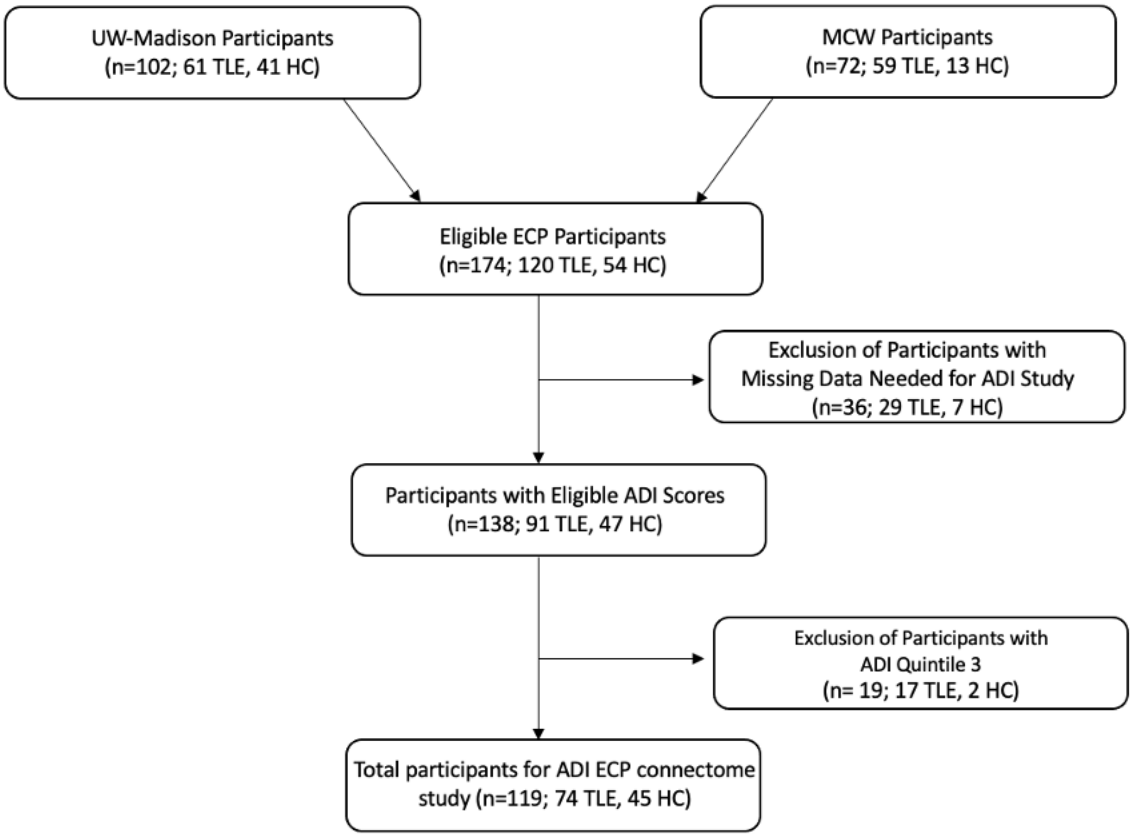

Supplementary Figure S2. Flowchart of patient inclusion and exclusion of the ECP DWI connectome study. UW-Madison = University of Wisconsin Madison, MCW = Medical College of Wisconsin, ECP = epilepsy connectome project, TLE = temporal lobe epilepsy, HC = healthy controls, DWI = diffusion weighted imaging.

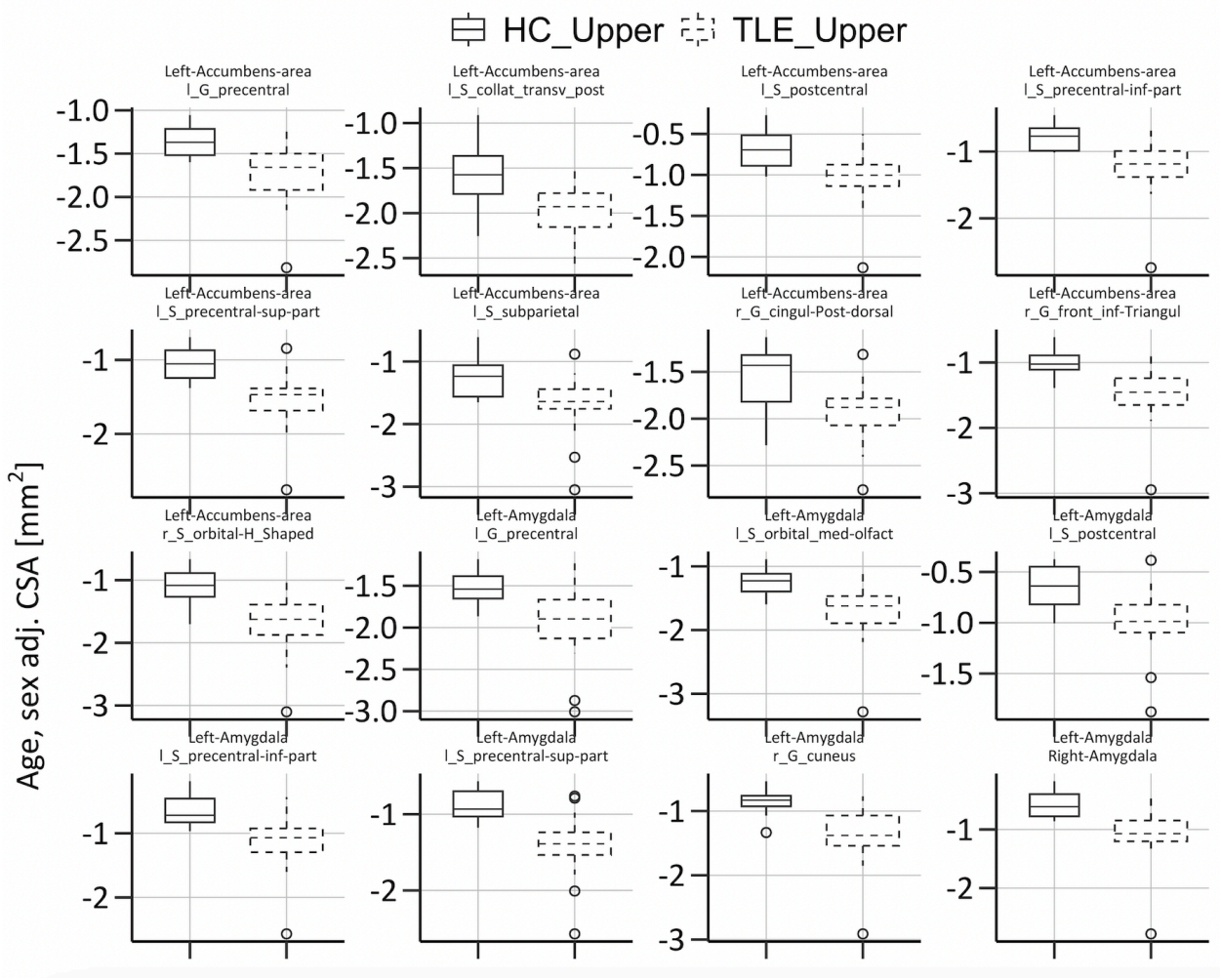

Supplementary Figure S3. Representative More Disadvantaged TLE vs. More Disadvantaged HC ADI Analyses. Depicted are 16 representative corrected analyses showing upper (more disadvantaged) ADI TLE patients vs. upper (more disadvantaged) HC patients. The results indicate that TLE patients who are more disadvantaged exhibit significantly lower white matter tract age and sex adjusted expected CSA when compared HCs in the same ADI group. The originating nodes and region locations are identified above each box plot. Lower = less disadvantaged ADI groups; Upper = more disadvantaged ADI groups; CSA = cross-sectional area of the white matter.

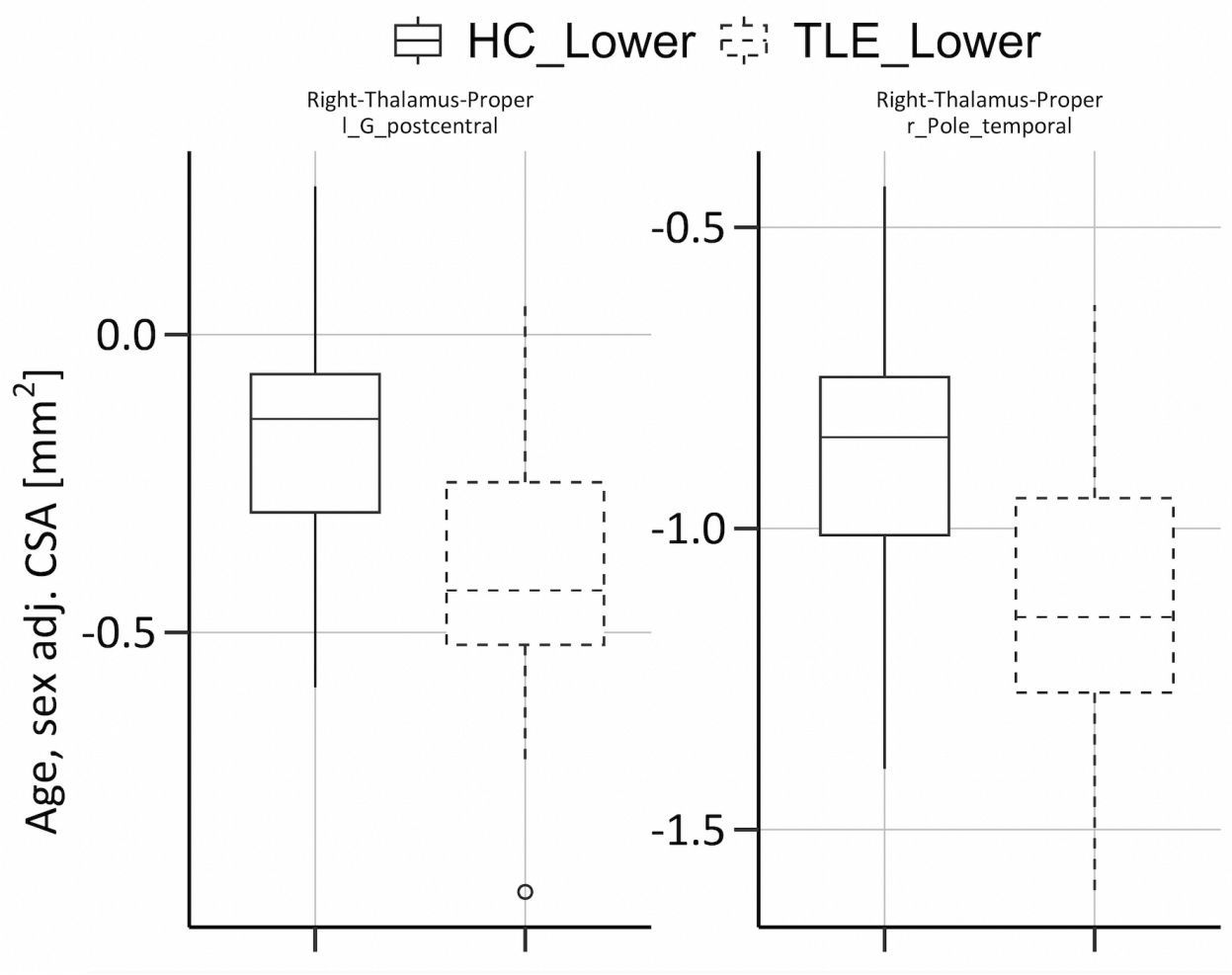

Supplementary Figure S4. Representative Less Disadvantaged TLE vs. Less Disadvantaged HC ADI Analyses. Depicted are 2 corrected analyses showing lower (less disadvantaged) ADI TLE patients vs. lower (less disadvantaged) HC patients. The results indicate that TLE patients who are less disadvantaged exhibit significantly lower white matter tract age and sex adjusted expected CSA when compared to HC of the same ADI category. The originating nodes and region locations are identified above each box plot. Lower = less disadvantaged ADI groups; Upper = more disadvantaged ADI groups; CSA = cross-sectional area

REFERENCES

1. Zack MM, Kobau R. National and State Estimates of the Numbers of Adults and Children with Active Epilepsy - United States, 2015. MMWR Morb Mortal Wkly Rep. 2017;66(31):821-5.
2. Global, regional, and national burden of neurological disorders, 1990-2016: a systematic analysis for the Global Burden of Disease Study 2016. Lancet Neurol. 2019;18(5):459-80.
3. Fisher RS, Acevedo C, Arzimanoglou A, Bogacz A, Cross JH, Elger CE, et al. ILAE official report: a practical clinical definition of epilepsy. Epilepsia. 2014;55(4):475-82.
4. Organization WH. Neurological Disorders – public health challenges. **Geneva**: World Health Organization; 2006. p. 232.
5. Begley CE, Famulari M, Annegers JF, Lairson DR, Reynolds TF, Coan S, et al. The cost of epilepsy in the United States: an estimate from population-based clinical and survey data. Epilepsia. 2000;41(3):342-51.
6. Berg AT. Epilepsy, cognition, and behavior: The clinical picture. Epilepsia. 2011;52 Suppl 1(Suppl 1):7-12.
7. LaFrance WC, Jr., Kanner AM, Hermann B. Psychiatric comorbidities in epilepsy. Int Rev Neurobiol. 2008;83:347-83.
8. Rakitin A, Liik M, Oun A, Haldre S. Mortality risk in adults with newly diagnosed and chronic epilepsy: a population-based study. Eur J Neurol. 2011;18(3):465-70.
9. Loscher W, Klitgaard H, Twyman RE, Schmidt D. New avenues for anti-epileptic drug discovery and development. Nat Rev Drug Discov. 2013;12(10):757-76.
10. Brodie MJ, Barry SJ, Bamagous GA, Norrie JD, Kwan P. Patterns of treatment response in newly diagnosed epilepsy. Neurology. 2012;78(20):1548-54.
11. Spencer SS, Berg AT, Vickrey BG, Sperling MR, Bazil CW, Shinnar S, et al. Predicting long-term seizure outcome after resective epilepsy surgery: the multicenter study. Neurology. 2005;65(6):912-8.
12. Téllez-Zenteno JF, Ronquillo LH, Moien-Afshari F, Wiebe S. Surgical outcomes in lesional and non-lesional epilepsy: A systematic review and meta-analysis. Epilepsy Research. 2010;89(2):310-8.
13. Téllez-Zenteno JF, Hernández-Ronquillo L. A review of the epidemiology of temporal lobe epilepsy. Epilepsy Res Treat. 2012;2012:630853.
14. Blümcke I, Thom M, Aronica E, Armstrong DD, Bartolomei F, Bernasconi A, et al. International consensus classification of hippocampal sclerosis in temporal lobe epilepsy: A Task Force report from the ILAE Commission on Diagnostic Methods. Epilepsia. 2013;54(7):1315-29.
15. Huff JS MN. Seizure. Treasure Island, Florida: StatPearls Publishing; 2023.
16. Anderson JS, Ferguson MA, Lopez-Larson M, Yurgelun-Todd D. Reproducibility of single-subject functional connectivity measurements. AJNR Am J Neuroradiol. 2011;32(3):548-55.
17. Baillet S, Friston K, Oostenveld R. Academic software applications for electromagnetic brain mapping using MEG and EEG. Comput Intell Neurosci. 2011;2011:972050.
18. Hermann B, Seidenberg M, Sager M, Carlsson C, Gidal B, Sheth R, et al. Growing old with epilepsy: the neglected issue of cognitive and brain health in aging and elder persons with chronic epilepsy. Epilepsia. 2008;49(5):731-40.
19. Bell B, Lin JJ, Seidenberg M, Hermann B. The neurobiology of cognitive disorders in temporal lobe epilepsy. Nat Rev Neurol. 2011;7(3):154-64.
20. Berg AT. The natural history of mesial temporal lobe epilepsy. Curr Opin Neurol. 2008;21(2):173-8.
21. Rosenow F, Lüders H. Presurgical evaluation of epilepsy. Brain. 2001;124(Pt 9):1683-

700.
22. Frauscher B. Localizing the epileptogenic zone. Curr Opin Neurol. 2020;33(2):198-206.
23. Gonzalez-Martinez JA. The Stereo-Electroencephalography: The Epileptogenic Zone. J Clin Neurophysiol. 2016;33(6):522-9.
24. Wiebe S, Blume WT, Girvin JP, Eliasziw M. A randomized, controlled trial of surgery for temporal-lobe epilepsy. N Engl J Med. 2001;345(5):311-8.
25. Téllez-Zenteno JF, Dhar R, Wiebe S. Long-term seizure outcomes following epilepsy surgery: a systematic review and meta-analysis. Brain. 2005;128(Pt 5):1188-98.
26. van Mierlo P, Carrette E, Hallez H, Vonck K, Van Roost D, Boon P, et al. Accurate epileptogenic focus localization through time-variant functional connectivity analysis of intracranial electroencephalographic signals. Neuroimage. 2011;56(3):1122-33.
27. Bernhardt BC, Bernasconi N, Concha L, Bernasconi A. Cortical thickness analysis in temporal lobe epilepsy: reproducibility and relation to outcome. Neurology. 2010;74(22):1776-84.
28. Morgan VL, Chang C, Englot DJ, Rogers BP. Temporal lobe epilepsy alters spatio-temporal dynamics of the hippocampal functional network. Neuroimage Clin. 2020;26:102254.
29. Maccotta L, He BJ, Snyder AZ, Eisenman LN, Benzinger TL, Ances BM, et al. Impaired and facilitated functional networks in temporal lobe epilepsy. Neuroimage Clin. 2013;2:862-72.
30. Richardson MP. Large scale brain models of epilepsy: dynamics meets connectomics. J Neurol Neurosurg Psychiatry. 2012;83(12):1238-48.
31. Stefan H, Lopes da Silva FH. Epileptic neuronal networks: methods of identification and clinical relevance. Front Neurol. 2013;4:8.
32. Terry JR, Benjamin O, Richardson MP. Seizure generation: the role of nodes and networks. Epilepsia. 2012;53(9):e166-9.
33. Hardy SG, Miller JW, Holmes MD, Born DE, Ojemann GA, Dodrill CB, et al. Factors predicting outcome of surgery for intractable epilepsy with pathologically verified mesial temporal sclerosis. Epilepsia. 2003;44(4):565-8.
34. Arfanakis K, Hermann BP, Rogers BP, Carew JD, Seidenberg M, Meyerand ME. Diffusion tensor MRI in temporal lobe epilepsy. Magn Reson Imaging. 2002;20(7):511-9.
35. Dow C, Seidenberg M, Hermann B. Relationship between information processing speed in temporal lobe epilepsy and white matter volume. Epilepsy Behav. 2004;5(6):919-25.
36. Janecek JK, Swanson SJ, Sabsevitz DS, Hammeke TA, Raghavan M, M ER, et al. Language lateralization by fMRI and Wada testing in 229 patients with epilepsy: rates and predictors of discordance. Epilepsia. 2013;54(2):314-22.
37. Zahn R, Moll J, Iyengar V, Huey ED, Tierney M, Krueger F, et al. Social conceptual impairments in frontotemporal lobar degeneration with right anterior temporal hypometabolism. Brain. 2009;132(Pt 3):604-16.
38. Birn RM, Molloy EK, Patriat R, Parker T, Meier TB, Kirk GR, et al. The effect of scan length on the reliability of resting-state fMRI connectivity estimates. Neuroimage. 2013;83:550-8.
39. Gross DW. Diffusion tensor imaging in temporal lobe epilepsy. Epilepsia. 2011;52 Suppl 4:32-4.
40. Winston GP, Vos SB, Caldairou B, Hong SJ, Czech M, Wood TC, et al. Microstructural imaging in temporal lobe epilepsy: Diffusion imaging changes relate to reduced neurite density. Neuroimage Clin. 2020;26:102231.
41. Bernhardt BC, Fadaie F, Liu M, Caldairou B, Gu S, Jefferies E, et al. Temporal lobe epilepsy: Hippocampal pathology modulates connectome topology and controllability. Neurology. 2019;92(19):e2209-e20.
42. Cook CJ, Hwang G, Mathis J, Nair VA, Conant LL, Allen L, et al. Effective Connectivity Within the Default Mode Network in Left Temporal Lobe Epilepsy: Findings from the Epilepsy Connectome Project. Brain Connect. 2019;9(2):174-83.

43. Struck AF, Boly M, Hwang G, Nair V, Mathis J, Nencka A, et al. Regional and global resting-state functional MR connectivity in temporal lobe epilepsy: Results from the Epilepsy Connectome Project. Epilepsy Behav. 2021;117:107841.
44. Hwang G, Dabbs K, Conant L, Nair VA, Mathis J, Almane DN, et al. Cognitive slowing and its underlying neurobiology in temporal lobe epilepsy. Cortex. 2019;117:41-52.
45. Rivera Bonet CN, Hermann B, Cook CJ, Hwang G, Dabbs K, Nair V, et al. Neuroanatomical correlates of personality traits in temporal lobe epilepsy: Findings from the Epilepsy Connectome Project. Epilepsy Behav. 2019;98(Pt A):220-7.
46. Rivera Bonet CN, Hwang G, Hermann B, Struck AF, C JC, V AN, et al. Neuroticism in temporal lobe epilepsy is associated with altered limbic-frontal lobe resting-state functional connectivity. Epilepsy Behav. 2020;110:107172.
47. Garcia-Ramos C, Adluru N, Chu DY, Nair V, Adluru A, Nencka A, et al. Multi-shell connectome DWI-based graph theory measures for the prediction of temporal lobe epilepsy and cognition. Cereb Cortex. 2023.
48. Chu DY, Adluru N, Nair VA, Choi T, Adluru A, Garcia-Ramos C, et al. Association of neighborhood deprivation with white matter connectome abnormalities in temporal lobe epilepsy. Epilepsia. 2023;64(9):2484-98.
49. Gross DW, Bastos A, Beaulieu C. Diffusion tensor imaging abnormalities in focal cortical dysplasia. Can J Neurol Sci. 2005;32(4):477-82.
50. Bast T, Ramantani G, Seitz A, Rating D. Focal cortical dysplasia: prevalence, clinical presentation and epilepsy in children and adults. Acta Neurol Scand. 2006;113(2):72-81.
51. Maynard LM, Leach JL, Horn PS, Spaeth CG, Mangano FT, Holland KD, et al. Epilepsy prevalence and severity predictors in MRI-identified focal cortical dysplasia. Epilepsy Res. 2017;132:41-9.
52. Barkovich AJ, Guerrini R, Kuzniecky RI, Jackson GD, Dobyns WB. A developmental and genetic classification for malformations of cortical development: update 2012. Brain. 2012;135(5):1348-69.
53. Lee DA, Lee H-J, Kim HC, Park KM. Alterations of structural connectivity and structural co-variance network in focal cortical dysplasia. BMC neurology. 2021;21(1):1-8.
54. Rezayev A, Feldman HA, Levman J, Takahashi E. Bilateral thalamocortical abnormalities in focal cortical dysplasia. Brain Res. 2018;1694:38-45.
55. Lee S-K, Kim DI, Mori S, Kim J, Kim HD, Heo K, et al. Diffusion tensor MRI visualizes decreased subcortical fiber connectivity in focal cortical dysplasia. NeuroImage. 2004;22(4):1826-9.
56. Stasenko A, Lin C, Bonilha L, Bernhardt BC, McDonald CR. Neurobehavioral and Clinical Comorbidities in Epilepsy: The Role of White Matter Network Disruption. Neuroscientist. 2022:10738584221076133.
57. Eriksson S, Rugg-Gunn F, Symms M, Barker G, Duncan J. Diffusion tensor imaging in patients with epilepsy and malformations of cortical development. Brain. 2001;124(3):617-26.
58. Fonseca Vde C, Yasuda CL, Tedeschi GG, Betting LE, Cendes F. White matter abnormalities in patients with focal cortical dysplasia revealed by diffusion tensor imaging analysis in a voxelwise approach. Front Neurol. 2012;3:121.
59. Beyer T, Bailey DL, Birk UJ, Buvat I, Catana C, Cheng Z, et al. Medical Physics and Imaging–A Timely Perspective. Frontiers in Physics. 2021;9.
60. Berger A. Magnetic resonance imaging. Bmj. 2002;324(7328):35.
61. Alexander AL, Lee JE, Lazar M, Field AS. Diffusion Tensor Imaging of the Brain. Neurotherapeutics. 2007;4(3):316-29.
62. Peters JM, Taquet M, Prohl AK, Scherrer B, van Eeghen AM, Prabhu SP, et al. Diffusion tensor imaging and related techniques in tuberous sclerosis complex: review and future directions. Future Neurol. 2013;8(5):583-97.
63. Soares J, Marques P, Alves V, Sousa N. A hitchhiker's guide to diffusion tensor imaging.

Frontiers in Neuroscience. 2013;7.
64. Qiu A, Mori S, Miller MI. Diffusion tensor imaging for understanding brain development in early life. Annu Rev Psychol. 2015;66:853-76.
65. Maier-Hein KH, Neher PF, Houde J-C, Côté M-A, Garyfallidis E, Zhong J, et al. The challenge of mapping the human connectome based on diffusion tractography. Nature Communications. 2017;8(1):1349.
66. Bernhardt BC, Bonilha L, Gross DW. Network analysis for a network disorder: The emerging role of graph theory in the study of epilepsy. Epilepsy Behav. 2015;50:162-70.
67. Bonilha L, Jensen JH, Baker N, Breedlove J, Nesland T, Lin JJ, et al. The brain connectome as a personalized biomarker of seizure outcomes after temporal lobectomy. Neurology. 2015;84(18):1846-53.
68. Taylor PN, Sinha N, Wang Y, Vos SB, de Tisi J, Miserocchi A, et al. The impact of epilepsy surgery on the structural connectome and its relation to outcome. Neuroimage Clin. 2018;18:202-14.
69. Caiafa CF, Pestilli F. Multidimensional encoding of brain connectomes. Scientific Reports. 2017;7(1):11491.
70. Baggio HC, Abos A, Segura B, Campabadal A, Garcia-Diaz A, Uribe C, et al. Statistical inference in brain graphs using threshold-free network-based statistics. Hum Brain Mapp. 2018;39(6):2289-302.
71. Hampton OL, Buckley RF, Manning LK, Scott MR, Properzi MJ, Pena-Gomez C, et al. Resting-state functional connectivity and amyloid burden influence longitudinal cortical thinning in the default mode network in preclinical Alzheimer's disease. Neuroimage Clin. 2020;28:102407.
72. Kuang L, Han X, Chen K, Caselli RJ, Reiman EM, Wang Y, et al. A concise and persistent feature to study brain resting-state network dynamics: Findings from the Alzheimer's Disease Neuroimaging Initiative. Hum Brain Mapp. 2019;40(4):1062-81.
73. Kaiser RH, Andrews-Hanna JR, Wager TD, Pizzagalli DA. Large-Scale Network Dysfunction in Major Depressive Disorder: A Meta-analysis of Resting-State Functional Connectivity. JAMA Psychiatry. 2015;72(6):603-11.
74. Lynall ME, Bassett DS, Kerwin R, McKenna PJ, Kitzbichler M, Muller U, et al. Functional connectivity and brain networks in schizophrenia. J Neurosci. 2010;30(28):9477-87.
75. Viviano JD, Buchanan RW, Calarco N, Gold JM, Foussias G, Bhagwat N, et al. Resting-State Connectivity Biomarkers of Cognitive Performance and Social Function in Individuals With Schizophrenia Spectrum Disorder and Healthy Control Subjects. Biol Psychiatry. 2018;84(9):665-74.
76. Di Martino A, Yan CG, Li Q, Denio E, Castellanos FX, Alaerts K, et al. The autism brain imaging data exchange: towards a large-scale evaluation of the intrinsic brain architecture in autism. Mol Psychiatry. 2014;19(6):659-67.
77. Sato W, Uono S. The atypical social brain network in autism: advances in structural and functional MRI studies. Curr Opin Neurol. 2019;32(4):617-21.
78. Lee DA, Lee HJ, Kim HC, Park KM. Alterations of structural connectivity and structural co-variance network in focal cortical dysplasia. BMC Neurol. 2021;21(1):330.
79. Lee SK, Kim DI, Mori S, Kim J, Kim HD, Heo K, et al. Diffusion tensor MRI visualizes decreased subcortical fiber connectivity in focal cortical dysplasia. Neuroimage. 2004;22(4):1826-9.
80. Eriksson SH, Rugg-Gunn FJ, Symms MR, Barker GJ, Duncan JS. Diffusion tensor imaging in patients with epilepsy and malformations of cortical development. Brain. 2001;124(Pt 3):617-26.
81. Hong SJ, Bernhardt BC, Schrader DS, Bernasconi N, Bernasconi A. Whole-brain MRI phenotyping in dysplasia-related frontal lobe epilepsy. Neurology. 2016;86(7):643-50.
82. Whelan CD, Altmann A, Botia JA, Jahanshad N, Hibar DP, Absil J, et al. Structural brain

abnormalities in the common epilepsies assessed in a worldwide ENIGMA study. Brain. 2018;141(2):391-408.
83. Chen AA, Srinivasan D, Pomponio R, Fan Y, Nasrallah IM, Resnick SM, et al. Harmonizing Functional Connectivity Reduces Scanner Effects in Community Detection. Neuroimage. 2022:119198.
84. Fortin JP, Parker D, Tunc B, Watanabe T, Elliott MA, Ruparel K, et al. Harmonization of multi-site diffusion tensor imaging data. Neuroimage. 2017;161:149-70.
85. Pinto MS, Paolella R, Billiet T, Van Dyck P, Guns PJ, Jeurissen B, et al. Harmonization of Brain Diffusion MRI: Concepts and Methods. Front Neurosci. 2020;14:396.
86. Zhong J, Wang Y, Li J, Xue X, Liu S, Wang M, et al. Inter-site harmonization based on dual generative adversarial networks for diffusion tensor imaging: application to neonatal white matter development. Biomed Eng Online. 2020;19(1):4.
87. Widjaja E, Zarei Mahmoodabadi S, Otsubo H, Snead OC, Holowka S, Bells S, et al. Subcortical alterations in tissue microstructure adjacent to focal cortical dysplasia: detection at diffusion-tensor MR imaging by using magnetoencephalographic dipole cluster localization. Radiology. 2009;251(1):206-15.
88. Amarreh I, Meyerand ME, Stafstrom C, Hermann BP, Birn RM. Individual classification of children with epilepsy using support vector machine with multiple indices of diffusion tensor imaging. NeuroImage: Clinical. 2014;4:757-64.
89. Tournier JD, Smith R, Raffelt D, Tabbara R, Dhollander T, Pietsch M, et al. MRtrix3: A fast, flexible and open software framework for medical image processing and visualisation. Neuroimage. 2019;202:116137.
90. Jenkinson M, Beckmann CF, Behrens TE, Woolrich MW, Smith SM. FSL. Neuroimage. 2012;62(2):782-90.
91. Tustison NJ, Avants BB, Cook PA, Zheng Y, Egan A, Yushkevich PA, et al. N4ITK: improved N3 bias correction. IEEE Trans Med Imaging. 2010;29(6):1310-20.
92. Ades-Aron B, Veraart J, Kochunov P, McGuire S, Sherman P, Kellner E, et al. Evaluation of the accuracy and precision of the diffusion parameter EStImation with Gibbs and NoisE removal pipeline. Neuroimage. 2018;183:532-43.
93. Wechsler D. Wechsler Intelligence Scale for Children–Fifth Edition (WISC–V). Pearson. 2014.
94. Smith SM, Johansen-Berg H, Jenkinson M, Rueckert D, Nichols TE, Miller KL, et al. Acquisition and voxelwise analysis of multi-subject diffusion data with tract-based spatial statistics. Nat Protoc. 2007;2(3):499-503.
95. Smith SM, Nichols TE. Threshold-free cluster enhancement: addressing problems of smoothing, threshold dependence and localisation in cluster inference. Neuroimage. 2009;44(1):83-98.
96. Mori S, Oishi K, Faria AV. White matter atlases based on diffusion tensor imaging. Curr Opin Neurol. 2009;22(4):362-9.
97. Mori S, Oishi K, Jiang H, Jiang L, Li X, Akhter K, et al. Stereotaxic white matter atlas based on diffusion tensor imaging in an ICBM template. Neuroimage. 2008;40(2):570-82.
98. Keihaninejad S, Zhang H, Ryan NS, Malone IB, Modat M, Cardoso MJ, et al. An unbiased longitudinal analysis framework for tracking white matter changes using diffusion tensor imaging with application to Alzheimer's disease. NeuroImage. 2013;72:153-63.
99. Goodlett C, Davis B, Jean R, Gilmore J, Gerig G. Improved correspondence for DTI population studies via unbiased atlas building. Med Image Comput Comput Assist Interv. 2006;9(Pt 2):260-7.
100. Zavaliangos-Petropulu A, Nir TM, Thomopoulos SI, Reid RI, Bernstein MA, Borowski B, et al. Diffusion MRI Indices and Their Relation to Cognitive Impairment in Brain Aging: The Updated Multi-protocol Approach in ADNI3. Front Neuroinform. 2019;13:2.
101. Beer JC, Tustison NJ, Cook PA, Davatzikos C, Sheline YI, Shinohara RT, et al.

Longitudinal ComBat: A method for harmonizing longitudinal multi-scanner imaging data. Neuroimage. 2020;220:117129.
102. Kamali A, Flanders AE, Brody J, Hunter JV, Hasan KM. Tracing superior longitudinal fasciculus connectivity in the human brain using high resolution diffusion tensor tractography. Brain Struct Funct. 2014;219(1):269-81.
103. Min ZG, Shan HR, Xu L, Yuan DH, Sheng XX, Xie WC, et al. Diffusion tensor imaging revealed different pathological processes of white matter hyperintensities. BMC Neurol. 2021;21(1):128.
104. Otte WM, van Eijsden P, Sander JW, Duncan JS, Dijkhuizen RM, Braun KP. A meta-analysis of white matter changes in temporal lobe epilepsy as studied with diffusion tensor imaging. Epilepsia. 2012;53(4):659-67.
105. Chang YA, Marshall A, Bahrami N, Mathur K, Javadi SS, Reyes A, et al. Differential sensitivity of structural, diffusion, and resting-state functional MRI for detecting brain alterations and verbal memory impairment in temporal lobe epilepsy. Epilepsia. 2019;60(5):935-47.
106. Leyden KM, Kucukboyaci NE, Puckett OK, Lee D, Loi RQ, Paul B, et al. What does diffusion tensor imaging (DTI) tell us about cognitive networks in temporal lobe epilepsy? Quant Imaging Med Surg. 2015;5(2):247-63.
107. Rodriguez-Cruces R, Velazquez-Perez L, Rodriguez-Leyva I, Velasco AL, Trejo-Martinez D, Barragan-Campos HM, et al. Association of white matter diffusion characteristics and cognitive deficits in temporal lobe epilepsy. Epilepsy Behav. 2018;79:138-45.
108. Catani M, Howard RJ, Pajevic S, Jones DK. Virtual in vivo interactive dissection of white matter fasciculi in the human brain. Neuroimage. 2002;17(1):77-94.
109. Kim H, Harrison A, Kankirawatana P, Rozzelle C, Blount J, Torgerson C, et al. Major white matter fiber changes in medically intractable neocortical epilepsy in children: a diffusion tensor imaging study. Epilepsy Res. 2013;103(2-3):211-20.
110. Dumas de la Roque A, Oppenheim C, Chassoux F, Rodrigo S, Beuvon F, Daumas-Duport C, et al. Diffusion tensor imaging of partial intractable epilepsy. Eur Radiol. 2005;15(2):279-85.
111. Widjaja E, Skocic J, Go C, Snead OC, Mabbott D, Smith ML. Abnormal white matter correlates with neuropsychological impairment in children with localization-related epilepsy. Epilepsia. 2013;54(6):1065-73.
112. Caeyenberghs K, Siugzdaite R, Drijkoningen D, Marinazzo D, Swinnen SP. Functional Connectivity Density and Balance in Young Patients with Traumatic Axonal Injury. Brain Connect. 2015;5(7):423-32.
113. Madaan P, Gupta D, Agrawal D, Kumar A, Jauhari P, Chakrabarty B, et al. Neurocognitive Outcomes and Their Diffusion Tensor Imaging Correlates in Children With Mild Traumatic Brain Injury. J Child Neurol. 2021;36(8):664-72.
114. Suprano I, Kocevar G, Stamile C, Hannoun S, Fourneret P, Revol O, et al. White matter microarchitecture and structural network integrity correlate with children intelligence quotient. Sci Rep. 2020;10(1):20722.
115. Amarreh I, Meyerand ME, Stafstrom C, Hermann BP, Birn RM. Individual classification of children with epilepsy using support vector machine with multiple indices of diffusion tensor imaging. Neuroimage Clin. 2014;4:757-64.
116. Hatton SN, Huynh KH, Bonilha L, Abela E, Alhusaini S, Altmann A, et al. White matter abnormalities across different epilepsy syndromes in adults: an ENIGMA-Epilepsy study. Brain. 2020;143(8):2454-73.
117. Tuch DS, Reese TG, Wiegell MR, Wedeen VJ. Diffusion MRI of complex neural architecture. Neuron. 2003;40(5):885-95.
118. Moeller S, Yacoub E, Olman CA, Auerbach E, Strupp J, Harel N, et al. Multiband multislice GE-EPI at 7 tesla, with 16-fold acceleration using partial parallel imaging with application to high spatial and temporal whole-brain fMRI. Magn Reson Med. 2010;63(5):1144-

53.
119. Bullmore E, Sporns O. Complex brain networks: graph theoretical analysis of structural and functional systems. Nat Rev Neurosci. 2009;10(3):186-98.
120. Sotiropoulos SN, Jbabdi S, Xu J, Andersson JL, Moeller S, Auerbach EJ, et al. Advances in diffusion MRI acquisition and processing in the Human Connectome Project. Neuroimage. 2013;80:125-43.
121. Fortin JP, Parker D, Tunç B, Watanabe T, Elliott MA, Ruparel K, et al. Harmonization of multi-site diffusion tensor imaging data. Neuroimage. 2017;161:149-70.
122. Avants BB, Tustison N, Song G. Advanced normalization tools (ANTS). Insight j. 2009;2(365):1-35.
123. Hermann B, Conant LL, Cook CJ, Hwang G, Garcia-Ramos C, Dabbs K, et al. Network, clinical and sociodemographic features of cognitive phenotypes in temporal lobe epilepsy. NeuroImage: Clinical. 2020;27:102341.
124. Morgan VL, Sainburg LE, Johnson GW, Janson A, Levine KK, Rogers BP, et al. Presurgical temporal lobe epilepsy connectome fingerprint for seizure outcome prediction. Brain Communications. 2022;4(3).
125. Gleichgerrcht E, Keller SS, Drane DL, Munsell BC, Davis KA, Kaestner E, et al. Temporal Lobe Epilepsy Surgical Outcomes Can Be Inferred Based on Structural Connectome Hubs: A Machine Learning Study. Ann Neurol. 2020;88(5):970-83.
126. Kodankandath TV, Theodore D, Samanta D. Generalized Tonic-Clonic Seizure. StatPearls. Treasure Island (FL): StatPearls Publishing
Copyright © 2023, StatPearls Publishing LLC.; 2023.
127. Kaestner E, Balachandra AR, Bahrami N, Reyes A, Lalani SJ, Macari AC, et al. The white matter connectome as an individualized biomarker of language impairment in temporal lobe epilepsy. Neuroimage Clin. 2020;25:102125.
128. Munsell BC, Wu G, Fridriksson J, Thayer K, Mofrad N, Desisto N, et al. Relationship between neuronal network architecture and naming performance in temporal lobe epilepsy: A connectome based approach using machine learning. Brain and Language. 2019;193:45-57.
129. Balachandra AR, Kaestner E, Bahrami N, Reyes A, Lalani S, Macari AC, et al. Clinical utility of structural connectomics in predicting memory in temporal lobe epilepsy. Neurology. 2020;94(23):e2424-e35.
130. King-Stephens D, Mirro E, Weber PB, Laxer KD, Van Ness PC, Salanova V, et al. Lateralization of mesial temporal lobe epilepsy with chronic ambulatory electrocorticography. Epilepsia. 2015;56(6):959-67.
131. Thornton RL, Glover CM, Cené CW, Glik DC, Henderson JA, Williams DR. Evaluating Strategies For Reducing Health Disparities By Addressing The Social Determinants Of Health. Health Aff (Millwood). 2016;35(8):1416-23.
132. Cockerham WC, Hamby BW, Oates GR. The Social Determinants of Chronic Disease. Am J Prev Med. 2017;52(1s1):S5-s12.
133. Price JH, Khubchandani J, McKinney M, Braun R. Racial/ethnic disparities in chronic diseases of youths and access to health care in the United States. Biomed Res Int. 2013;2013:787616.
134. Quiñones AR, Botoseneanu A, Markwardt S, Nagel CL, Newsom JT, Dorr DA, et al. Racial/ethnic differences in multimorbidity development and chronic disease accumulation for middle-aged adults. PLoS One. 2019;14(6):e0218462.
135. Shaw KM, Theis KA, Self-Brown S, Roblin DW, Barker L. Chronic Disease Disparities by County Economic Status and Metropolitan Classification, Behavioral Risk Factor Surveillance System, 2013. Prev Chronic Dis. 2016;13:E119.
136. Singh GK. Area deprivation and widening inequalities in US mortality, 1969-1998. Am J Public Health. 2003;93(7):1137-43.
137. Kind AJH, Buckingham WR. Making Neighborhood-Disadvantage Metrics Accessible -

The Neighborhood Atlas. The New England journal of medicine. 2018;378(26):2456-8.
138. Burneo JG, Jette N, Theodore W, Begley C, Parko K, Thurman DJ, et al. Disparities in epilepsy: report of a systematic review by the North American Commission of the International League Against Epilepsy. Epilepsia. 2009;50(10):2285-95.
139. Maloney EM, Corcoran P, Costello DJ, O'Reilly ÉJ. Association between social deprivation and incidence of first seizures and epilepsy: A prospective population-based cohort. Epilepsia. 2022;63(8):2108-19.
140. Pickrell WO, Lacey AS, Bodger OG, Demmler JC, Thomas RH, Lyons RA, et al. Epilepsy and deprivation, a data linkage study. Epilepsia. 2015;56(4):585-91.
141. Steer S, Pickrell WO, Kerr MP, Thomas RH. Epilepsy prevalence and socioeconomic deprivation in England. Epilepsia. 2014;55(10):1634-41.
142. Louis S, Rabah N, Rammo R, Bingaman W, Jehi L. Disparities in the nationwide distribution of epilepsy centers. Epilepsy & Behavior. 2021;125:108409.
143. Schiltz NK, Koroukian SM, Singer ME, Love TE, Kaiboriboon K. Disparities in access to specialized epilepsy care. Epilepsy Res. 2013;107(1-2):172-80.
144. DeSalvo MN, Douw L, Tanaka N, Reinsberger C, Stufflebeam SM. Altered structural connectome in temporal lobe epilepsy. Radiology. 2014;270(3):842-8.
145. Slinger G, Sinke MR, Braun KP, Otte WM. White matter abnormalities at a regional and voxel level in focal and generalized epilepsy: A systematic review and meta-analysis. NeuroImage Clinical. 2016;12:902-9.
146. Rodríguez-Cruces R, Bernhardt BC, Concha L. Multidimensional associations between cognition and connectome organization in temporal lobe epilepsy. Neuroimage. 2020;213:116706.
147. Horsley JJ, Schroeder GM, Thomas RH, de Tisi J, Vos SB, Winston GP, et al. Volumetric and structural connectivity abnormalities co-localise in TLE. NeuroImage: Clinical. 2022;35:103105.
148. Reyes A, Kaestner E, Bahrami N, Balachandra A, Hegde M, Paul BM, et al. Cognitive phenotypes in temporal lobe epilepsy are associated with distinct patterns of white matter network abnormalities. Neurology. 2019;92(17):e1957-e68.
149. Uğurbil K, Xu J, Auerbach EJ, Moeller S, Vu AT, Duarte-Carvajalino JM, et al. Pushing spatial and temporal resolution for functional and diffusion MRI in the Human Connectome Project. Neuroimage. 2013;80:80-104.
150. Adluru G, Gur Y, Anderson JS, Richards LG, Adluru N, DiBella EV. Assessment of white matter microstructure in stroke patients using NODDI. Annu Int Conf IEEE Eng Med Biol Soc. 2014;2014:742-5.
151. Kim WH, Adluru N, Chung MK, Okonkwo OC, Johnson SC, B BB, et al. Multi-resolution statistical analysis of brain connectivity graphs in preclinical Alzheimer's disease. Neuroimage. 2015;118:103-17.
152. Adluru N, Destiche DJ, Lu SY, Doran ST, Birdsill AC, Melah KE, et al. White matter microstructure in late middle-age: Effects of apolipoprotein E4 and parental family history of Alzheimer's disease. Neuroimage Clin. 2014;4:730-42.
153. Hunt JF, Buckingham W, Kim AJ, Oh J, Vogt NM, Jonaitis EM, et al. Association of neighborhood-level disadvantage with cerebral and hippocampal volume. JAMA neurology. 2020;77(4):451-60.
154. Hunt JF, Vogt NM, Jonaitis EM, Buckingham WR, Koscik RL, Zuelsdorff M, et al. Association of neighborhood context, cognitive decline, and cortical change in an unimpaired cohort. Neurology. 2021;96(20):e2500-e12.
155. Witt JA, Nass RD, Baumgartner T, von Wrede R, Elger CE, Surges R, et al. Does the accumulated antiepileptic drug load in chronic epilepsy reflect disease severity? Epilepsia. 2020;61(12):2685-95.
156. Boorgu DSSK, Venkatesh S, Lakhani CM, Walker E, Aguerre IM, Riley C, et al. The

impact of socioeconomic status on subsequent neurological outcomes in multiple sclerosis. Multiple sclerosis and related disorders. 2022;65:103994.
157. Vassilaki M, Aakre JA, Castillo A, Chamberlain AM, Wilson PM, Kremers WK, et al. Association of neighborhood socioeconomic disadvantage and cognitive impairment. Alzheimer's & Dementia. 2022.
158. Zuelsdorff M, Larson JL, Hunt JF, Kim AJ, Koscik RL, Buckingham WR, et al. The Area Deprivation Index: a novel tool for harmonizable risk assessment in Alzheimer's disease research. Alzheimer's & Dementia: Translational Research & Clinical Interventions. 2020;6(1):e12039.
159. Rakesh D, Seguin C, Zalesky A, Cropley V, Whittle S. Associations between neighborhood disadvantage, resting-state functional connectivity, and behavior in the adolescent brain cognitive development study: the moderating role of positive family and school environments. Biological Psychiatry: Cognitive Neuroscience and Neuroimaging. 2021;6(9):877-86.
160. Pase MP, Rowsthorn E, Cavuoto MG, Lavale A, Yassi N, Maruff P, et al. Association of Neighborhood-Level Socioeconomic Measures With Cognition and Dementia Risk in Australian Adults. JAMA network open. 2022;5(3):e224071-e.
161. Powell WR, Zuelsdorff M, Keller SA, Betthauser TJ, Rissman RA, Bendlin BB, et al. Association of Neighborhood-Level Disadvantage With Neurofibrillary Tangles on Neuropathological Tissue Assessment. JAMA Network Open. 2022;5(4):e228966-e.
162. Bell KL, Purcell JB, Harnett NG, Goodman AM, Mrug S, Schuster MA, et al. White matter microstructure in the young adult brain varies with neighborhood disadvantage in adolescence. Neuroscience. 2021;466:162-72.
163. Brown AF, Liang L-J, Vassar SD, Stein-Merkin S, Longstreth Jr W, Ovbiagele B, et al. Neighborhood disadvantage and ischemic stroke: the Cardiovascular Health Study (CHS). Stroke. 2011;42(12):3363-8.
164. Symonds JD, Elliott KS, Shetty J, Armstrong M, Brunklaus A, Cutcutache I, et al. Early childhood epilepsies: epidemiology, classification, aetiology, and socio-economic determinants. Brain. 2021;144(9):2879-91.
165. Löscher W, Stafstrom CE. Epilepsy and its neurobehavioral comorbidities: Insights gained from animal models. Epilepsia. 2023;64(1):54-91.
166. Kotloski RJ, Sutula TP. Environmental enrichment: evidence for an unexpected therapeutic influence. Exp Neurol. 2015;264:121-6.
167. Kwan P, Arzimanoglou A, Berg AT, Brodie MJ, Allen Hauser W, Mathern G, et al. Definition of drug resistant epilepsy: consensus proposal by the ad hoc Task Force of the ILAE Commission on Therapeutic Strategies. Epilepsia. 2010;51(6):1069-77.